0063

NASA CR-54677
HRL-6272 S

GPO PRICE $ _____

CFSTI PRICE(S) $ 5.00

Hard copy (HC) _____

Microfiche (MF) 1.00

ff 653 July 65

FACILITY FORM 602

| | |
|---|---|
| N66 30489 (ACCESSION NUMBER) | (THRU) |
| 176 (PAGES) | 3 (CODE) |
| CR-54677 (NASA CR OR TMX OR AD NUMBER) | 15 (CATEGORY) |

# ALLOY IONIZER FABRICATION


by

R. R. TURK and W. E. McKEE


Prepared for

NATIONAL AERONAUTICS and SPACE ADMINISTRATION

CONTRACT NO. NAS 3-6272


HUGHES

HUGHES AIRCRAFT COMPANY

RESEARCH LABORATORIES

3011 MALIBU CANYON ROAD

MALIBU, CALIFORNIA

NOTICE

This report was prepared as an account of Government sponsored work. Neither the United States, nor the National Aeronautics and Space Administration (NASA), nor any person acting on behalf of NASA:

A. Makes any warranty or representation, expressed or implied, with respect to the accuracy, completeness or usefulness of the information contained in this report, or that the use of any information, apparatus, method, or process disclosed in this report may not infringe privately owned rights; or

B. Assumes any liabilities with respect to the use of, or for damages resulting from the use of any information, apparatus, method or process disclosed in this report.

As used above, "person acting on behalf of NASA" includes any employee or contractor of NASA, or employee of such contractor, to the extent that such employee or contractor of NASA, or employee of such contractor prepares, disseminates, or provides access to, any information pursuant to his employment or contract with NASA, or his employment with such contractor.

Requests for copies of this report should be referred to

National Aeronautics and Space Administration
Office of Scientific and Technical Information
Attention: AFSS-A
Washington, D.C. 20546

NASA CR-54677
HRL-6272S

# SUMMARY REPORT

# ALLOY IONIZER FABRICATION

by

R. R. Turk and W. E. McKee

prepared for

NATIONAL AERONAUTICS AND SPACE ADMINISTRATION

May 1966

CONTRACT NAS 3-6272

Technical Management
NASA-Lewis Research Center
Cleveland, Ohio

HUGHES RESEARCH LABORATORIES
A Division of Hughes Aircraft Company
Malibu, California

BLANK PAGE

TABLE OF CONTENTS


LIST OF ILLUSTRATIONS . . . . . vii

ABSTRACT . . . . . xi

SUMMARY . . . . . xiii

PART 1

I. INTRODUCTION . . . . . 3

II. POROUS IRIDIUM FABRICATION . . . . . 5

A. Iridium Powder . . . . . 5

B. Pressing and Sintering Iridium . . . . . 6

C. Welding Iridium . . . . . 10

III. POROUS SPECIMENS FROM PRE-ALLOYED POWDER . . . 21

A. 5 Re-95 W Powder . . . . . 25

B. 25 Re-75 W Powder . . . . . 26

C. 50 Ir-50 W Powder . . . . . 32

D. Pressing Problems . . . . . 34

IV. SOLID PELLETS FROM POWDER MIXTURES . . . . . 37

A. Unalloyed Tungsten . . . . . 37

B. Iridium-Tungsten Powder Mixtures . . . . . 39

C. Rhenium-Tungsten Powder Mixtures . . . . . 44

V. SINTERING KINETICS OF SPHERICAL TUNGSTEN POWDERS . . . . . 47

A. Sintering Kinetics Program Description . . . . . 47

B. Powders . . . . . 50

C. Pellet Fabrication . . . . . 50

D. Equipment . . . . . 56

E. Initial Kinetics Runs . . . . . 59

F. Permeability Testing . . . . . 63

VI. SUMMARY OF WORK DONE . . . . . 71

VII. RECOMMENDATIONS FOR FUTURE WORK . . . . . 81

PART 2

I. INTRODUCTION . . . . . 85

II. TESTING PROCEDURES . . . . . 89

III. IRIDIUM COATING OF POROUS TUNGSTEN . . . . . 95

A. Coating by Impregnation in an Iridium Solution . . . . . 95

B. Coating with Iridium by Sputtering . . . . . 117

C. Coating with Iridium by Combining Sputtering and Immersion . . . . . 118

D. Coating by Spraying with Iridium Solutions . . . . . 120

E. Testing of Iridium Coated Tungsten . . . . . 129

F. Conclusions and Recommendations Concerning Coating with Iridium . . . . . 135

IV. RHENIUM COATING OF POROUS TUNGSTEN . . . . . 137

A. Coating with Rhenium by Electroplating . . . . . 137

B. Coating by Immersion in a Rhenium Solution . . . . . 139

C. Coating by Spraying with a Rhenium Solution . . . . . 143

D. Coating with Rhenium by Vapor Plating . . . . . 148

E. Coating with Rhenium by Sputtering . . . . . 149

F. Testing of Rhenium Coated Tungsten . . . . . 149

G. Conclusions and Recommendations Concerning Coating with Rhenium . . . . . 155

APPENDIX I – SPECTROGRAPHIC ANALYSIS OF PRE-ALLOYED SPHERICAL POWDER . . . 157

DISTRIBUTION LIST . . . . . 159

BLANK PAGE

## LIST OF ILLUSTRATIONS


Fig. 1. Photomicrograph (2000x) of the 3.7 μ fraction of spherical iridium powder . . . . . 7

Fig. 2. Surface of porous iridium pellet . . . . . 11

Fig. 3. Cracking in molybdenum-iridium weld . . . . . 14

Fig. 4. Single crack through columbium-iridium weld . . . 14

Fig. 5. Rhenium annulus with iridium pellet in center and outer ring of molybdenum . . . . . 15

Fig. 6. Rhenium pellet with iridium core . . . . . 17

Fig. 7. Molybdenum-rhenium weld . . . . . 17

Fig. 8. Iridium-rhenium weld . . . . . 18

Fig. 9. Iridium-rhenium weld . . . . . 18

Fig. 10. Iridium-rhenium weld . . . . . 19

Fig. 11. Iridium-rhenium weld . . . . . 19

Fig. 12. Phase diagram for tungsten-rhenium . . . . . 23

Fig. 13. Phase diagram for tungsten-iridium system . . . . 24

Fig. 14. Warm pressing setup . . . . . 27

Fig. 15. Photomicrograph (400x) of as-pressed pellet of powder supplied as 25 Re-75 W "pre-alloyed" material . . . . . 33

Fig. 16. Photomicrograph (30x) of weld between porous pellet of pre-alloyed rhenium-tungsten powder and a molybdenum holder . . . . . 33

Fig. 17. Setup for vacuum sintering . . . . . 40

Fig. 18. Repeated sintering of 50 Ir-50 W pellet No. 229 at 2200°C . . . . . 45

Fig. 19. 3.1 μ spherical tungsten powder . . . . . 51

Fig. 20. 3.9 μ spherical tungsten powder . . . . . 51

Fig. 21. 5.4 μ spherical tungsten powder . . . . . 52

Fig. 22. 7.4 μ spherical tungsten powder . . . . . 52

Fig. 23. One-half inch diameter pellets machined by trepanning from a pressed-powder tungsten plate, with trepanning tool . . . . . 53

Fig. 24. Heating arrangement for long term vacuum sintering of tungsten pellets . . . . . 60

Fig. 25. Heater circuits for long term sintering kinetics studies . . . . . 61

Fig. 26. Specimen holders used during permeability testing . . . . . 64

Fig. 27. Testing apparatus . . . . . 65

Fig. 28. Final permeability testing apparatus . . . . . 67

Fig. 29. Specimen holder used for permeability testing . . . . . 68

Fig. 30. Pellets fabricated under contract effort . . . . 72

Fig. 31. Pellet No. 214 . . . . . 73

Fig. 32. Pellet No. 192 . . . . . 74

Fig. 33. Pellet No. 226 . . . . . 75

Fig. 34. Work function as a function of neutral efflux for iridium and tungsten-rhenium alloys . . . . 86

Fig. 35. Schematics of test apparatus used at HRL . . . 91

Fig. 36. Uncoated No. 477 Mod E ionizer tungsten . . . . 102

Fig. 37. No. 477-2 Mod E ionizer tungsten after six impregnations with iridium . . . . . 102

Fig. 38. No. 477-1 Mod E ionizer tungsten after six impregnations with iridium . . . . . 103

Fig. 39. No. 477-2 Mod E ionizer tungsten after 11 impregnations with iridium . . . . . 103

Fig. 40. No. 466 flat Mod E tungsten after six impregnations with iridium . . . . . 104

Fig. 41. No. 466 flat Mod E tungsten after 11 impregnations with iridium . . . . . 104

Fig. 42. No. 466 flat Mod E tungsten after 11 impregnations with iridium . . . . . 104

Fig. 43. Photomicrograph (2000x) of a section of an iridium impregnated single strip ionizer hydrogen fired at 1500°C for 54-1/2 hours . . . . . 111

Fig. 44. Photomicrograph (2000x) of another section of the same piece of iridium impregnated single strip ionizer shown in Fig. 10 . . . . . 111

Fig. 45. Photomicrograph (2000x) of another section of the same piece of iridium impregnated single strip ionizer shown in Figs. 10 and 11 . . . . . 112

Fig. 46. Photomicrograph (2000x) of another section of the same piece of iridium impregnated single strip ionizer shown in Figs. 10 through 12 . . . 112

Fig. 47. Photomicrograph (2000x) of a section of an iridium impregnated single strip ionizer hydrogen fired at 1500°C for 21-1/2 hours . . . 113

Fig. 48. Photomicrograph (2000x) of another section of the same piece of iridium impregnated single strip ionizer shown in Fig. 14 . . . . . 113

Fig. 49. Pellet No. 104 . . . . . 115

Fig. 50. Sputtered iridium on Mod E tungsten . . . . . 119

Fig. 51. Sputtered iridium on Mod E tungsten after 4 hours at 1800°C in vacuum . . . . . 119

Fig. 52. Sample I-12 Mod E . . . . . 122

Fig. 53. Sample No. 3 Ir . . . . . 122

Fig. 54. Sample No. 3 Ir . . . . . 124

Fig. 55. Sample No. 3 Ir . . . . . 124

Fig. 56. Sample 4V Ir . . . . . 128

Fig. 57. Sample 4V Ir . . . . . 128

Fig. 58. Phase diagram for tungsten-iridium system . . . 132

Fig. 59. Sample PW Re No. 3 . . . . . 140

Fig. 60. Pellet No. 66, Sample PW Re No. 4 . . . . . 140

Fig. 61. Sample PW Re No. 5 . . . . . 145

Fig. 62. Sample 1 R . . . . . 145

Fig. 63. Photomicrograph (2000x) of a sample of Mod E tungsten sputter coated with a 0.5 μ thick coating of rhenium . . . . . 150

Fig. 64. Photomicrograph (2000x) of Mod E tungsten sputter coated with rhenium . . . . . 150

Fig. 65. Photomicrograph (2000x) of Mod E tungsten sputter coated with rhenium . . . . . 151

## ABSTRACT

30489

### PART 1

Fabrication of porous refractory ionizer material from pre-alloyed, spherical powders of narrow size range was investigated. Alloy powders used were 50 Ir-50W, 5 Re-95W, and 25 Re-75W (pure iridium was also included). Pellets from mixtures of elemental powders of the same elements were prepared in high density form. Fabrication techniques which were studied included warm pressing, joining methods, and surface treatment to keep pores open.

### PART 2

Methods have been investigated for depositing high work function, porous coatings of iridium and rhenium up to 2 to 3 μ thick on porous tungsten. Thermal stability tests showed that 0.5 to 1 μ surface layers of iridium were converted into a tungsten-iridium alloy which remained essentially unchanged and intact for at least 200 hours at 1500°C in vacuum. Preliminary short term measurements of the electron work function of various iridium coatings indicated values between 4.9 and 5.3 eV, compared with 4.5 eV for pure tungsten. The cesium ionization efficiency of these coatings was 2 to 20 times better than that of pure tungsten.

Less complete results on rhenium coatings indicated a similar improvement in work function and ionization efficiency. The thermal stability of these coatings may be somewhat less than that of iridium coatings.

BLANK PAGE

ALLOY IONIZER FABRICATION

by

R. R. Turk and W. E. McKee
Hughes Research Laboratories

## SUMMARY

PART 1

Methods for fabricating improved refractory ionizer alloys were investigated. Eight different alloys were used, including both pre-alloyed and mechanically mixed powders of iridium-tungsten and rhenium-tungsten. High-density (low porosity) alloys were made from elemental powder mixtures, and porous pellets from pre-alloyed powders.

Iridium was spheroidized, classified, pressed, sintered, impregnated, machined, polished, boiled out and welded for complete fabrication into a porous ionizer. The difficult problems associated with preparing the surface by cathodic etching and welding to molybdenum using a rhenium interface material were solved in a way suitable for application to reproducible fabricating procedures.

Porous pellets of pre-alloyed powder of 25 Re-75W were fabricated following the same nine steps. The problems were different, arising in pressing and from nonhomogeneity of powder alloying, but they were both either solved or detailed for possible solution.

Pre-alloyed 5 Re - 95W and 50 Ir - 50W were also fully investigated for fabrication of porous ionizers, and also presented pressing problems.

Mixtures of alloy element powders were formed successfully from 2 Ir - 98W, 4 Ir - 96W, 50 Ir - 50W, and 23 Re - 77W. Most of these mixtures were sintered to high densities above 90% and delivered to NASA. The 50 Ir - 50W mixture exhibited marked resistance to densification, and gave a possibility of highly stable material for fine-pored structures.

Solid tungsten was prepared in a 5/8 in. diameter by 5/8 in. long cylinder by warm-pressing techniques in a special die, then sintered to 94% of theoretical density, machined, and delivered to NASA.

Sintering kinetics of four sizes of spherical tungsten powder was initiated, with samples prepared from 3.1, 3.9, 5.4, and 7.4 μ powder. Runs were made at 1200, 1400, 1600, 1800, and 2000°C, for various times from 2 to 180 hours. Densities and permeabilities were measured, but permeability measurements were found to be inaccurate. Nitrogen transmission test equipment was modified and calibrated, and a system was set up for measuring comparative permeability constants.

PART 2

A number of methods for depositing very thin porous coatings of high work function refractory metals on porous tungsten have been investigated. Primary emphasis has been on the chemical deposition of iridium coatings up to 1.5 μ thick. A relatively minor amount of development work was performed on rhenium and other metals. The principal methods for testing these coatings for stability on an ionizer surface have been porosity measurements, x-ray diffraction studies, and metallographic examination before and after heating at 1500°C. Preliminary work function and cesium ionization measurements taken on these coatings are very encouraging.

The purpose of this work was to demonstrate, on a porous substrate, the reduction in neutral efflux expected from a surface with higher work function than that of the commonly used tungsten. The use of a thin coating of high work function refractory material allowed this test to be made on a porous tungsten substrate with known metallurgical characteristics. Encouraging results of the coating test should give sufficient confidence to allow fabrication of high work function longer bodies.

The most promising chemical method for depositing iridium involves spraying an aqueous solution of $IrCl_3$ on the surface of porous tungsten heated to 120°C, so that most of the $IrCl_3$ is deposited on the surface by evaporation. Subsequent hydrogen firing at 1000°C reduces the chloride to metallic iridium. This process can be repeated until the desired thickness of iridium has been deposited. The coating is then bonded and diffused into the porous surface by heating two or more hours at 1500°C. The resulting diffusion coating has been tentatively estimated to be 50% iridium or more.

Thermal tests for 200 hours at 1500°C in vacuum (150-250°C higher than ionizer temperatures) showed that a coating of 1.5 mg iridium/$cm^2$ with an estimated average thickness of 0.5 μ showed little change in thickness after the first few hours of heating. X-ray diffraction also showed the surface composition was stable. Surface porosity did not change more than that of the underlying porous tungsten substrate.

In another chemical technique for depositing iridium, the porous tungsten was immersed in and saturated with an ammonia solution of $IrCl_3$. After drying and firing in hydrogen, the iridium was found to be concentrated primarily on the surfaces of the outer two or three pores. Compared with the spray method, the immersion method does not give as heavy a coating on the extreme outer surface for an equal addition of iridium. However, the immersion technique gives a better coverage to the underlying pores. In general, because more of the iridium deposited deeper in the tungsten pores, less surface coating could be achieved by this method for a given loss of surface porosity than by the spray method. The thermal stability of the coatings from the two types of application appeared to be about the same.

Another method considered briefly for depositing iridium was the reduction of thin films of $IrCl_3$ by low energy electron bombardment. However, the vapor pressure of $IrCl_3$ was too low for practical application of this method.

A few specimens were sputter coated by Philips Metalonics with 0.5 μ and 1.5 μ coatings of iridium. This method produced a very uniform coverage on the outer surface, but little coverage in the pores. Sputter coatings 1.5 μ thick were found to remain on the surface when heated at 1800°C for 4 hours. The sputter coating was deposited at a relatively low temperature so that there was little interaction between the iridium and tungsten. Comparison of the coating thickness before and after heating at 1500°C or above showed that the coating increased in thickness approximately 100%. This leads to a rough estimate that a 50:50 alloy was formed. Preliminary x-ray diffraction studies tend to confirm this estimate. A promising variation of this method is the combination of sputtering followed by chemical impregnation to coat the pores.

A similar but less extensive program was carried out in the chemical deposition of rhenium. It was found that $ReCl_5$ could be dissolved in tetrahydrofuran, or alcohol. The solutions could then be impregnated into the porous tungsten by immersion or spraying. Wet hydrogen firing at 1000°C reduced deposited $ReCl_5$ to the metal. The same general immersion and spray conditions were used as in the case of iridium, except that the evaporation took place at about 80°C. However, when the immersion technique was used, the high volatility of these solvents apparently caused the $ReCl_5$ to deposit deeper within the pores rather than on the surface. The spray technique worked very well. Preliminary thermal stability tests indicated that thin rhenium coatings may be more affected by inward diffusion than iridium.

Rhenium was also successfully sputter coated on porous tungsten without impairing surface porosity. One small ionizer coated in this manner showed some evidence of lack of coating adhesion, but this is not necessarily characteristic of this method.

It was also found possible to electroplate thin rhenium coatings on porous tungsten without impairing porosity. Using commercial plating solutions, coatings up to 0.8 μ thick were made. They appear to be subject to a considerable amount of shrinkage during subsequent hydrogen firing, so that the coatings may become discontinuous. The thermal stability or electrical properties of these coatings were not studied further.

The electrical properties exhibited by both iridium and rhenium coatings, as determined by relative short term tests, were very encouraging and definitely warrant more critical long term tests. Vacuum work functions in the range of 4.8 to 5.3 eV have been measured under various conditions for both iridium and rhenium and are reported in detail in other contract reports by Dr. R. G. Wilson under Contracts NAS 3-5249 and NAS 3-6278 and by Dr. O. K. Husmann under Contract NAS 3-6270. Measured neutral fractions for iridium coatings have ranged from 1% to 50% of the neutral fraction obtained from pure tungsten. As these were not optimized coatings and were applied in various thicknesses from 0.2 to more than 1.5 μ thick, the ultimate improvement could not be expected at this time.

One short test with a small cesium ionizer indicated that similarly promising improvements should be expected from rhenium coatings.

# PART 1

# IONIZER FABRICATION

# I. INTRODUCTION

This contract effort was directed toward the development of fabrication methods for improved porous refractory ionizers for use in cesium contact ion engines. Although the final product was to be porous, both porous and solid alloy specimens were produced on the program. The solid alloys were delivered to NASA-Lewis for surface tests of work function, while porous alloys were to be tested at Hughes Research Laboratories.

An improved ionizer is one which will ionize a greater percentage of the cesium atoms evaporating from its surface. Efficient ionization is necessary because cesium atoms which are not ionized upon evaporation from the surface are subsequently ionized by charge exchange in the beam of accelerated ions. These unfocused ions bombard the acceleration electrodes and result in sputter damage.

A surface with a high affinity for electrons (a high work function) is essential for ionization of cesium. Tungsten, with a work function of 4.54 eV, is now used as a cesium contact ionizer. However, cesium flow rates which are sufficient to produce higher thrusts, tend to flood the ionizing surface, so that cesium atoms experience the lower work function of a "cesiated" surface and evaporate as neutral atoms. Porous tungsten, with a large number of pores per square centimeter of surface, distributes cesium more uniformly so that the surface work function is not depressed as low as that resulting from high surface cesium density. Therefore, ionization efficiency increases with pore density, but stability of the high pore density structure at ionizing temperatures is lower. A portion of this contract effort was devoted to an evaluation of the sintering kinetics of various grades of porous tungsten at and above ion engine operation temperatures.

---

The draft of this report was submitted December 20, 1965. Approval was received on February 14, 1966.



PRECEDING PAGE BLANK NOT FILMED.

Ionization efficiency can be improved significantly if a higher work function surface is used to provide a greater affinity for electrons (a larger percentage of cesium atoms will be ionized). Iridium and rhenium, refractory metals with work functions higher than tungsten, were believed to be most promising as alloy materials for improved ionizers. Comparative work functions and melting temperatures are shown in Table I.

TABLE I

Work Functions and Melting Temperatures of Potential Ionizer Materials

| Metal | Work Function, eV | Melting Temperature, °C |
|---|---|---|
| Tungsten | 4.54 | 3410 |
| Iridium | 5.30 | 2443 |
| Rhenium | 5.10 | 3145 |

The tungsten, iridium, and rhenium studies under this contract may be considered under four classifications: (1) porous iridium fabrication; (2) porous specimens of pre-alloyed powder; (3) solid specimens from powder mixtures; (4) sintering kinetics of porous tungsten.

## II. POROUS IRIDIUM FABRICATION

### A. IRIDIUM POWDER

Iridium powder of -325 mesh size was procured from Engelhard Industries. A certified analysis of this material is shown in Table II.

TABLE II

Quantitative Analysis of Iridium Powder
From Engelhard Industries, Lot No. 9358-3

| Element | ppm | Element | ppm |
|---|---|---|---|
| Platinum | <200 | Copper | <10 |
| Rhodium | <100 | Silicon | 16 |
| Palladium | 560 | Magnesium | < 2 |
| | < 70 | Calcium | <30 |
| Silver | < 6 | Aluminum | < 2 |
| Lead | 96 | Nickel | <10 |
| Tin | ND[a] | Chromium | ND |
| Zinc | ND | Manganese | ND |
| Iron | <100 | Antimony | ND |
| [a]Not Detectable | | | |

Ten troy ounces of this material (311 grams) were obtained. Microscopic examination showed it to consist of unagglomerated solid particles, approximately 90% of which were below 10 μ. The iridium was spheroidized in a plasma flame by Advanced Materials and Processes Company, Palo Alto, California. Spheroidization loss was about 50% by weight. Subsequent size separation of the spheres (at the same company) resulted in narrow size fractions in the amounts listed in Table III.

TABLE III

Size Fractions of Spherical Iridium Powder
(obtained by microscopic count)

| Fraction | Size, μ | Standard Deviation | Amount, g |
|---|---|---|---|
| 1 | | | 2 |
| 2 | | | 2 |
| 3 | 3.7 | 0.62 | 14 |
| 4 | 5.1 | 0.62 | 18 |
| 5 | 7.6 | 1.59 | 56 |
| 6 | 10-11 | | 53 |
| 7 | $15^+$ | | 17 |
| | | | 162 TOTAL |

Figure 1 is a 2000x photomicrograph of the 3.7 μ fraction. Note the clean particle surfaces. This material was found to be contaminated by phosphor materials in the separating apparatus. Contaminants were removed by chemical cleaning in a hot 50-50 mixture of concentrated HF and $HNO_3$. Table IV gives analyses of fractions 3 and 5 before and after cleaning.

Note that the phosphor material – zinc (probably as zinc sulfide) was found after separation only in the lighter fraction, because it is a low-density material.

## B. PRESSING AND SINTERING IRIDIUM

Spherical fractions of iridium powder were warm pressed in a 1/2 in. diameter tungsten carbide pressing die. A temperature of 400°C, pressure of 70,000 psi, and a dwell time of 60 min. were used. Ten pellets were pressed, each 1/8 in. thick and weighing 4 g. No cracking was observed, and green strength was excellent. Results are given in Table V.

1211

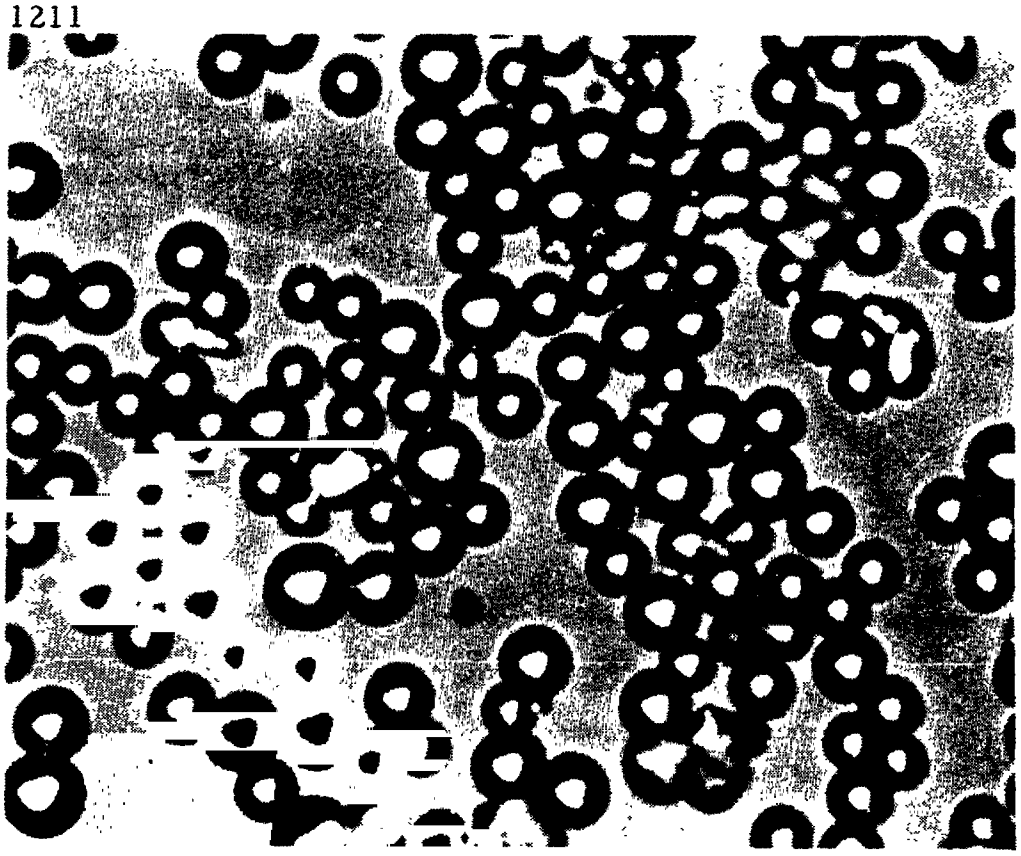

Fig. 1. Photomicrograph (2000x) of the 3.7 μ fraction of spherical iridium powder.

TABLE IV

Analyses of Iridium Powder Fractions
Before And After Chemical Cleaning

| | Element | ppm | |
|---|---|---|---|
| | | Contaminated | Cleaned |
| Fraction No. 3 | | | |
| | Silicon | 360 | 52 |
| | Magnesium | 19 | 3 |
| | Calcium | 5 | < 2 |
| | Zinc | 1200 | ND[a] (<200) |
| Fraction No. 5 | | | |
| | Silicon | 140 | <20 |
| | Magnesium | 6 | < 1 |
| | Calcium | 1 | ND (<10) |
| | Zinc | ND (<200) | ND (<200) |

[a]Not Detected

TABLE V

Pressing and Sintering of Spherical Iridium Powder Fractions

| Pellet Number | Powder Size, μ | Density % Pressed | Density % Sintered | Sintering °C | Sintering Min. |
|---|---|---|---|---|---|
| 161[a] | 10-11 | 78.4 | 77.4 ($H_2$) | 1500 | 60 |
| 164 | 6-9 | 75.6 | | | |
| 166 | 6-9 | 76.5 | | | |
| 171[a] | 6-9 | 74.6 | 78.6 (Vac) | 1630 | 90 |
| 172[a] | 3.7 | 75.3 | 83.1 (Vac) | 1630 | 60 |
| 173[a] | 5.0 | 74.0 | 84.6 (Vac) | 1700 | 60 |
| 174 | 3.7 | 74.3 | | | |
| 175[a] | 5.0 | 74.6 | 81.9 (Vac) | 1600 | 60 |
| 177[a] | 5.0 | 74.6 | 81.4 (Vac) | 1600 | 60 |
| 182 | 6-9 | 81.5 | | | |

[a]Silver-impregnated pellets

Six pellets were sintered (one in hydrogen, five in vacuum) with results shown in Table V. Densification rates were found to be very dependent on particle size, with finer sizes sintering to higher densities (Table V).

Six sintered pellets were impregnated with high-purity silver (Table VI) in a hydrogen atmosphere at 1080°C for 15 min. All pellets filled completely, and are indicated in Table V.

TABLE VI

Analysis of Silver Used for Impregnation of Porous Iridium

| Element | ppm |
|---|---|
| Antimony | ND[a] (<1) |
| Thallium | ND |
| Magnesium | 1 |
| Manganese | ND |
| Lead | ND (<1) |
| Tin | ND (<1) |
| Silicon | <1 |
| Chromium | ND (<0.1) |
| Iron | ND (<0.7) |
| Nickel | ND (<1) |
| Bismuth | ND (<0.1) |
| Aluminum | ND |
| Calcium | ND |
| Copper | 2 |
| Indium | ND |
| Zirconium | ND |
| Gold | ND |
| Cadmium | ND |

[a]Not Detectable

Machining of impregnated pellets offered no problems, and two test pellets were made for ionizer testing (Nos. 175 and 177).

Following machining, an attempt was made to polish pellet surfaces prior to evaporation of the silver, so that a reproducible surface could be obtained for pore evaluation and ionizer source tests. Softness of the iridium resulted in smearing during machining and metallographic preparation. It was difficult to remove the disturbed material because iridium is resistant to chemical attack. Electrolytic removal of material resulted in preferential silver attack, with no iridium surface improvement. Success in surface preparation was achieved using a combination of cathodic bombardment with argon ions and metallographic polishing (Fig. 2).

Subsequent evaporation of the silver left a representative porous surface. Pore counts are shown in Table VII.

Variation in the direct number of counts over the five representative areas photographed was about ±10% of the average. Figure 2 is a typical area at 2000x magnification. These results may be compared to a count of approximately $3.0 \times 10^6$ pores/cm$^2$ obtained for a 5.3 μ tungsten material similarly prepared to the same density. This shows pore count to be a function of spherical particle size and unaffected by material used.

## C. WELDING IRIDIUM

Electron beam welding of an iridium pellet into a molybdenum holder was attempted with poor results. Cracking of the weld was visible throughout the weld zone (Fig. 3). This was attributed to three causes: (1) a poor machining fit required excessive amounts of melted material as "filler"; (2) hard phases existed throughout the weld zone; (3) there was a large difference in coefficient of thermal expansion between iridium ($6.8 \times 10^6/^\circ C$) and molybdenum ($4.9 \times 10^6/^\circ C$). Vickers

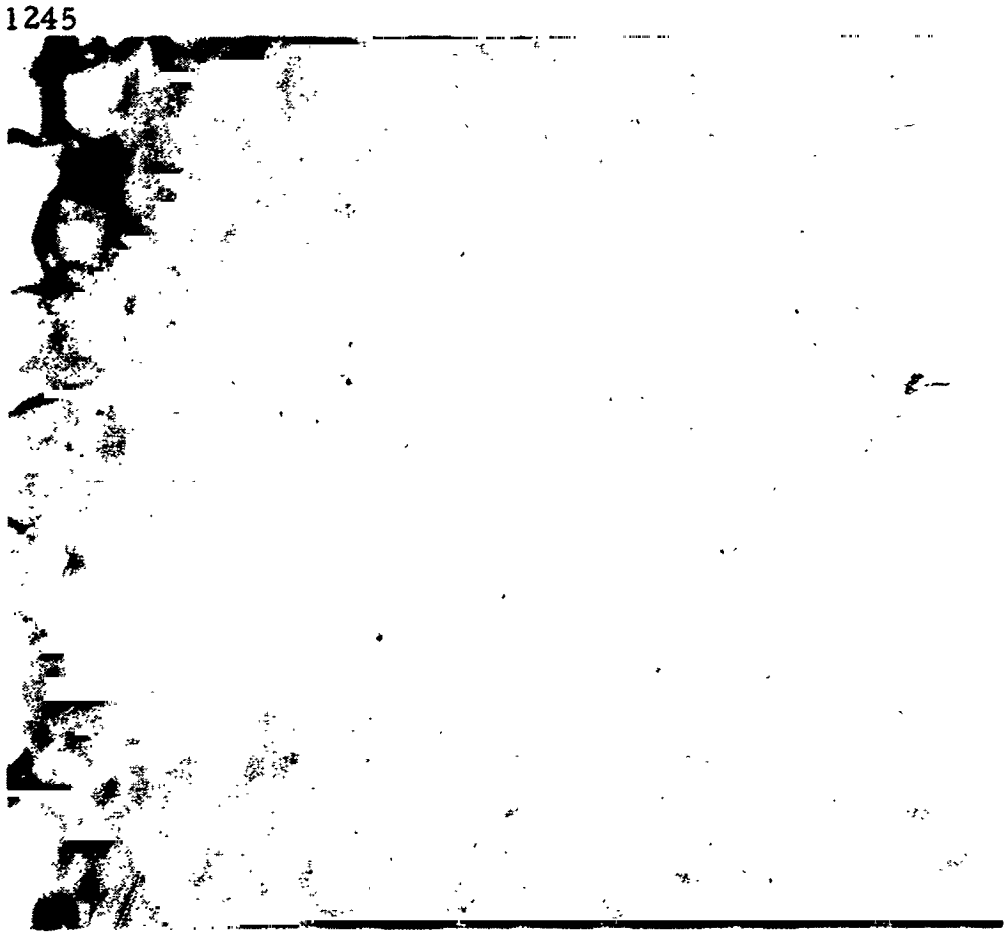


Fig. 2. Surface of porous iridium pellet.

TABLE VII

Pore Counts Obtained From 2000x Photomicrographs of Iridium Pellet No. 175 After Cathodic Etching and Silver Evaporation (5.0 μ Particles)

| Negative Number | Direct Count | | Line – Intercept | |
|---|---|---|---|---|
| | Number Pores | Density pores/cm | Average Pore Size | Average Pore Distance |
| 1250 | 388 | $3.39 \times 10^6$ | 1.60μ | 8.24μ |
| 1248 | 375 | $3.27 \times 10^6$ | 1.33μ | 9.48μ |
| 1247 | 385 | $3.37 \times 10^6$ | 1.30μ | 9.82μ |
| 1246 | 450 | $3.73 \times 10^6$ | 1.41μ | 7.17μ |
| 1245 | 424 | $3.46 \times 10^6$ | 1.42μ | 8.40μ |
| Averages | | $3.44 \times 10^6$ | 1.42μ | 8.53μ |

pyramid hardness averaged 1300 over the weld cross section, compared with 134 and 190 for iridium and molybdenum, respectively. Welding of another pellet was attempted with three changes; (1) a close machined fit was obtained; (2) only the higher-melting molybdenum was melted, providing a semi-braze joint without extensive formation of hard weld material; (3) heating of the assembly was minimized in an effort to minimize the effects of expansion differences. With all these changes, the weld region still showed cracks. For a final attempt, the molybdenum was reduced to a thin section at the joint to relieve contraction stresses with an undercut in back of the thin section to provide further stress relief. This approach showed slight promise, but cracks still appeared along the weld. It was decided then to abandon a direct iridium-molybdenum weld as too unreliable for ionizer fabrication.

Welding of an iridium pellet to columbium was attempted, but all welds cracked (Fig. 4). Tests with rhenium pieces showed promise, and rhenium was prepared for testing as an intermediate material for a "graded" joint, to avoid crack formation during welding. Two rhenium pieces were prepared directly from rhenium powder in a 1/2 in. diameter double action pressing die. One piece approximately 1/8 in. thick was pressed, sintered to 81% of theoretical density, and machined to accommodate a 1/4 in. diameter iridium pellet at the center, with a molybdenum external ring (Fig. 5). The second piece was pressed as a composite with a central section of iridium powder, by filling internal and external annular portions of the die cavity individually using a thin-wall tube as a removable separator. The sintered piece showed the effect of the difference in sintering rates between the two powders, with greater shrinkage visible in the rhenium. A weld pass along the juncture zone of this "co-pressed" pellet gave an uncracked weld, but slight shrinkage cracks occured adjacent to the weld zone in the rhenium portion of the pellet (Fig. 6). Microhardness traverses of the weld area showed a change from 148 Vickers Pyramid Hardness in the iridium, to a maximum of 623 VPH at the weld center, to 161 VPH in the rhenium.

M 4086

Fig. 3.
Cracking in molybdenum-iridium weld. (Representative of tests No. 1, 2, and 3), 30x.

M 4087

Fig. 4.
Single crack through columbium-iridium weld (test No. 4), 30x.

M 3873

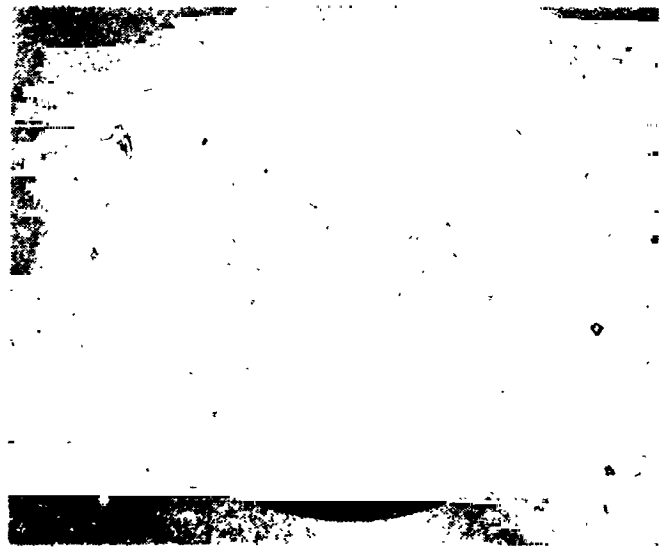

Fig. 5.
Rhenium annulus with iridium pellet in center and outer ring of molybdenum.

These are not severe differences, and should not contribute to cracking. The machined rhenium annulus, with a separate iridium pellet at its center and an external molybdenum annulus, was welded with good results. The rhenium-molybdenum and rhenium-iridium welds were examined in cross section and found to be free from cracks (Figs. 7 and 8). Several welding tests were made with rhenium to determine proper penetration parameters and machining tolerances required. Final results are shown in Fig. 9, 10, and 11.

Table VIII summarizes the efforts to weld porous iridium. The following can be concluded:

1. Iridium alloys are extremely brittle and crack sensitive. Of several refractory metals attempted, rhenium alloyed with iridium gives the necessary ductility to overcome this tendency to crack.

2. Porosity along the iridium side of the weld appears to be greater than normal, but it can be controlled by proper heat-up prior to welding.

3. Parts must fit within 0.0005 in.

In summary, it is concluded that porous iridium, while presenting some unusual problems in surface preparation and joining, can be fabricated into useful ionizers. Some modification of mounting and manifolding will be necessary, but the high work function of the final product will justify the changes. The rate of structural change with time at temperature is still not well known, but use of a coarse material of low pore density and high stability would be warranted, because of the manifold increase in ionization efficiency as a result of the increased work function. However, the high raw material cost suggests that the more economical method of surface coating of an existing porous tungsten ionizer should be thoroughly investigated before complete engine ionizers are made of porous iridium.

M 4093

Fig. 6.
Rhenium pellet with iridium core showing separation crack that continues along side of weld (test No. 5), 30x.

M 4092

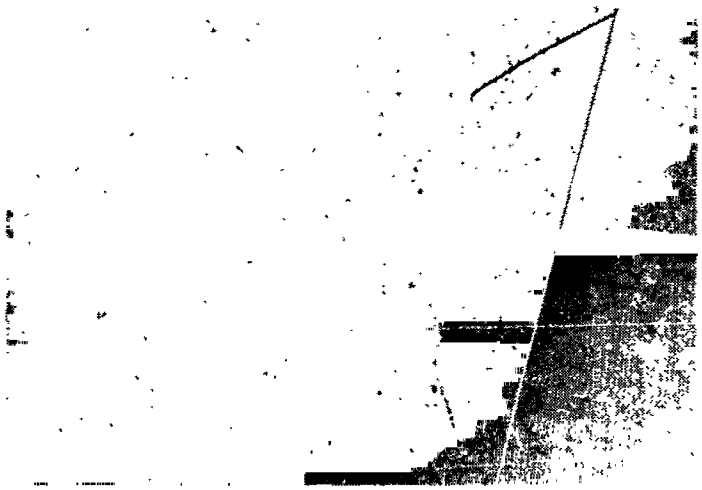

Fig. 7.
Molybdenum-rhenium weld, free of cracks but with excessive penetration (test No. 6), 30x.

M 4089

Fig. 8..
Iridium-rhenium weld made with extremely heavy penetration but free of cracks (test No. 6), 30x.

M 4088

Fig. 9.
Iridium-rhenium weld with 100% penetration and free of cracks (test No. 7), 30x.

M 4083

Fig. 10.
Iridium-rhenium weld of test No. 8, 30x.

M 4082

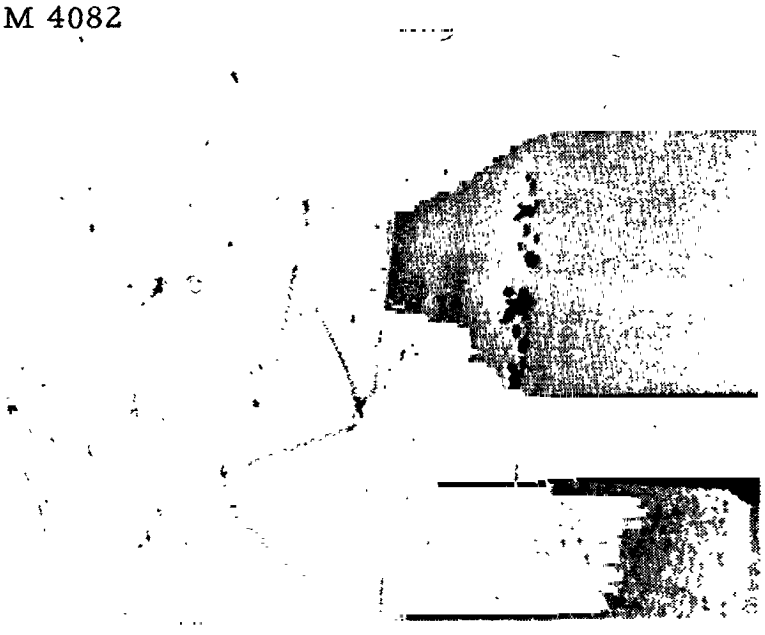

Fig. 11.
Iridium-rhenium weld of test No. 9, 30x.

## TABLE VIII

### Welding of Porous Iridium

| Test Number | Materials | Setup | Result | Corresponding Figure Number |
|---|---|---|---|---|
| 1 & 2 | Iridium Molybdenum | Standard molybdenum holder and fully machined iridium button | Alloy material in the welds extremely brittle and cracked in many places | 3 |
| 3 | Iridium Molybdenum | Flat iridium pellet (0.250 in. by 0.040 in.) fitted into molybdenum holder (0.125 in. thick) with stress relieving undercut | Same as tests Nos. 1 & 2 | |
| 4 | Iridium Columbium | Same as test No. 3 with columbium holder instead of molybdenum | Weld failed, but it had only a single crack as opposed to numerous cracks in molybdenum welds | 4 |
| 5 | Iridium Rhenium | A rhenium pellet with an iridium "core" pressed and sintered as a unit | Separation crack between iridium and rhenium, due to variance in their respective sintering kinetics, followed the outside (rhenium side) of the weld. Weld itself was crack free. | 6 |
| 6 | Iridium Rhenium Molybdenum | A rhenium "washer" was used as a ductile buffer between the iridium pellet and the molybdenum holder | Excessive welding schedule was used, causing deep penetration as well as excessive porosity at the iridium to rhenium junction | 7 (Mo-Re) 8 (Re-Ir) |
| 7 | Iridium Rhenium Molybdenum | Same as Test No. 6 | Schedule was still too heavy but better than Test No. 6. Crack at molybdenum-rhenium weld due to poor fit of parts prior to welding. | 9 (Re-Ir) |
| 8 | Iridium Rhenium Molybdenum | Same as Tests No. 6 and 7. Iridium button was fitted into rhenium washer after washer was welded to molybdenum holder | Welds look good although schedules were too light. Porosity still apparent on iridium side of weld, but joint is tight | 10 (Re-Ir) |
| 9 | Iridium Rhenium Molybdenum | Same as Tests No. 6, 7, and 8 | Heavier schedule used on rhenium to iridium weld resulting in 100% penetration. Porosity is still apparent at iridium junction, but joint is tight. | 11 (Re-Ir) |

## III. POROUS SPECIMENS FROM PRE-ALLOYED POWDER

It was decided to use pre-alloyed spherical powder to fabricate high efficiency ionizers. There were several reasons for this decision: (1) Ion source research had shown a strong tendency for a peak in work function with increasing amounts of alloy elements in tungsten so that at some composition between pure tungsten and pure rhenium (or iridium), a work function higher than that of either component might be found. (2) Alloy additions had shown tendencies toward stabilizing the porous structure of tungsten, permitting use of high pore density material at higher temperatures (and higher cesium ion currents) than possible with unalloyed tungsten. (3) The coating approach to ionizer fabrication demanded a substrate which was not only stable, but which would not readily accept alloy element atoms diffusing into its lattice and effectively diluting the coating. It was believed that a tungsten substrate phase saturated with alloy would discourage this diffusion.

Tungsten alloys with rhenium and with iridium were chosen as the materials most likely to confer high work function characteristics and contribute to high temperature stability. Single phase alloys were chosen, to avoid patchy work function characteristics resulting from varying crystal structures at the ionizing surface. Pre-alloyed material, since it was fully interdiffused, was felt to be more stable than mixtures of alloy element powders requiring long times at high temperature for interdiffusion. In addition, the heat-treatment required to interdiffuse mixtures of these high-melting elements would result in a high density structure without interconnected porosity. Spherical powder shapes were desired to permit close packing of powders and prediction of pore density. These also helped to evaluate stability by comparison with known values of sintering kinetics for spherical tungsten of similar size.

Rhenium-tungsten compositions were chosen at 5 wt. % rhenium and 25 wt. % rhenium. Figure 12, the constitution diagram for tungsten-rhenium, shows both of these alloys to be in the single phase, body-centered-cubic terminal solid solution region at the tungsten side of the diagram. Note that the 25% rhenium alloy at lower temperatures is saturated with rhenium with respect to the beta, or body-centered-cubic, phase.

An iridium-tungsten composition at 50 wt. % iridium was chosen to provide a maximum atomic surface coverage of iridium while retaining the high temperature stability of an iridium-alloyed tungsten body. The Ir-W constitution diagram (Fig. 13) shows this composition to be in the epsilon region — a single phase, close packed hexagonal structure of high hardness.

The 5% Re alloy was spheroidized by plasma melting of powder at Linde Air Products. The 25% Re and 50% Ir alloys were produced at Advanced Materials and Processes by triple arc melting, crushing, and plasma melting into microspheres. Tap densities of the powders are listed in Table IX. Spectrographic analyses are listed in Appendix I.

TABLE IX

Pre-Alloyed Spherical Powder Evaluation

| Alloy | Size, μ | Standard Deviation, μ | Tap Density, in % of Theoretical. Container Diameter = 1.13 cm | Appearance | Treatment |
|---|---|---|---|---|---|
| 5 Re-95 W | 3.3 | 1.2 | 54% at 5 $cm^3$ | Spherical, clumpy | Vacuum dried |
| 25 Re-75 W | 2.5 | 0.8 | 46.5% at 5 $cm^3$ | Spherical, dark, some irregular shapes, composition not homogeneous | Washed to lighter color in NaOH, followed by HCl |
| 25 Re-75 W | 4-5 | | 53.6% at 4 $cm^3$ | | |
| 25 Re-75 W | 6-7 | | 57.8% at 5 $cm^3$ | | |
| 50 Ir-50 W | 2-5 | | 55.4% at 5 $cm^3$ | Partly spherical | |

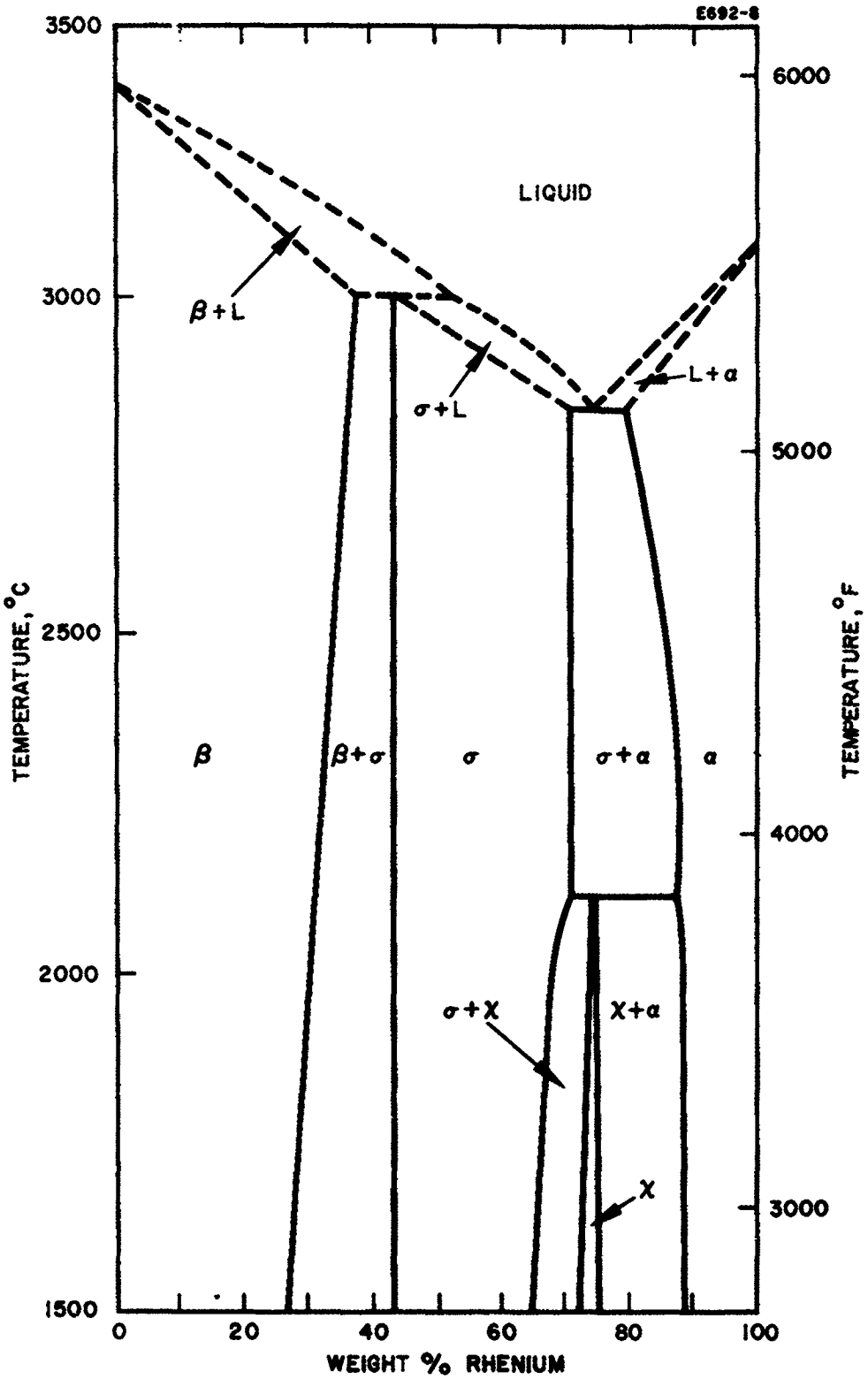


Fig. 12. Phase diagram for tungsten-rhenium from DMIC report No. 183, February 7, 1963, (84-1)-63.

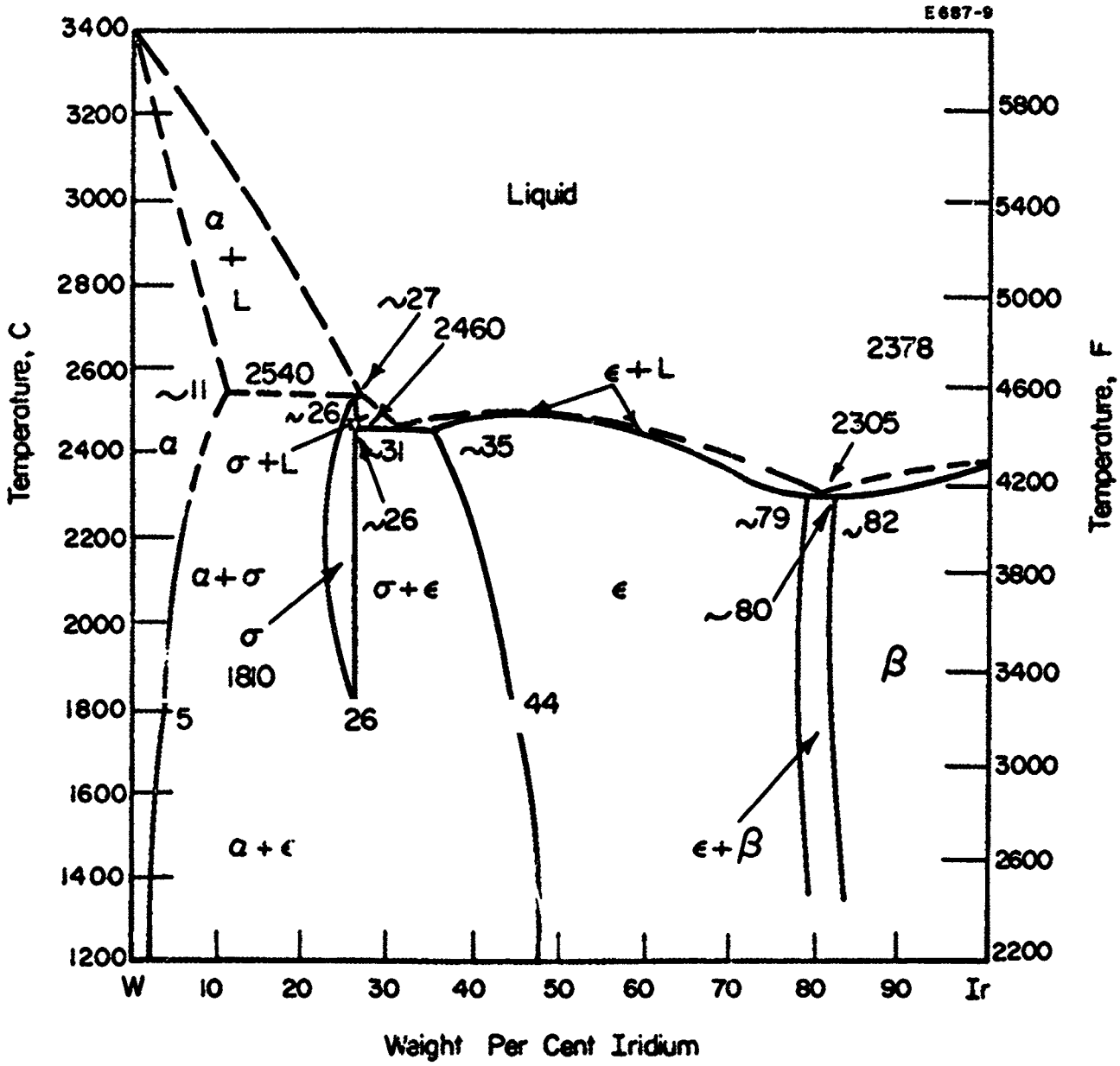


Fig. 13. Phase diagram for tungsten-iridium system. From DMIC Report No. 183, February 7, 1963 (84-1)-63.

## A. 5 Re-95 W POWDER

Microscopic examination of the 5 Re-95 W material showed the powder to be completely spheroidized, but with a tendency to stick together in clumps. The powder was vacuum dried to improve flowability, and slides were prepared for counting. Photomicrographs of eight areas were made and counted (see Table X). Note the uniformly wide size spread from 2 to 5 μ.

TABLE X

Distribution of 5% Re-95% W Pre-Alloyed Spherical Powder

| Diameter, μ | Percent By Count | Cumulative Percent | |
|---|---|---|---|
| | | Count | Weight |
| 1.0 | 2.84 | 2.84 | 0.06 |
| 1.5 | 6.20 | 9.04 | 0.49 |
| 2.0 | 10.47 | 19.51 | 2.22 |
| 2.5 | 13.82 | 33.33 | 6.69 |
| 3.0 | 18.60 | 51.93 | 17.08 |
| 3.5 | 13.29 | 65.22 | 28.87 |
| 4.0 | 13.11 | 78.33 | 46.23 |
| 4.5 | 8.84 | 87.17 | 62.90 |
| 5.0 | 7.42 | 94.59 | 82.10 |
| 5.5 | 3.25 | 97.84 | 93.29 |
| 6.0 | 1.12 | 98.96 | 98.30 |
| 6.6 | 0.30 | 99.26 | 100.00 |

Total Number Counted = 984 particles

Mean Diameter By Count $\bar{x}$ = 3.28 μ

Standard Deviation By Count o = 1.15 μ

All samples were pressed in double action in a heated cylindrical tungsten carbide die of 1/2 in. diameter (Fig. 14). Pressing of the 5% Re alloy was first tried using a "tandem" die to press two pellets at the same time (Nos. 231 and 232). The pieces were in series, with pressure transmitted through the top punch, through the top compact, through a separating punch to the bottom compact, to the bottom punch. The total effect was that of a long compact, with central sections (bottom of top piece and top of bottom piece) of lowered density due to wall friction. The remaining pellets were pressed individually, for a total of 15 samples. Note (Table XI) that all of these alloy pellets except one showed cracks before or after sintering. These resemble pressing-type cracks, and are thought to be indicative of strains from the pressing process. Variations in technique were made to eliminate pressing cracks which appeared either before or after sintering. Results are given in Table XI.

General conclusions which may be drawn from Table XI are that higher pressing temperatures give less cracking and that higher ejection temperatures reduce even those cracks which appear after sintering. It is believed that the higher pressing temperatures reduce resilient "spring-back" during ejection and increase bond strength. Higher ejection temperatures reduce the radial compression normally occurring upon cooling to room temperature. This compression results from the difference in expansion coefficient between a 1/2 in. diameter tungsten compact ($4.3 \times 10^{-6}/^{\circ}C$) and the WC die ($5.4 \times 10^{-6}/^{\circ}C$), a total of 0.0002 in. upon cooling from $400^{\circ}C$.

## B. 25 Re-75 W POWDER

Pre-alloyed powder of 25 Re-75 W was received in three spherical size fractions. These sizes corresponded to the 2 to 3, 4 to 5, and 6 to 7 μ ranges. All powder was dark in color. Prior to pressing, tap tests were run to determine relative packing abilities of different size

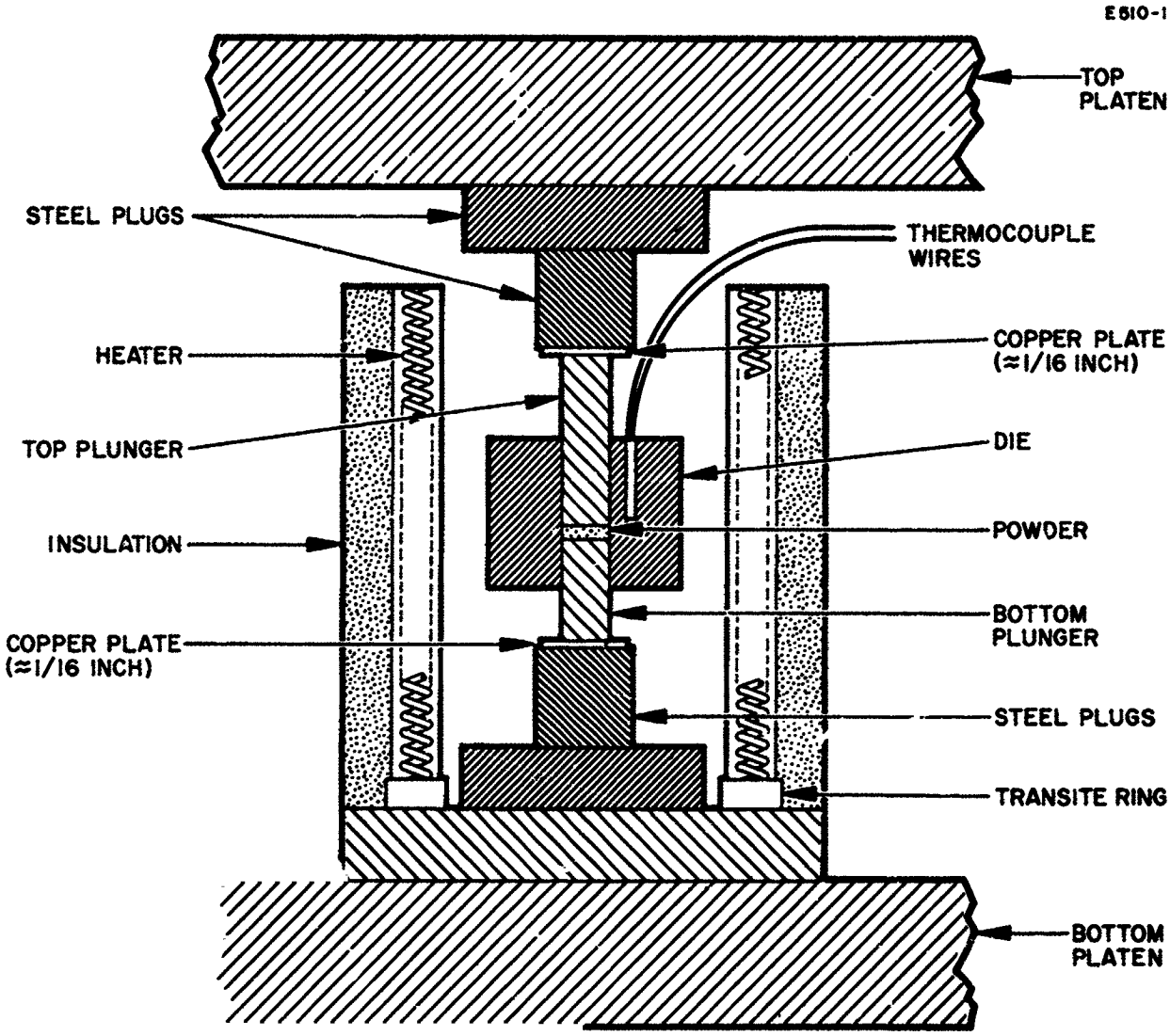


Note: Firebrick insulation and aluminum foil wrapped heat shield are placed around entire assembly after sufficient load is applied to hold assembly in place (approx. 1000 lb.) Copper plates distribute load uniformly over the tungsten carbide plunger.

Fig. 14. Warm pressing setup (heated in an argon atmosphere).

# TABLE XI

## Summary of Pressing and Sintering Results for 5 Re-95 W Pre-alloyed Spherical Powders

| Pressing Data | | | | | | Sintering Data | | | |
|---|---|---|---|---|---|---|---|---|---|
| Pellet Number | Pressure psi x $10^3$ | Temperature, °C | Ejection Temperature, °C | Density, % of Theoretical | Remarks | Temperature, °C | Time Hours | Density, % of Theoretical | Remarks |
| 231 | 75 | 400 | <100 | 70.8 | Looked Good | 1700 | 8 | 83.7 | Slight cracking |
| 232 | 75 | 400 | <100 | 72.1 | Looked Good | 1700 | 8 | 84.3 | Heavy cracking |
| 233 | 75 | 400 | <100 | 72.4 | Looked Good | 1700 | 8 | 85.4 | Slight cracking |
| 234 | 75 | 400 | <100 | 72.8 | Looked Good | 1700 | 8 | 85.1 | Slight cracking |
| 235 | 75 | 400 | <100 | 72.8 | Looked Good | 1700 | 8 | 84.5 | Heavy cracking |
| 236 | 75 | 400 | <100 | 71.7 | Looked Good | 1700 | 8 | 84.3 | |
| 237 | 75 | 400 | <100 | 72.0 | Looked Good | 1700 | 8 | 79.5 | Radial and lamination cracks |
| 261 | 75[a] | 400 | <100 | 73.0 | Looked Good | 1600 | 4 | 77.6 | Possible circumferential crack |
| 262 | 75[a] | 400 | <100 | 73.3 | Looked Good | 1600 | 4 | 78.1 | Circumferential crack, radial crack |
| 263 | 75[a] | 25 | <100 | — | Laminated (crumbled) | — | | | |
| 264 | 60[a] | 200 | <100 | — | Laminated (crumbled) | — | | | |
| 265 | 60[b] | 200 | 200 | 69.3 | Cracks on edge and face | 1600 | 8 | 76.9 | Laminations, cracks |
| 266 | 75[b] | 200 | 200 | 71.3 | Severe cracks, Laminations | — | | | |
| 267 | 75[b] | 400 | 200 | 72.9 | Looked good | 1600 | 8 | 78.7 | Very slight lamination |
| 269 | 75[b] | 500 | 250 | 72.8 | Looked good | 1600 | 8 | 78.5 | Very slight lamination |

[a]Pressure applied before raising temperature.

[b]Pressure applied after raising temperature.

fractions. Table IX gives the tap test results, and shows that the finer powder packs to a lower density than does the coarser powder. Compared with clean tungsten powders, this material packs approximately 3 to 4% less densely.

Powder was loaded into the pressing die in an argon-filled dry-box, using a long funnel to avoid coating the die walls. Loads of 4.5 g were used, and the die was tapped to level the charge before inserting the top plunger. Pressing was done in an argon atmosphere, using clam-shell heaters and insulation, as shown in Fig. 14.

Ten pressings were made, using high-temperature ejection techniques. The first five compacts of unwashed powder had a very powdery appearance, especially on the side walls. Pressed densities were low, of the order of 60%, indicating poor packing and low green strength. High springback occurred on the diameter of all compacts, of the order of 0.4%, compared with a typical tungsten springback of 0.2%. A major difficulty experienced during hot ejection was the inability of the back pressure pads to withstand the necessary punch temperatures. Deterioration of the pads caused tilting of the upper punch during ejection, with consequent breaking of the compact. Substitution of a high melting, resilient material (Viton), for the rubber pads which supply back pressure gave a measure of success, especially with subsequent cleaned powder.

Because of the low density and fragility of the pressed compacts, along with the low tap density, it was decided to attempt to clean the powder in a way similar to that used for unalloyed tungsten. The A-B fraction (2 to 3 μ) was washed as follows:

a. ≈30 g powder
   30 g $H_2O$
   30 g NaOH
   in 250 ml beaker of copper

b. mixture brought to boil and held 1/2 hour

c. mixture diluted to 250 ml, stirred, allowed to settle, and supernatant liquid decanted

d. two more rinses with water (second rinse was very black)

e. concentrated HCl added to slurry, diluted, and decanted

f. one more water rinse

g. slurry vacuum dried at 100°C in copper (25 g remained).

The final powder was light gray in color. Upon pressing (pellet No. 287), the compact was not at all powdery on the surface, but it laminated because the upper punch tilted on ejection. It is believed that the actual pressed strength may have been higher than that of previous pellets. Two succeeding pellets of cleaned powder were ejected using Viton pads for back pressure, and were free of cracks. Powder of larger size could not be pressed successfully. All pressing results for this alloy are listed in Table XII. Note that a pressing temperature of 700°C was used for one pellet (No. 286), but did not improve pressed density. Pellets No. 288 and 289 were not checked for pressed density, thus avoiding breakage during measurement.

The 25 Re-75 W pre-alloyed powder was sintered in vacuum at temperatures of 1600 to 2000°C, and times up to 300 min. Short-term or low temperature heating caused a decrease in density, with a diametral growth greater than 3%. Subsequent sintering at higher temperatures for longer times increased the density to desired values near 80% (see Table XII). This behavior, while typical of a mixture of elemental powders exhibiting the Kirkendall effect,* was unexplainable for pre-alloyed powder, except possibly as the familiar gas-evolution expansion in a powder compact (because of rhenium oxide volatility). However, the reason for this behavior became evident upon metallographic examination of these powder particles in cross section.

*Kirkendall effect — generation of porosity near an interface between two materials, because of a difference in rate of diffusion (faster atoms leave vacancies).

# TABLE XII

## Pre-alloyed Spherical 25 Re-75 W Powder

| Sample Number | Size, μ | Pressing | | | | | Sintering | | | Remarks |
|---|---|---|---|---|---|---|---|---|---|---|
| | | Temperature, °C | Pressure, psi x $10^{-3}$ | Ejection Temperature, °C | Density % of Theoretical | Remarks | Temperature, °C | Time, min | Density % of Theoretical | |
| 277 | 2-3 | 400 | 75 | 250 | Low | Powdery sides, high "spring back", ≈ 0.4% | 1600<br>1800<br>2000 | 120<br>300<br>240 | ≈ 81 | Machined, polished, boiled-out and held for reserve |
| 278 | 2-3 | 300 | 65 | 300 | 59.1 | Powdery, back pressure failed. Broken edge | 1600<br>1800<br>1800<br>2000 | 120<br>120<br>300<br>240 | 50.4<br>62.5<br>68.4<br>82.2 | Machined, polished, boiled-out and used for test weld |
| 282 | 4-5 | 300 | 75 | 300 | Loose | Crumbled | — | — | — | — |
| 285 | 2.3 | 400 | 85 | 200 | 61.0 | Powdery, broke on measuring | — | — | — | — |
| 286 | 2-3 | 700 | 75 | 200 | 58.2 | Powdery, layers stuck to plungers, no cracks | 1800<br>1800<br>2000 | 120<br>300<br>240 | 64.4<br>67.5<br>80.9 | Machined, polished, boiled-out and used test weld |
| 287 | 2-3 | 400 | 75 | 200 | — | Washed powder, not powdery after pressing, uminated and broke | — | — | — | — |
| 288 | 2-3 | 400 | 75 | 200 | — | Looked good – used viton pads for pushout | 2000 | 180 | ≈ 85 | Laminations |
| 289 | 2-3 | 400 | 75 | 200 | — | Looked good – used viton pads for pushout | 1800(?) Malfunction of furnace | 50 | 75 | Machined, polished, boiled-out, pore counts made, sent for electrical testing |
| 291 | 6-7 | 400 | 75 | 200 | — | Broke when handled | — | — | — | — |
| 292 | 4-5 | 400 | 75 | 200 | — | Crumbled | — | — | — | — |

Particles of two distinct phases were present; one phase was easily etched, and the other was very etch resistant.* The etch resistant particles had a Vickers Pyramid Hardness of over 1800; the easily etched particles, 410 to 450 VPH (Fig. 15). It is believed that the hard phase is the sigma-phase rhenium-tungsten alloy of 50 to 60% rhenium, while the softer material is a phase rich in tungsten, with only the slight solid-solution hardening of 5 to 10% rhenium. This probably happened despite the preparation by triple arc-melting, because of the extremely slow interdiffusion of rhenium and tungsten and the rapid cooling rates inherent in the arc-melting process. Subsequent crushing prior to plasma-melting effectively separated brittle material from soft material, and the softer high-tungsten material, with its higher melting point, was partly nonspheroidized (note elongated etched particles in Fig. 15).

Pellets were machined from impregnated porous specimens No. 277 and 289. These were polished and boiled out in preparation for ion source testing. Welding to molybdenum was successful (Fig. 16), in spite of powder inhomogeneity, probably because the material homogenized during 2000 $^{\circ}$C sintering.

## C. 50 Ir-50 W POWDER

A solid piece of 50% Ir-50% W alloy was received from Advanced Materials and Processes Co. This alloy was made by triple arc melting (for homogeneity) the component materials. The piece was mounted and polished for x-ray and hardness tests. X-ray diffraction showed a uniform single-phase structure throughout, with the parameters of the hexagonal 50-50 epsilon phase. Microhardness was high and uniform, averaging 1050 Vickers Pyramid Hardness. This material was granulated, spheroidized, and separated at Advanced Materials and Processes Corporation.

*Dilute alkaline ferricyanide etchant was used, 450 $cm^3$ $H_2O$, 15 g $K_3Fe(CN)_6$, 2 g NaOH.

M 4080

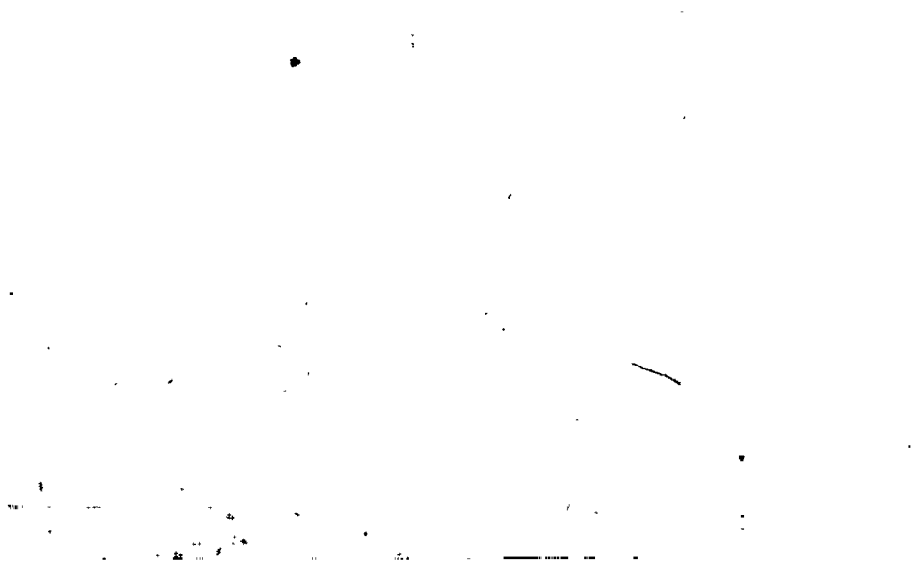

Fig. 15. Photomicrograph (400x) of as-pressed pellet of powder supplied as 25 Re-75 W "pre-alloyed" material. Note the copper impregnant (dark background), the spherical and elongated particles with black edges (probably partly alloyed tungsten) with a hardness of 410 to 450 VPH, and the remaining spherical particles of hardness over 1800 VPH (probably Re-W alloy of over 30% Re — see upper right corner).

M 4081

Fig. 16. Photomicrograph (30x) of weld between porous pellet of pre-alloyed rhenium-tungsten powder and a molybdenum holder. The dark material is the pellet, while the weld is shown by a crescent of columnar grains indicating melted material.

The pre-alloyed spherical 50 Ir-50 W powder was pressed unsuccessfully. Four pellets were pressed as shown in Table XIII. A smoky discoloration of punches and die occurred upon all pressing runs with this alloy, and was removable only with emery paper. Chemical check of the powder showed no impurities. Results shown in Table XIII indicate no improvement in compacting of this brittle alloy with increased pressing temperatures to 700°C, or with an ejection temperature higher than the pressing temperature (to expand the die and accommodate spring-back resilience).

## D. PRESSING PROBLEMS

Pressing of all of these pre-alloyed spherical refractory powders was more difficult than pressing of any other powder on this program. In the attempts to make crack-free compacts, the variables of the pressing process were carefully examined, and considerable understanding was gained. The benefits of hot ejection were demonstrated, eliminating stresses caused by differential shrinkage due to cooling of the die. Attempts were made to lower the load to that required to maintain back pressure without fully releasing pressure to insert push-out jigs, but these proved infeasible and were abandoned. Pressing of two compacts at one time was found to be poor, with wall friction excessive despite a polished (2 μin.) tungsten carbide surface. Hot pressing temperatures up to 700°C at 75,000 psi were used for stubborn materials, with little success. A total of 29 pre-alloyed pellets were pressed, with about half strong enough for sintering. It is believed that the technique of warm pressing for forming strong compacts of spherical refractory powders was fully investigated as the best technique available. Hot pressing at temperatures of over 1400°C would not have given porous compacts with complete interconnection of pores or reproducible structures typical of spherical powder. It might not have been successful for the more difficult alloys, especially since

TABLE XIII

Pressing of 50 Ir-50 W Pre-Alloyed Spherical Powder

| Pellet Number | Pressure, psi x $10^{-3}$ | Temperature, °C | Ejection Temperature, °C | Density % of Theoretical | Remarks |
|---|---|---|---|---|---|
| 257 | 75 | 520 | <100 | — | Crumbled, powdery |
| 258 | 90 | 400 | <100 | — | Severe lamination |
| 259 | 50 | 700 | <100 | — | Powdery, laminated |
| 276 | 75 | 100 | 250 | ≈ 63.5 | Powdery |

the lower pressures required by available high temperature die materials would have materially reduced the bonding strength.

It is felt that use of a binder for difficult-to-press materials might be warranted, if exotic methods of carbon removal were developed (such as pressurized wet hydrogen flow at high temperatures, etc.).

## IV. SOLID PELLETS FROM POWDER MIXTURES

Nonporous material was ordered by NASA for electrical testing. This material was to be over 93% of theoretical density, made from mixtures of suitable alloy element powders with tungsten. As before, the alloy elements chosen were iridium and rhenium because of their high work function characteristics. Mixtures of elemental powders were used because it was felt that homogeneity of structure and composition would be attained at the high temperatures and long times required for sintering to densities in excess of 93%. In addition to being more economical than pre-alloyed powder, densification rates of these mixtures would give some insight into kinetics of interdiffusion and possible stabilizing effects of additional elements.

Unalloyed tungsten was chosen as a comparative base material. The base material was made from a powder which has a high densification rate and was used for all subsequent powder mixtures. Iridium compositions of 2 and 4 wt. % iridium in tungsten were selected as representative of the tungsten terminal solid solution region (Fig. 13). A 50% iridium alloy was used to investigate the hexagonal epsilon phase (Fig. 13). A rhenium mixture at 23% rhenium in tungsten was selected as a saturated condition of rhenium in tungsten solid solution, to give maximum work function and stabilizing effects in a single-phase, ductile material.

### A. UNALLOYED TUNGSTEN

Powder for fabrication of alloy samples greater than 93% dense was prepared by blending a 50-50 mixture by weight of 3 μ and 6 μ tungsten spheres. This mixture helps in obtaining a high density sample because the fine fraction contributes to the sintering rate of the mixture. Size distribution data for this powder are given in Table XIV. Note the maxima occurring in the distribution at both 3 and 6 μ, reflecting the

TABLE XIV

Size Distribution of Mixture of Tungsten Microspheres for High Density Specimens

| Size, μ | Percent by Count |
|---|---|
| 1.5 | 2.37 |
| 2.0 | 3.40 |
| 2.5 | 10.01 |
| 3.0 | 13.83 |
| 3.5 | 13.83 |
| 4.0 | 12.07 |
| 4.5 | 6.91 |
| 5.0 | 8.98 |
| 5.5 | 7.74 |
| 6.0 | 11.04 |
| 6.5 | 4.50 |
| 7.0 | 2.68 |
| 7.5 | 1.34 |
| 8.0 | 0.93 |
| 8.5 | 0.31 |
| Total Number Counted | = 969 Particles |
| Mean Particle Diameter | = 4.27 μ |
| Standard Deviation | = 1.72 μ |

mixture of two widely varying particle sizes. Since large specimens of this material were desired (5/8 in. diameter by 1/2 in. long), a warm-pressing die was designed and fabricated. This die was of Cromovan die steel (12 Cr, 1 V, 1 Mo, 1.55 C, balance Fe), and was hardened to 58 Rockwell "C." The die cavity was cylindrical, 4 in. long by 0.725 in. in diameter, and two plungers were lapped to tolerances of 0.0002 in. All mating and pressing surfaces were polished to a 4 μin. finish. A thermocouple well adjacent to the die cavity permitted temperature control during warm pressing.

Three samples were pressed and sintered, because two were needed for delivery and one cracked during pressing. The pieces were pressed approximately 0.750 in. long by 0.725 in. diameter, to allow for sintering shrinkage and machining losses. Pressing conditions were 75,000 psi, 150°C, 60 min dwell. It was found necessary to expand the die (by heating) both during pressure release (to avoid compressive cracking due to "springback") and during extraction of the sample. Details are shown in Table XV. Note that sintering had to be repeated to increase the density to acceptable values. Pressed density was lower than that usually obtained because of the high length-to-diameter ratio. The setup for vacuum sintering is shown in Fig. 17.

## B. IRIDIUM-TUNGSTEN POWDER MIXTURES

Iridium powder for alloy mixtures was composed of nonspherical, irregularly shaped particles of 2 to 6 μ. This material, along with the basic spherical tungsten powder blend, was weighed on an analytical balance, then blended in a double-cone blender for 4 hours. The double-cone blender is a highly efficient machine for uniformly combining powders of varying size and differing densities.

For purposes of comparison, theoretical density of alloys prepared from mixtures was computed as follows: (specific volume A x % A + specific volume B x % B)$^{-1}$ x 100. For a 2 Ir-98 W alloy:

E491-1

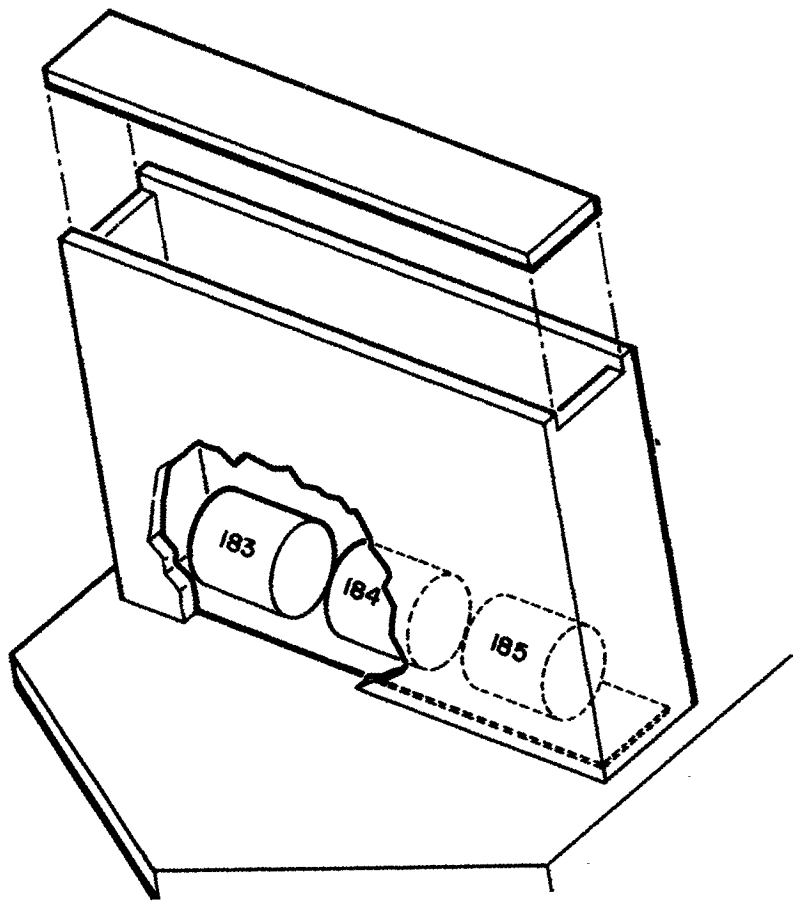


Fig. 17. Setup for vacuum sintering. Note plates used as radiation baffles.

$$\text{Volume tungsten} = \frac{98}{19.3} \qquad 5.078$$

$$\text{Volume iridium} = \frac{2}{22.5} \qquad \underline{0.089}$$

$$\text{Total volume (100 g)} \qquad 5.167$$

$$\text{Theoretical density} = \frac{100}{5.167} \qquad 19.35\ g/cm^3 \ .$$

TABLE XV

Pressing and Sintering of High-Density Tungsten Cylinders

| Sample Number | Pressed Density, % | Sintered Density, % | Sintering Conditions | |
|---|---|---|---|---|
| | | | Temp. °C | Time, min |
| 183 | 69.7 | 92.1 (cracked) | 2200 | 180 |
| 184 | 69.8 | 91.5 | 2200 | 180 |
| 185 | 69.6 | 91.5 | 2200 | 180 |
| Reheated | | | | |
| 183 | | 93.9 | 2400 | 120 |
| 184 | | 93.3 | 2400 | 120 |
| 185 | | 93.1 | 2400 | 120 |
| Machined | | | | |
| 184 | | 94.1 | | |
| 185 | | 93.9 | | |

This computation assumes no deviation from Vegard's Law, which stipulates a linear relation between the lattice parameter of the alloy and that of the constituent alloy elements.

Compacts were made from six gram samples and warm pressed in a tungsten carbide die (Fig. 14) to a 1/2 in. diameter by 1/8 in. thickness. Pressing conditions were varied to increase pressed density in hopes of increasing sintered density (Table XVI). A total of eight compacts of each type were prepared for delivery to NASA, with additional pieces for test purposes. Table XVI lists pressing and sintering results for the three iridium-tungsten alloys made.

In the attempt to obtain final densities in excess of 93% of theoretical, high pressed densities were obtained by pressing at 100,000 psi, 400°C. Dwell time did not affect the results, so a 30 min. dwell was used to insure temperature and pressure equilibrium. A protective atmosphere of argon was used for all fabrication steps except the vacuum sintering.

The required density of over 93% was not attained for the iridium alloys. Despite the ability of the tungsten powder blend to densify, addition of iridium seemed to set a top limit of densification depending upon the amount of iridium added. For 2% iridium, 91.8% was obtained. For 4% iridium, the limit was 90.8%, even when heated to 2400°C (almost 100° above the eutectic melting temperature of iridium-tungsten (Fig. 13). The 50% alloy decreased in density 8% with the same heat treatment. This decrease might be due to Kirkendall effect (porosity due to difference in diffusion rates of alloy atoms). It may also be attributed to the formation of four different crystalline phases ranging from body centered cubic tungsten to face centered cubic iridium. These phases would include the terminal solid solutions of iridium in tungsten and tungsten in iridium, the hexagonal close-packed eta phase (50-80% iridium), and the high-temperature sigma phase existing at 26% iridium and corresponding to $W_3Ir$ (see Fig. 13). Considering the slow diffusion rates shown by

## TABLE XVI

### Pressing and Sintering of Alloy Pellets from Mixed Powders

| Sample Number | Powders Mixed, % | Pressing | | | Sintering | | |
|---|---|---|---|---|---|---|---|
| | | Pressure, psi x $10^{-3}$ | Temperature, °C | Density, in % of Theoretical | Temperature, °C | Time, min | Density, in % of Theoretical |
| 207 | 2 Ir-98 W | 100 | 400 | 77.4 | 2200 | 360 | 91.2 |
| 208 | 2 Ir-98 W | 100 | 400 | 76.2 | 2200 | 360 | 90.9 |
| 210 | 2 Ir-98 W | 100 | 400 | 76.0 | 2200 | 360 | 91.7 |
| 211 | 2 Ir-98 W | 100 | 400 | 80.4 | 2200 | 360 | 91.0 |
| 212 | 2 Ir-98 W | 100 | 400 | 79.5 | 2200 | 360 | 91.8 |
| 213 | 2 Ir-98 W | 100 | 400 | 79.5 | 2200 | 360 | 91.8 |
| 214 | 2 Ir-98 W | 100 | 400 | 79.4 | 2200 | 360 | 91.8 |
| 215 | 2 Ir-98 W | 100 | 400 | 79.8 | 2200 | 360 | 91.2 |
| 216 | 2 Ir-98 W | 100 | 400 | 79.4 | 2200 | 360 | 91.8 |
| 191 | 4 Ir-96 W | 80 | 170 | 73.0 | 2400 | 240 | 90.9 |
| 192 | 4 Ir-96 W | 90 | 160 | 74.2 | 2400 | 240 | 90.0 |
| 194 | 4 Ir-96 W | 90 | 160 | 75.5 | 2200 | 360 | 90.6 |
| 195 | 4 Ir-96 W | 100 | 400 | 79.2 | 2200 | 360 | 90.7 |
| 196 | 4 Ir-96 W | 100 | 400 | Broken | — | – | — |
| 199 | 4 Ir-96 W | 100 | 400 | 79.5 | 2200 | 360 | 90.8 |
| 200 | 4 Ir-96 W | 100 | 400 | 79.6 | 2200 | 360 | 90.8 |
| 201 | 4 Ir-96 W | 100 | 400 | 79.5 | 2200 | 360 | 91.0 |
| 202 | 4 Ir-96 W | 100 | 400 | 79.4 | 2200 | 360 | 90.6 |
| 203 | 4 Ir-96 W | 100 | 400 | 80.0 | 2200 | 360 | 90.7 |
| 219 | 50 Ir-50 W | 100 | 400 | 78.7 | 2200 | 360 | 71.0[a] |
| 220 | 50 Ir-50 W | 100 | 400 | 78.6 | 2200 | 360 | 71.2[a] |
| 221 | 50 Ir-50 W | 100 | 400 | 77.8 | 2200 | 360 | 70.9[a] |
| 222 | 50 Ir-50 W | 100 | 400 | 78.0 | 2200 | 360 | 70.9[a] |
| 223 | 50 Ir-50 W | 100 | 400 | 78.6 | 2200 | 360 | 71.0[a] |
| 224 | 50 Ir-50 W | 100 | 400 | 77.8 | 2200 | 360 | 70.9[a] |
| 225 | 50 Ir-50 W | 100 | 400 | 78.6 | 2200 | 360 | 70.9[a] |
| 226 | 50 Ir-50 W | 100 | 400 | 78.1 | 2200 | 360 | 70.9[a] |
| 227 | 50 Ir-50 W | 100 | 400 | 77.9 | 2200 | 360 | 70.7[a] |

[a]Note 7% decrease in density after sintering.

this alloy system, it is likely that the almost stoichiometric phase still exists after cooling from sintering temperature. Sintering of a mixture of elemental powders must necessarily progress through all of the possible phases until equilibrium is reached. The unusual feature in this instance is the long time required to attain equilibrium at a temperature close to the melting point of the alloy (approximately 2470°C). Expansion of the material could be due to formation of expanded phases at each powder particle interface, thus multiplying a minor effect many times.

In an effort to determine the extent of iridium's stabilizing effect, a 50% sample (No. 227) was resintered repeatedly for 360-min periods at 2200°C, for a total of 2160 min, or 36 hours. Results of this heat treatment are shown in Fig. 18. A maximum density of 84.2% was reached after 36 hours at 2200°C. Permeability tests indicated existing porosity was interconnected. A permeability constant ($K_p$) of $2.4 \times 10^{-8}$ was measured, but this value is in question (see Section V). The high degree of stability contributed by the iridium can only be attributed to high-temperature inhibition of diffusion by the epsilon phase. It is recommended that this effect be investigated in future work with the aim of producing high-stability ionizers for high temperature operation.

## C. RHENIUM-TUNGSTEN POWDER MIXTURES

Powders were mixed for preparation of 5% Re-95% W compacts, but this work was re-directed by NASA, and a 23% Re-77% W mixture was made. Pellets of this material were pressed as follows:

| Pellet Number | Pressure, psi x $10^{-3}$ | Pressed Density | Remarks |
|---|---|---|---|
| 238* | 75 | 67.9% | Good |
| 239* | 75 | 68.5% | Good |
| 242 | 85 | 70.9% | Good |
| 243 | 85 | 70.8% | Good |

*Pressed in "tandem."

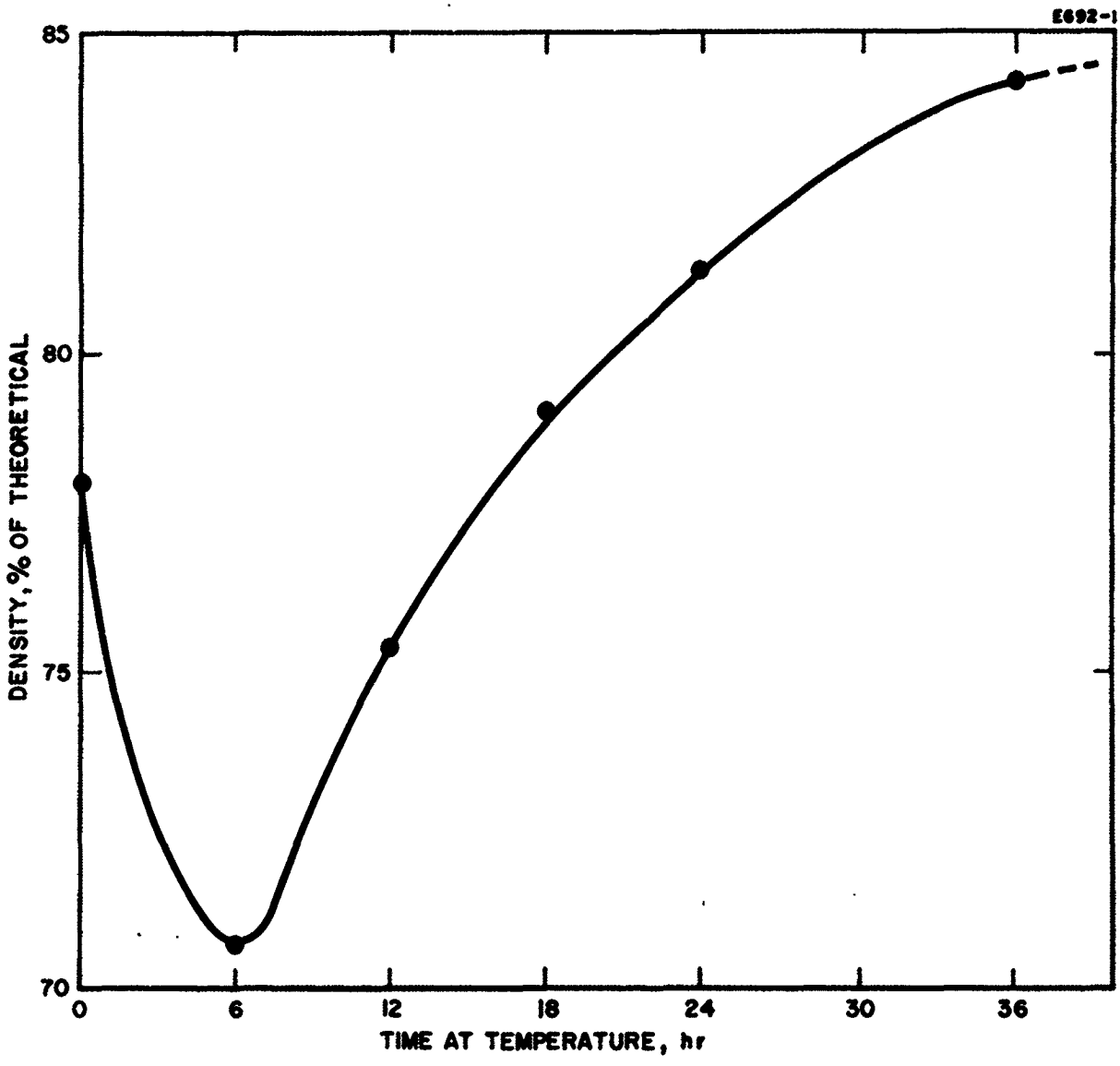


Fig. 18. Repeated sintering of 50 Ir-50 W pellet No. 229 at 2200°C. Density versus time at temperature.

Further work on this material was suspended by direction of NASA in favor of work on pre-alloyed powders. This is discussed under Section III.

## V. SINTERING KINETICS OF SPHERICAL TUNGSTEN POWDERS

Ion engines are proposed for missions of one year or greater. For maximum reliability, the life expectancy of all engine components should be predictable under operating conditions. The porous ionizer operates at 1100 to 1200°C, the highest temperatures encountered in the engine except for the heater and feed manifold. Although composed of tungsten, with a melting point of 3410°C and a recrystallization temperature over 1500°C, the porous structure is less stable than the solid metal. If used as a substrate for a coating of higher efficiency or directly as the ionizing surface, stability of the tungsten must be known, so that changes in such properties as permeability to cesium, surface pore density, and over-all dimension can be compensated for.

Stability is lower for a structure with a higher pore density, but the ionization efficiency is higher. Therefore, a compromise must be reached between the efficiency desired and lifetime of the structure at the temperature of operation. This compromise can be made to give the highest efficiency for the desired lifetime only if the structural change with time is known quantitatively. For these reasons, a program of tungsten sintering kinetics was started during this contract. (It is planned to complete this program during a follow-on contract.)

### A. Sintering Kinetics Program Description

Spherical tungsten powder of narrow size range, used for fabrication of ionizers of controlled uniform porosity, was chosen for kinetics studies. Four sizes of classified spherical tungsten powder were selected for this program: 3.1, 3.9, 5.4, and 7.4 μ. The finest powder, 3.1 μ, is felt to approach the smallest feasible size range for use in the present engine design because of its relatively rapid densification at elevated temperatures. The 3.9 μ size is being used for present engine ionizer material and represents the most intelligent compromise to date

between stability and ionization efficiency. The larger 5.4 μ powder may be a possible alternative for the 3.9 μ material, if increased stability at higher engine temperatures is needed. The coarsest powder, 7.4 μ, represents the most stable material (of this close-packed type) and may be considered for use as a possible coating substrate structure for future higher-temperature use.

Starting densities of all materials for this program are 71 to 72% of theoretical, to permit direct comparisons of density changes for the different powder sizes.

The test temperatures selected are 1200°C, 1400°C, 1600°C, 1800°C, and 2000°C, with a minimum of three different temperatures for each particle size. Time at temperature is divided into "short-term" and "long-term" runs. "Short-term" tests are defined as those lasting 2, 4, 8, 16, and 32 hours. "Long-term" tests require special vacuum heating facilities, and will be run 120 hours (5 days), 360 hours (15 days), 960 hours (40 days) and 2500 hours (104 days, 4 hours).

At densities approaching 87% of theoretical, permeability approaches zero, so material will not be tested above this upper limit. Samples will not be tested at any time and temperature combination where it is known that the resulting change in structure would be either negligible or excessive.

A set of three specimens from a powder lot is sintered together under the same conditions for increasing times at temperature, with measurements of density and permeability taken following each time interval. Two specimens start from the as-pressed condition, in order to obtain the total sintering change at temperature. The third specimen, previously sintered to 80% of theoretical density, is included to provide a measure of the change to be expected in a final ionizer when subjected to long term heating. This 80% specimen will also give a check against any future extrapolations of data to predict changes while at 80% density. The surface of the 80% dense specimen is polished (after filling with copper) and the copper removed by vacuum evaporation. The porous

surface is then examined after each heating interval to record surface changes during use. A summary of samples and runs for the total program is listed in Table XVII.

TABLE XVII

Sintering Kinetics Test Plan

| Powder Size, μ | Number of Samples to be Heated to Temperature* | | | | |
|---|---|---|---|---|---|
| | 1200°C | 1400°C | 1600°C | 1800°C | 2000°C |
| 3.1 | 3[a] | 3[a] | 3 | | |
| 3.9 | 3[a] | 3[a] | 3 | 3 | |
| 5.4 | | 3[a] | 6[b] | 3 | |
| 7.4 | | 3[a] | 3[a] | 3 | 3 |

*Samples without superscripts will be evaluated at the end of 2, 4, 8, 16 and 32 hours ("short-term" tests).

[a]These samples will be evaluated at the end of 120 hours (5 days), 360 hours (15 days), 960 hours (50 days), and 2500 hours (104 days, 4 hours) ["long-term" tests].

[b]Three "long-term," 3 "short-term" samples.

Results from these runs should give a quantitative understanding of sintering rates in warm-pressed spherical tungsten powder, with respect to temperature and particle size. Accurate prediction of changes

in permeability and dimension will be feasible. It should be possible to plot particle size versus permeability for various density parameters (78%, 80%, 82%).

## B. Powders

Each of the four sizes of tungsten powder has been photographed at 1000x magnification (see Figs. 19, 20, 21, and 22). Size measurements were made of over 700 particles of each size, and results are shown in Table XVIII. The results of tap-packing tests are presented in Table XIX.

All powders were cleaned in NaOH and HF to remove oxide and improve packing. The three finer fractions were supplied by Advanced Materials and Processes at Palo Alto, California. The coarse fraction is from Federal Mogul in Warren, Michigan.

## C. Pellet Fabrication

Pressed pellets, 1/2 in. in diameter by 1/8 in. thick, were cut from large pressed plates of each powder size. (See Table XX for details of pressing these plates.) Initially, this as-pressed material offered some problems in machining, with breakage and edge-chipping prevalent. Standard single and multitoothed machining tools proved ineffective. Final machining was done with a trepanning or coring tool, consisting of a hollow tube with diamonds impregnated on one end. This yielded sharp-edged pellets from all plates. Figure 23 shows a typical set of pellets machined from a pressed plate, along with the tool used. The additional number of samples made available by this technique permitted the choice of densities (and permeabilities) which were well matched, an important consideration in sintering tests.

M 4164

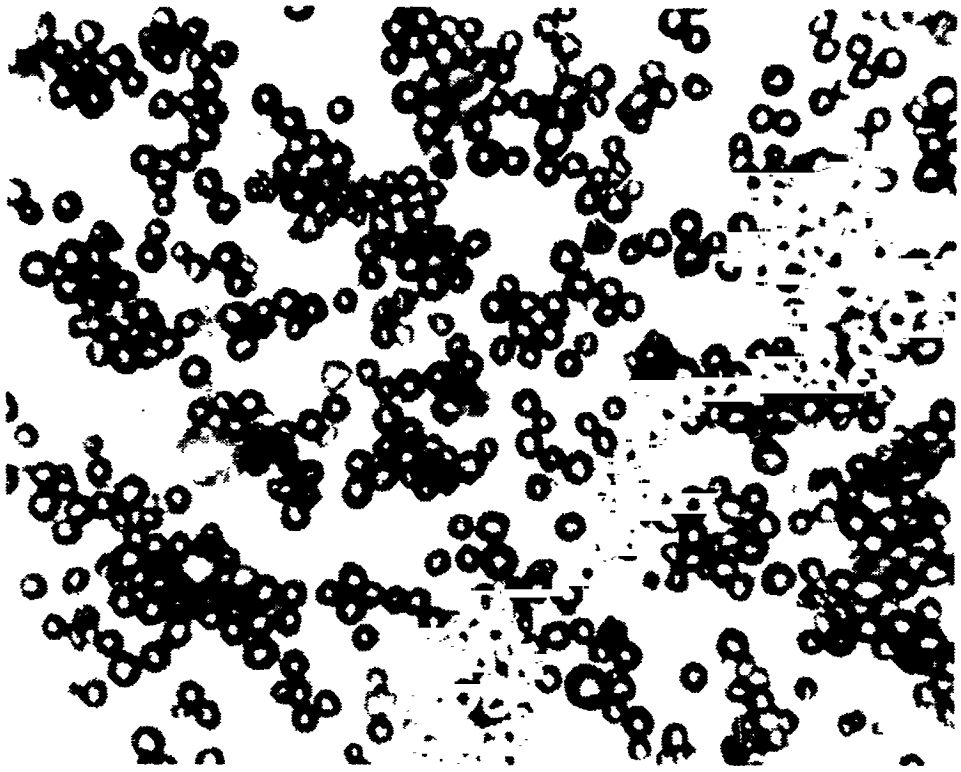

Fig. 19. 3.1 μ spherical tungsten powder, 1000x.

M 4167

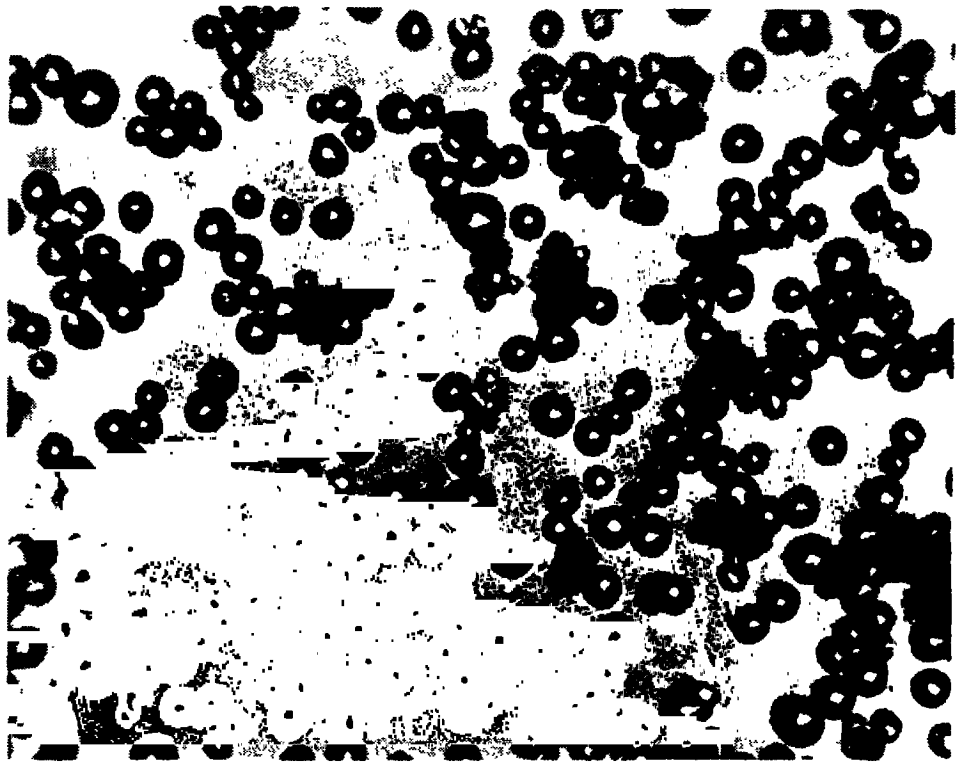

Fig. 20. 3.9 μ spherical tungsten powder, 1000x.

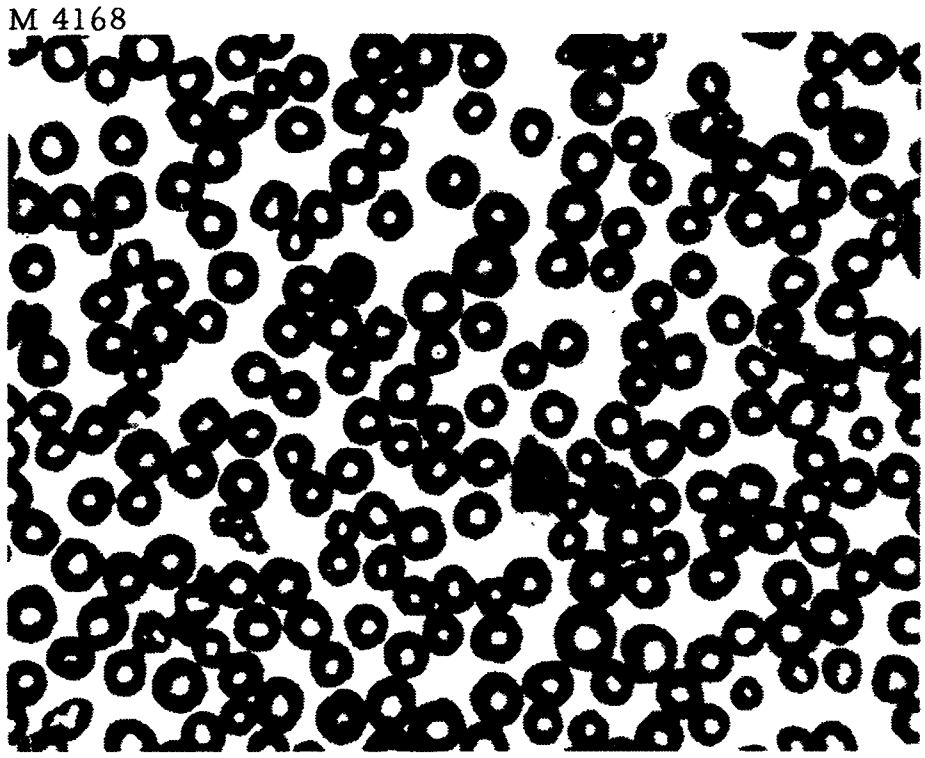


Fig. 21. 5.4 μ spherical tungsten powder, 1000x.

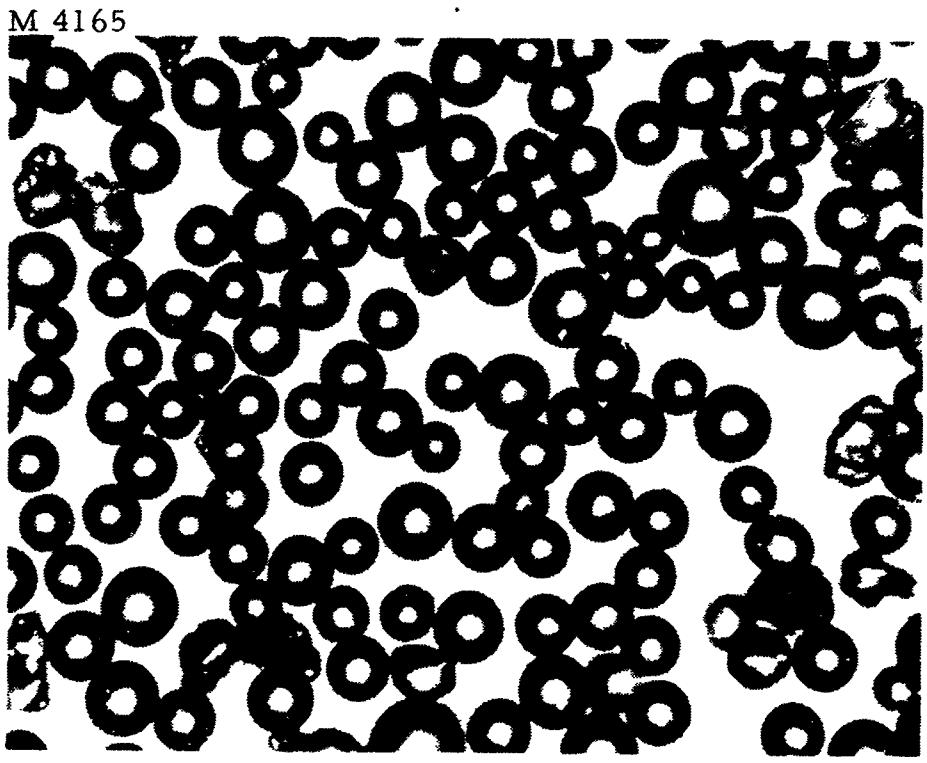


Fig. 22. 7.4 μ spherical tungsten powder, 1000x.

M 4166

Fig. 23. One-half inch diameter pellets machined by trepanning from a pressed-powder tungsten plate, with trepanning tool.

TABLE XVIII

Powder Distributions for Sintering Kinetics Studies

| Size, μ | Percent by Count | | | |
|---|---|---|---|---|
| 1.5 | 0.24 | | | |
| 2.0 | 0.96 | 0.66 | | |
| 2.5 | 23.34 | 1.80 | | |
| 3.0 | 46.20 | 11.93 | | |
| 3.5 | 22.38 | 30.59 | 0.55 | 0.09 |
| 4.0 | 6.14 | 26.99 | 3.31 | 0.37 |
| 4.5 | 0.24 | 15.81 | 7.59 | 0 |
| 5.0 | 0.48 | 8.14 | 24.55 | 0.37 |
| 5.5 | | 2.46 | 24.28 | 2.68 |
| 6.0 | | 1.04 | 20.96 | 7.86 |
| 6.5 | | 0.57 | 12.55 | 17.38 |
| 7.0 | | | 3.31 | 20.33 |
| 7.5 | | | 2.76 | 16.91 |
| 8.0 | | | 0.14 | 12.75 |
| 8.5 | | | | 9.52 |
| 9.0 | | | | 5.92 |
| 9.5 | | | | 3.60 |
| 10.0 | | | | 1.57 |
| 10.5 | | | | 0.09 |
| 11.0 | | | | 0.37 |
| 11.5 | | | | 0.18 |
| Mean Size, Microns | 3.06 | 3.92 | 5.39 | 7.41 |
| Standard Deviation | 0.46 | 0.71 | 0.80 | 1.08 |
| Number Counted | 831 | 1056 | 725 | 1082 |

TABLE XIX

Tap-Test Results for Spherical Tungsten Powder Used for Sintering Kinetics Studies

| Powder Size, μ | Tapped Density (% of Theoretical) | | | | |
|---|---|---|---|---|---|
| | 1 $cm^3$ [a] | 2 $cm^3$ | 3 $cm^3$ | 4 $cm^3$ | 5 $cm^3$ |
| 3.1 | 41.7 | 47.6 | 49.7 | 50.9 | 52.1 |
| 3.9 | 46.4 | 51.3 | 53.4 | 54.4 | 55.0 |
| 5.4 | 48.1 | 52.8 | 53.8 | 54.7 | 55.8 |
| 7.4 | 50.9 | 54.2 | 56.1 | 56.9 | 56.8 |

[a]Volume of powder after tapping. Cylinder used had 1.13 cm diameter.

TABLE XX

Fabrication of Pressed Tungsten Plates for Sintering Kinetics Specimens

| Powder Size, μ | Plate Number | Pressing Temperature, °C | Pressure, 1000 lb/in$^2$ | Total Number Specimens Machined |
|---|---|---|---|---|
| 3.06 | 191 | 190 | 80 | 16 |
| 3.92 | 342 | 180 | 75 | 29 |
| 5.39 | 318 | 165 | 75 | 16 |
| 7.41 | 341 | 170 | 50 | 21 |

Eighty-two pellets were trepanned from four pressed plates, and densities were computed from measurements of dimensions and weight. Although only 45 samples are required for kinetics runs, all 82 pellets were measured and weighed to permit a choice of specimens in each size range having the least variation in pressed density. Table XXI lists all densities obtained, showing those pieces chosen for kinetics runs.

For comparison, samples of each powder size were sintered to a density of 80% impregnated with copper, polished, and boiled out. Table XXII gives details of sintering runs for these samples. Note that enough pieces (15) were prepared for insertion of one 80% dense sample with each short-term and long-term temperature run. After boilout of copper (1600°C, 1 hour) from these pieces, an increase in density was noted (see Table XXII). This increase was about the same (0.4 to 0.5%) for all sizes except 3.1 μ (which was sensitive to the boilout time-temperature schedule). It was also found that each sample had experienced an equal diametral shrinkage. The inference drawn from these measurements is that the tungsten was actually densified due to contraction of the copper during cooling.

D. Equipment

Short-term vacuum heating runs are made in a Brew Corporation vacuum furnace. This unit is heated by resistance elements of tantalum sheet and is pumped by a 10 in. diffusion pump through a liquid nitrogen chevron trap. Operating vacuum at temperature is about $2 \times 10^{-6}$ Torr, and maximum temperature is 2450°C. Gettering action of tantalum shields improves vacuum in the heated zone beyond that registered by the ion gauge. The 7 in. hexagonal hot zone is 12 in. long and shielded to give black body conditions within most of the region (by test). Temperatures are measured optically through a shuttered window, with corrections made for window material.

Long-term vacuum heating will be conducted in four stainless steel bell jars, pumped by an 8 in. diffusion pump through a zeolite molecular sieve trap. Heating elements in each bell jar will consist

## TABLE XXI

### Density Data for Samples Measured in Preparation for Sintering Kinetics Tests

| 3.1 μ, Plate No. 191 | | 3.9 μ, Plate No. 342 | | 5.4 μ, Plate No. 306 | | 7.4 μ, Plate No. 341 | |
|---|---|---|---|---|---|---|---|
| Pressed Density, % of Theoretical | Pellet Number | Pressed Density, % of Theoretical | Pellet Number | Pressed Density, % of Theoretical | Pellet Number | Pressed Density, % of Theoretical | Pellet Number |
| 68.1 | 14 | 70.2 | 18 | 69.4 | 10 | 70.4 | 19 |
| 68.2 | 15 | 70.7[a] | 12 | 69.5 | 6 | 70.7 | 9 |
| 68.6 | 7 | 70.8 | 2 | 69.5 | 15 | 70.7 | 13 |
| 69.0 | 16 | 70.9 | 14 | 69.6 | 13 | 70.9 | 14 |
| 69.3 | 4 | 70.9 | 25 | 69.8 | 16 | 71.1[a] | 1 |
| 70.0[a] | 13 | 71.0 | 19 | 70.2 | 11 | 71.1[a] | 18 |
| 70.3[a] | 8 | 71.1 | 5 | 70.5[a] | 5 | 71.2[a] | 7 |
| 70.6[a] | 9 | 71.2 | 11 | 70.5[a] | 17 | 71.3[a] | 8 |
| 70.9[a] | 3 | 71.2 | 20 | 70.6[a] | 4 | 71.3[a] | 12 |
| 71.0[a] | 12 | 71.3 | 9 | 70.7[a] | 19 | 71.3[a, b] | 15 |
| 71.0[a] | 6 | 71.3 | 26 | 70.8[a] | 12 | 71.4[a] | 11 |
| 71.0[a] | 10 | 71.4[a] | 15 | 71.0[a] | 9 | 71.5[a] | 3 |
| 71.1[a] | 5 | 71.4 | 10 | 71.1[a] | 8 | 71.5[a] | 16 |
| 71.5[a] | 11 | 71.4 | 29 | 71.3[a] | 1 | 71.6[a] | 10 |
| 71.5[a] | 1 | 71.4 | 23 | 71.3[a] | 2 | 71.7[a, b] | 17 |
| 72.7 | 2 | 71.5 | 27 | 71.4[a] | 3 | 71.9[a] | 2 |
| | | 71.6[a] | 8 | 71.6[a] | 18 | 71.9[a] | 6 |
| | | 71.6 | 28 | 71.7[a] | 14 | 72.0[a] | 4 |
| | | 71.6[a] | 1 | 72.9[a] | 7 | 72.2 | 21 |
| | | 71.7[a] | 4 | | | 72.3 | 20 |
| | | 71.7[a] | 6 | | | 72.4 | 5 |
| | | 71.7[a] | 7 | | | | |
| | | 71.8[a] | 17 | | | | |
| | | 71.8[a] | 24 | | | | |
| | | 71.8[a] | 13 | | | | |
| | | 71.8[a] | 3 | | | | |
| | | 71.9[a] | 21 | | | | |
| | | 72.1 | 16 | | | | |
| | | 72.4 | 22 | | | | |

[a]Selected for sintering kinetics tests.

[b]Broken during permeability testing.

TABLE XXII

80% Dense Polished Specimens for Comparative Sintering Kinetics Studies

| Powder Size, μ | Pellet Number | Sintering Conditions | | Density, % of Theoretical | | |
|---|---|---|---|---|---|---|
| | | Temperature, °C | Time, Hour | Pressed | Sintered | After Boilout[a] |
| 3.1 | 191-3 | 1600 | 6 | 70.9 | 79.7 | 81.1 |
| 3.1 | 191-5 | 1600 | 6 | 71.1 | 80.0 | 81.0 |
| 3.1 | 191-6 | 1600 | 6 | 71.0 | 80.0 | 81.7 |
| 3.9 | 342-4 | 1800 | 1.5 | 71.7 | 80.7 | 81.2 |
| 3.9 | 342-6 | 1800 | 1.5 | 71.7 | 80.7 | 81.2 |
| 3.9 | 342-7 | 1800 | 1.5 | 71.7 | 80.7 | 81.1 |
| 3.9 | 342-8 | 1800 | 1.5 | 71.6 | 80.7 | 81.1 |
| 5.4 | 306-1 | 1800 | 3.5 | 71.3 | 80.4 | 80.9 |
| 5.4 | 306-2 | 1800 | 3.5 | 71.3 | 80.5 | 80.6 |
| 5.4 | 306-3 | 1800 | 3.5 | 71.4 | 80.4 | 80.8 |
| 5.4 | 306-8 | 1800 | 3.5 | 71.1 | 80.2 | 80.6 |
| 7.4 | 341-3 | 2000 | 2 | 71.5 | 80.6 | 81.4 |
| 7.4 | 341-7 | 2000 | 2 | 71.2 | 80.6 | 81.0 |
| 7.4 | 341-8 | 2000 | 2 | 71.3 | 80.6 | 81.1 |
| 7.4 | 341-10 | 2000 | 2 | 71.6 | 81.0 | 81.2 |

[a]Boilout - 1 hour at 1600°C.

of a heavy tungsten coil of 1/8 in. rod wound into a 1 in. o.d. helix, inside of which the sample pellets will be supported on an alumina plate (Fig. 24). This assembly, with radiation shields, will be sealed into a bell jar, and the temperature monitored both optically and by thermocouple. Power for each heater will come from a current transformer fed from an autotransformer. Line voltage variations will be compensated for by a three-phase powerstat controlled by a regulating positioner. The power circuit is shown in Fig. 25. Each heavy coil is designed to support eight pellets, 1/8 in. thick and 1/2 in. in diameter. Two of these pellets, one at each end, will serve as radiation baffles for temperature uniformity (in the absence of end heaters). The remaining six pellets will be test specimens. Timers will indicate time at temperature.

## E. Initial Kinetics Runs

A total of 40 pellets were sintered in 19 separate runs* of three pellets each (one starting at 81%, two as-pressed). Sintering times of 2 to 180 hours were used at temperatures of 1200 to 2000°C. Density results are listed in Table XXIII.

These initial sintering runs show some interesting trends. Initial densification of pressed specimens is greater for specimens starting at lower densities, while later sintering steps result in approximately equivalent changes. At 1600°C, the densification of 5.4 and 7.4 μ pellets after 60 hours indicates that the limiting value of 87% density will be reached before 360 hours, with discontinuance of the long-term tests for these materials.

*All runs were made in the Brew furnace. The long term tests will be completed in the special equipment being prepared for that purpose.

M 4675

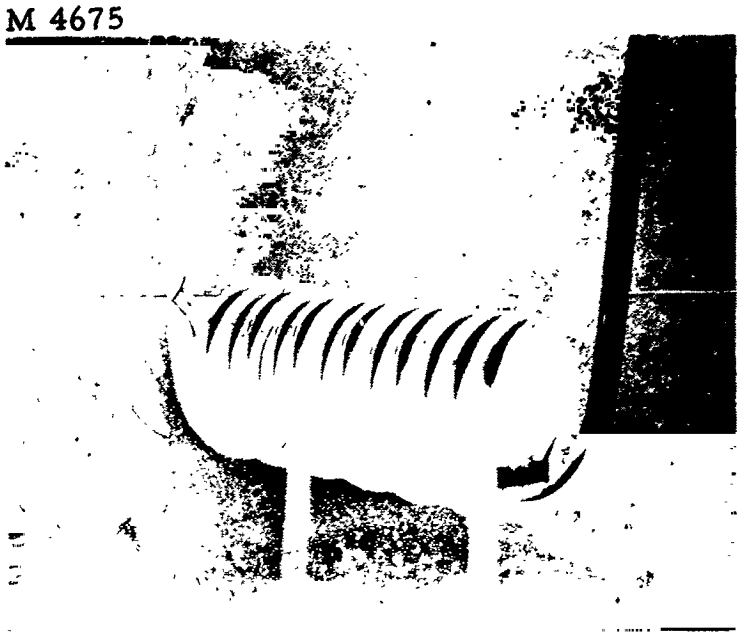

Fig. 24. Heating arrangement for long term vacuum sintering of tungsten pellets.

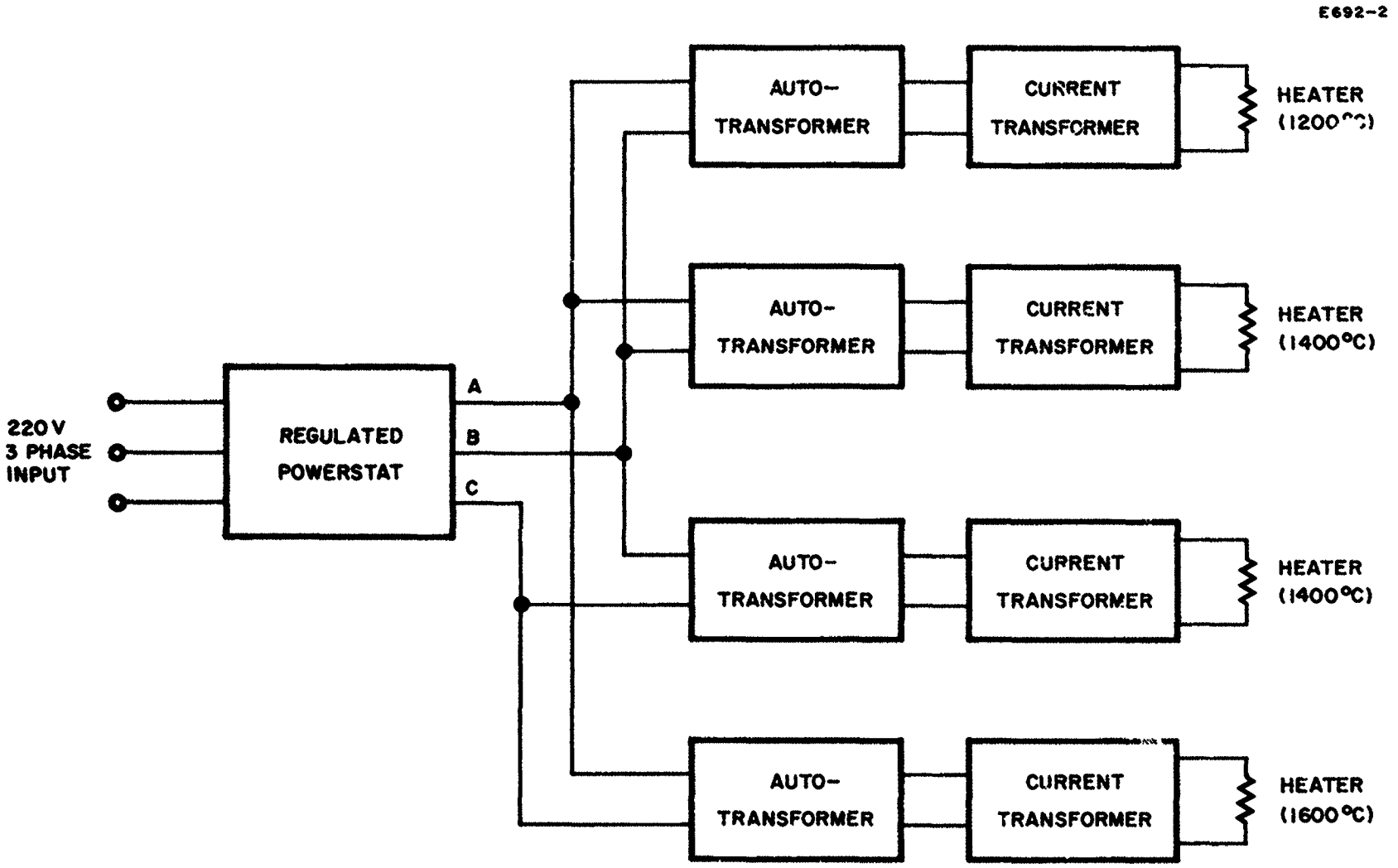


Fig. 25. Heater circuits for long term sintering kinetics studies.

## TABLE XXIII

### Results of Sintering Kinetics Runs

| Powder Size, μ | Pellet Number | Density, % of Theoretical | | | | | | | | |
|---|---|---|---|---|---|---|---|---|---|---|
| | | Initial | After Sintering Run | | | | | | | |
| | | | 1200°C | 1400°C | | | 1600°C | | 1800°C | 2000°C |
| | | | 120 hours | 60 hours | 120 hours | 180 hours | 2 hours | 60 hours | 2 hours | 2 hours |
| 3.1 | 191-3 | 81.1 | 81.5 | | | | | | | |
| | -1 | 71.5 | 72.2 | | | | | | | |
| | -8 | 70.3 | 71.1 | | | | | | | |
| | -5 | 81.0 | | 84.4 | 86.0 | 87.4 | | | | |
| | -9 | 70.6 | | 77.3 | 80.9 | 85.0 | | | | |
| | -11 | 71.5 | | 77.9 | 81.3 | 83.4 | | | | |
| | -13 | 70.0 | | 77.5 | 81.1 | | | | | |
| | -6 | 81.7 | | | | | 82.7 | | | |
| | -10 | 71.0 | | | | | 76.3 | | | |
| | -12 | 71.0 | | | | | 76.4 | | | |
| 3.9 | 342-4 | 81.2 | 81.1 | | | | | | | |
| | -1 | 71.6 | 71.9 | | | | | | | |
| | -3 | 71.8 | 72.0 | | | | | | | |
| | -6 | 81.2 | | 82.2 | 82.7 | 83.2 | | | | |
| | -12 | 70.7 | | 74.5 | 75.9 | 77.3 | | | | |
| | -13 | 71.8 | | 75.2 | 76.8 | 78.2 | | | | |
| | -7 | 81.1 | | | | | 81.7 | | | |
| | -15 | 71.4 | | | | | 74.1 | | | |
| | -17 | 71.8 | | | | | 74.4 | | | |
| | -8 | 81.1 | | | | | | | 84.5 | |
| | -21 | 71.9 | | | | | | | 81.1 | |
| | -24 | 71.8 | | | | | | | 81.0 | |
| 5.4 | 306-1 | 80.9 | | 81.6 | | | | | | |
| | -4 | 70.6 | | 73.8 | | | | | | |
| | -5 | 70.5 | | 73.9 | | | | | | |
| | -3 | 80.8 | | | | | | 86.7 | | |
| | -9 | 71.0 | | | | | | 85.0 | | |
| | -12 | 70.8 | | | | | | 84.8 | | |
| 7.4 | 341-3 | 81.4 | | 81.7 | 81.8 | 82.1 | | | | |
| | -2 | 71.9 | | 73.6 | 74.6 | 75.6 | | | | |
| | -11 | 71.4 | | 73.2 | 74.3 | 75.2 | | | | |
| | -7 | 81.0 | | | | | | 84.5 | | |
| | -4 | 72.0 | | | | | | 81.9 | | |
| | -12 | 71.3 | | | | | | 81.0 | | |
| | -8 | 81.1 | | | | | | | 81.6 | |
| | -1 | 71.1 | | | | | | | 75.1 | |
| | -6 | 71.9 | | | | | | | 76.0 | |
| | -10 | 81.7 | | | | | | | | 83.7 |
| | -16 | 71.5 | | | | | | | | 79.7 |
| | -18 | 71.1 | | | | | | | | 79.4 |

## F. Permeability Testing

Permeability of pellets was measured as throughput of nitrogen gas per unit area at a fixed pressure. The flat cylindrical pellet was sealed at the edges as shown in Fig. 26 and nitrogen was passed through at a constant pressure. Flow was measured on the high-pressure side of the pellet with a calibrated rotameter, and pressure was measured with an open-tube mercury manometer, as in Fig. 27(a).

Several problems were encountered during nitrogen transmission testing. A "hysteresis" was found; values of permeability measured upon increasing pressure were different from those measured upon decreasing pressure. The special low-flow rotameter tube was found to have a discontinuous flow response with pressure at 3 in. of mercury. Readings were not reproducible. The most important finding was that $K_p$, the permeability constant in Darcy's law (flow = $K_p \frac{\Delta PA}{\ell}$), was <u>not</u> constant with a change in pressure. Figure 27(b) shows the calibration apparatus used to test the original setup.

Each apparatus problem was solved in turn. The "discontinuous" rotameter tube was returned for replacement with a new one. Flow measurements were taken "downstream" from the pellet (on the low pressure side), thus avoiding inaccurate mathematical flow-corrections (rotameters were precalibrated at atmospheric pressure). The low pressure flow measurement also lessened the probability of leaks in the apparatus. The mercury manometer was replaced with an accurate and precise Kollsman pressure gauge. Finally, a calibrated "bubble" was used for measuring flow in collaboration with a timer, with the rotameter serving only as an approximate indicator. The "bubbler," made in Hughes' glass shop, consists of three glass tubes in series, with the diameter of each tube larger than the previous one (see Fig. 27(b) ). Each section of the "bubbler" was precalibrated by filling with water, weighing and marking, so that gas volumes of 1 $cm^3$, 10 $cm^3$, and 100 $cm^3$ were marked accurately. The top was open and a flexible soap-filled bulb at the bottom was squeezed to form a bubble above the

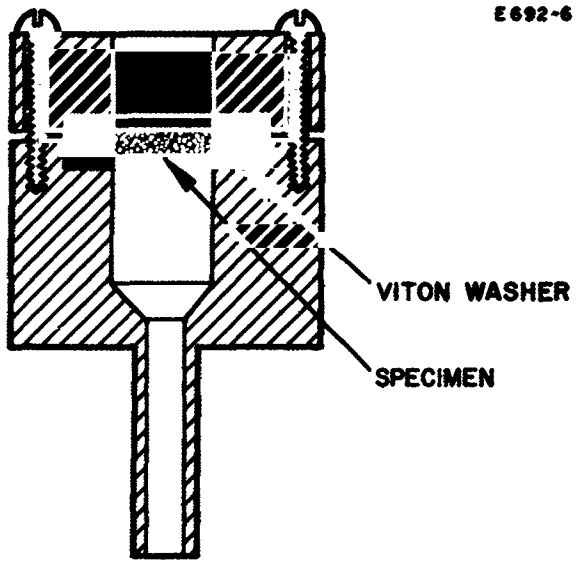


(a) SPECIMEN HOLDER USED FOR CHECKING PERMEABILITY UPSTREAM

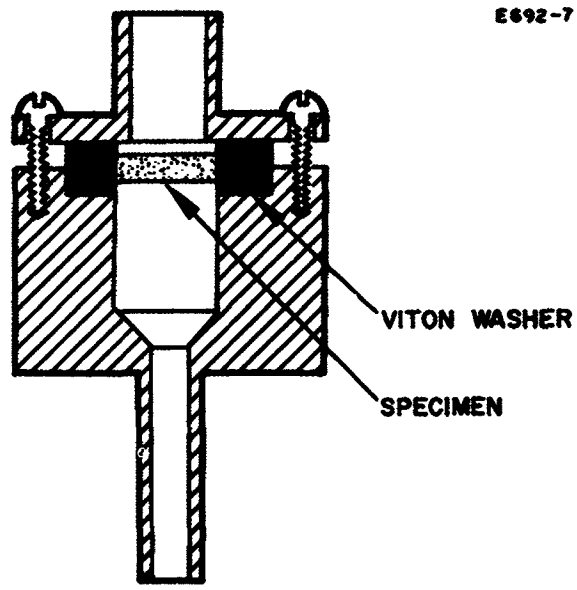


(b) SPECIMEN HOLDER MODIFIED FOR CHECKING PERMEABILITY DOWNSTREAM

Fig. 26. Specimen holders used during permeability testing.

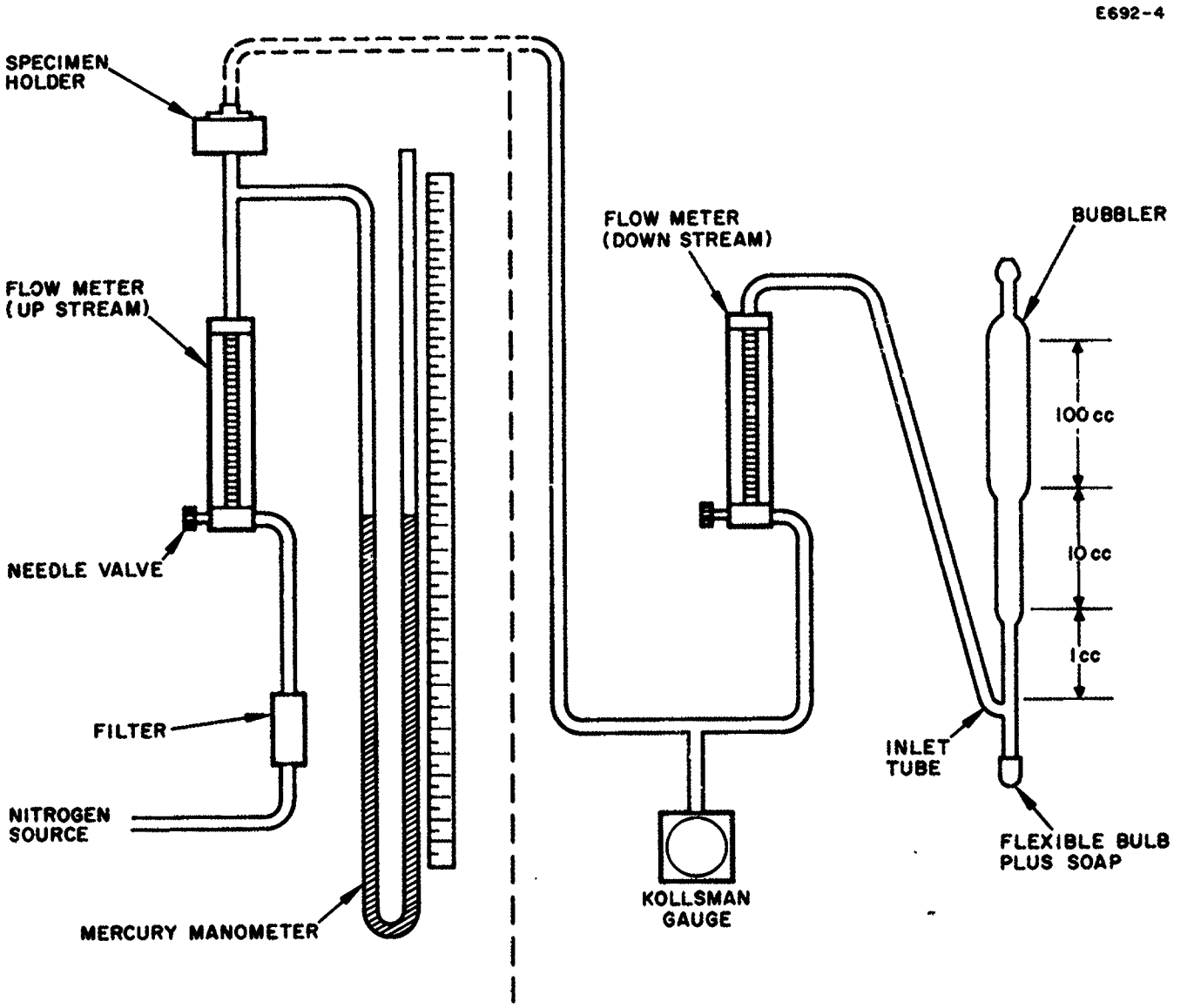


(a) Permeability testing apparatus with flowmeter on high pressureside of specimen.

(b) Flowmeter and bubbler used for calibration tests of original apparatus.

Fig. 27. Testing apparatus.

inlet tube (see Fig. 27(b) ). Incoming nitrogen flow raised the bubble, volume was measured versus time in each chamber, and an accurate measure of flow was obtained with virtually no back pressure (only that of the bubble). With this method of flow and pressure measurement, completely reproducible permeability values have been obtained over wide pressure ranges. The new apparatus (Fig. 28) can be used for testing two pellets at a time, and incorporates a pressure "reservoir" to reduce pressure differences due to rate of gas flow. An improved specimen holder (Fig. 29) provides a more positive seal and greater ease of specimen insertion.

The permeability constant $K_p$ from Darcy's law was still not constant with pressure, but varied in a regular fashion as pressure was increased or decreased. Reference to the literature* reveals why this is so. Gas flow through a porous body varies from molecular flow through a porous body at low pressures ($\approx 1$ Torr) to a mixture of laminar and turbulent flow at higher pressures (150 Torr). Darcy's law, in its simplest form (flow = $K_p \frac{\Delta PA}{\ell}$) assumes only laminar flow. The mixture of laminar and turbulent flow gives a varying $K_p$, approximating a second order equation. If five or more flow measurements are taken for each specimen, a least-squares data fit can give close values for $K_p$ for the several terms of the equation. The additional readings and computations (approximately 1100) are judged unnecessary, since only comparative permeabilities are meaningful. This is so because extrapolation of the curve to the region of operation ($\approx 10^{-2}$ Torr) using

*Theory and Applications of Controlled Permeability, by E. M. Cliffel, Jr., W. E. Smith, and A. D. Schwope, Clevite Corp., 1965 International Powder Metallurgy Conference.

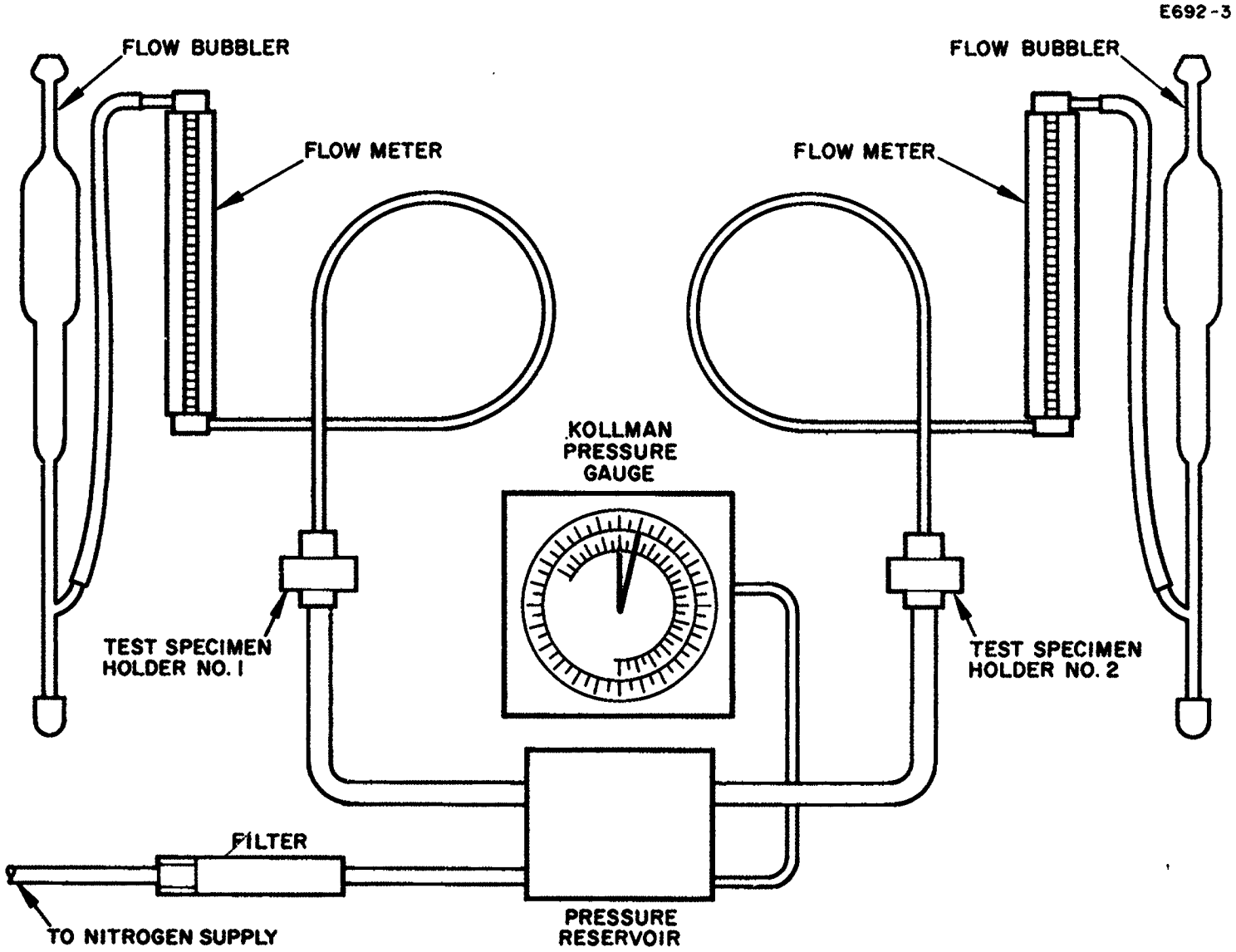


Fig. 28. Final permeability testing apparatus, with dual setups, flowmeters, and bubblers on low-pressure side of sample, and accurate pressure gauge.

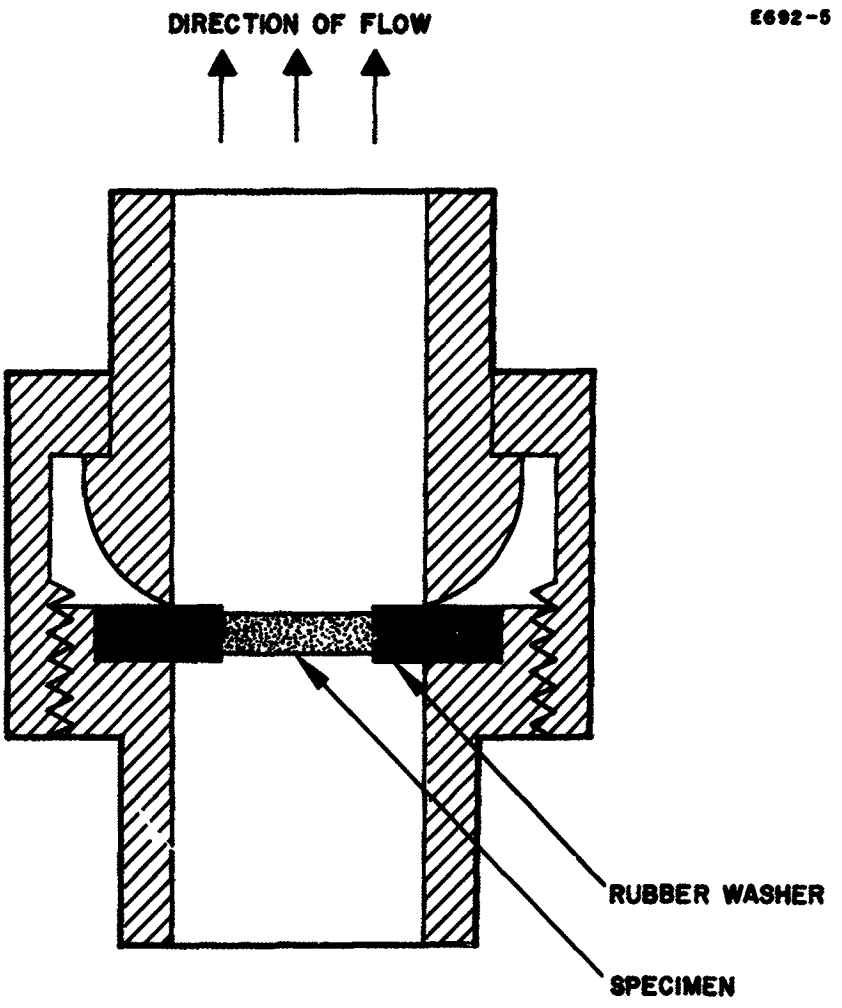


Fig. 29. Specimen holder used for permeability testing in improved, final apparatus of Fig. 28.

cesium ions in a mixture of molecular and laminar flow instead of nitrogen gas would be inaccurate. Therefore, future permeability measurements will be taken at a single, low pressure suitable for comparison between pellets of largest and smallest powders, at highest and lowest densities. Occasional five-point curves will be measured and computed to determine variations in shape of the curve with changing density and particle size.

While permeability measurements were made (originally) on all specimens before and after sintering, these were completely inaccurate, and will not be listed here. All measurements will be re-run in the future, using duplicate pressed specimens where samples have already been sintered, and curves of permeability versus density and particle size will be obtained.

BLANK PAGE

## VI. SUMMARY OF WORK DONE

During this contract effort, iridium was spheroidized, classified, pressed, sintered, impregnated, machined, polished, boiled out, and welded for complete fabrication into a porous ionizer. The difficult problems associated with preparing the surface by cathodic etching and welding to molybdenum using a rhenium interface material were solved in a way suitable for applying in reproducible fabricating procedures.

Porous pellets of pre-alloyed powder of 25 Re-75W were fabricated following the same nine steps. Problems were different, arising in pressing and from nonhomogeneity of powder alloying, but problems were either solved or detailed for possible solution.

Pre-alloyed 5 Re-95W and 50 Ir-50W were also fully investigated with respect to fabrication of porous ionizers, and also presented pressing problems.

Mixtures of alloy element powders were formed successfully from 2 Ir-98W, 4 Ir-96W, 50 Ir-50W, and 23 Re-77W. Most of these mixtures were sintered to high densities above 90% and delivered to NASA. The 50 Ir-50W mixture exhibited marked resistance to densification, and gave a possibility of highly stable material for fine-pored structures.

Solid tungsten was prepared in a 5/8 in. diameter by 5/8 in. long cylinder by warm-pressing techniques in a special die, then sintered to 94% of theoretical density, machined, and delivered to NASA.

The above pellets are pictured in Fig. 30. Note that there were 93 pellets plus 10 weld tests. Sintering kinetics specimens are not included in the photograph.

Table XXIV lists all of the alloy compacts, together with fabrication history.

Photomicrographs at 1000x are shown of mixture alloys 2 Ir-98W (Fig. 31), 4 Ir-96W (Fig. 32), and 50 Ir-50W (Fig. 33). Note microhardness indentations and values.

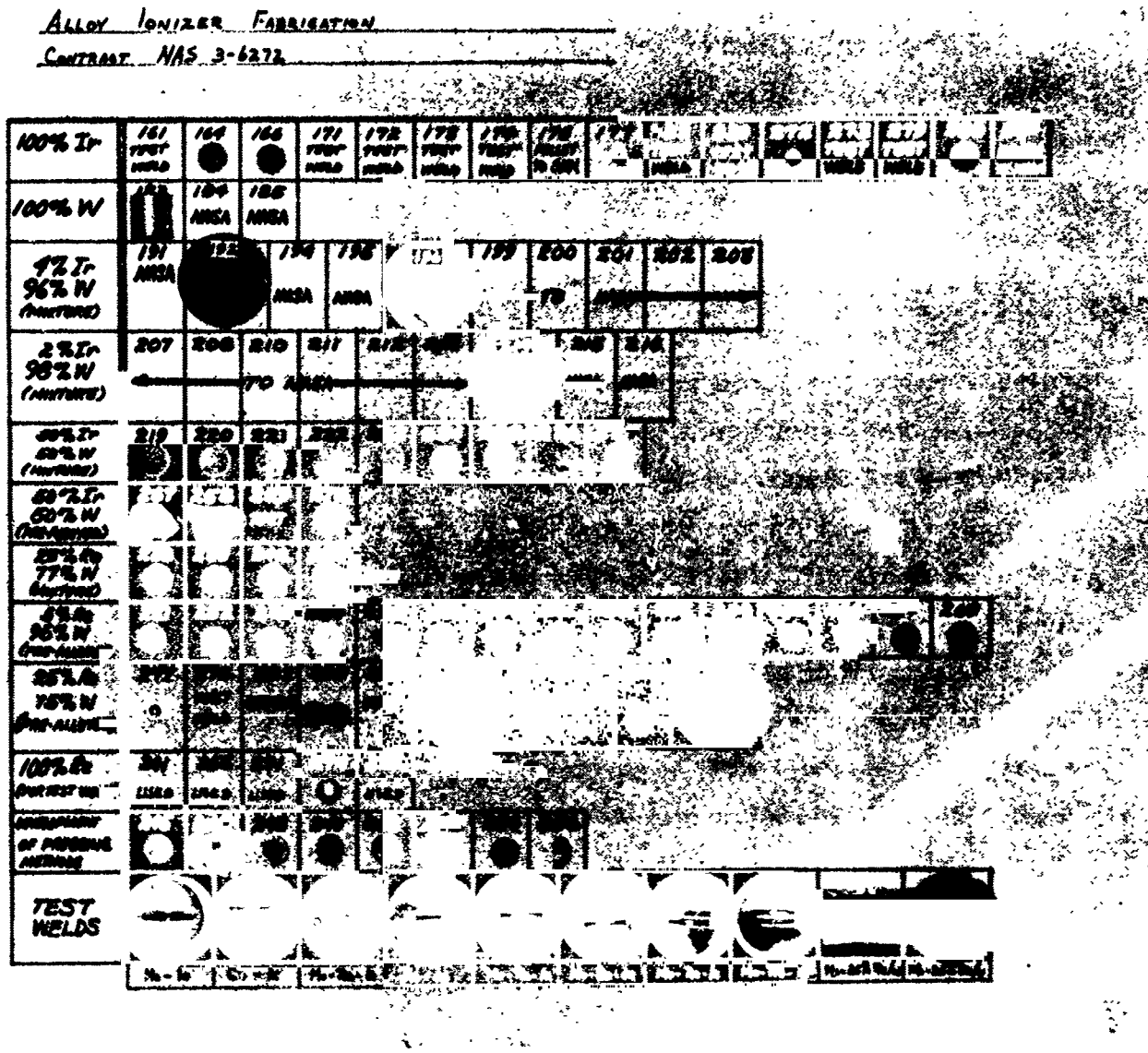


Fig. 30. Pellets fabricated under contract effort.

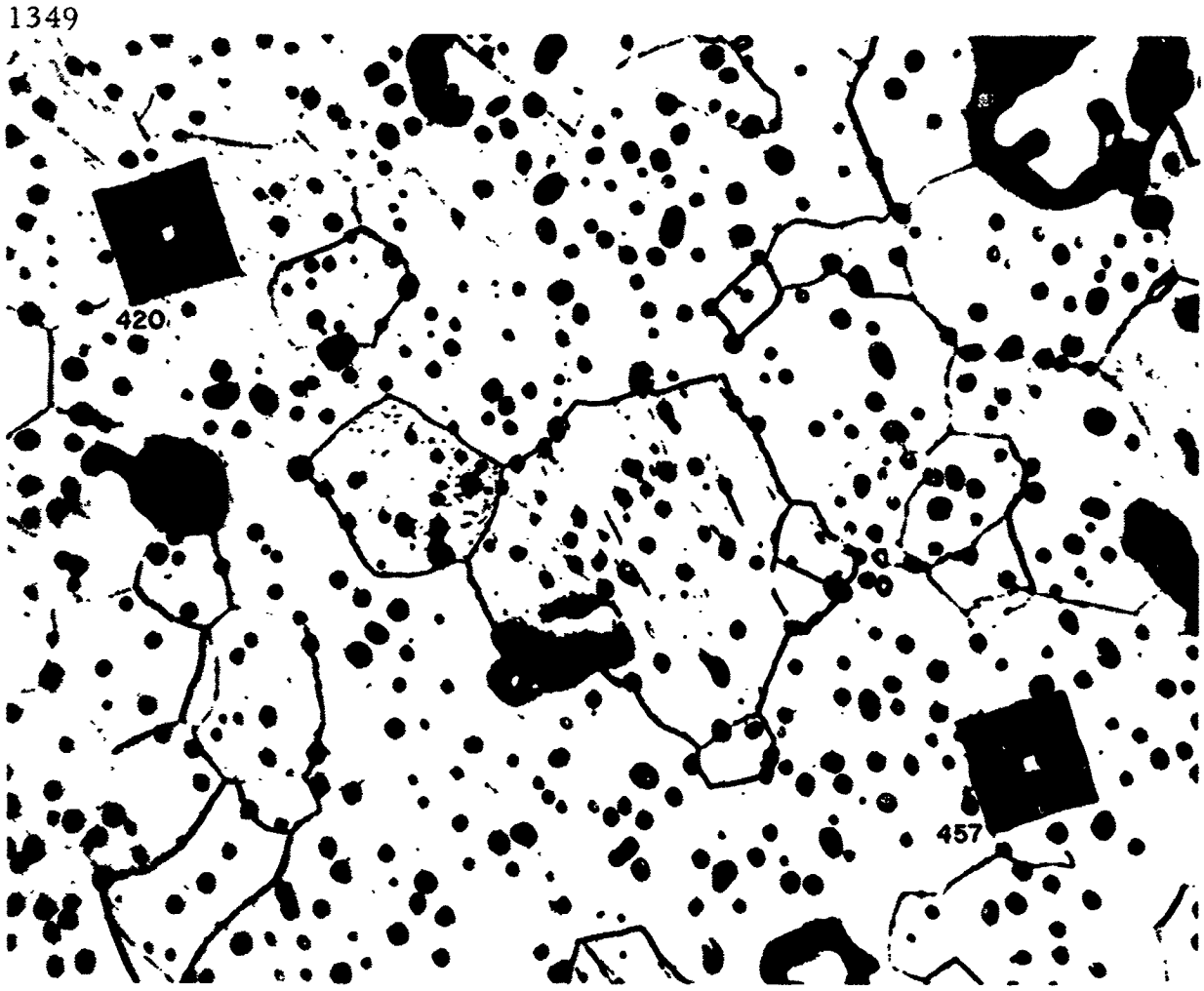


Fig. 31. Pellet No. 214; 92.1% dense, 396 to 468 VPH; 98 W-2 Ir; 1000x.

1348

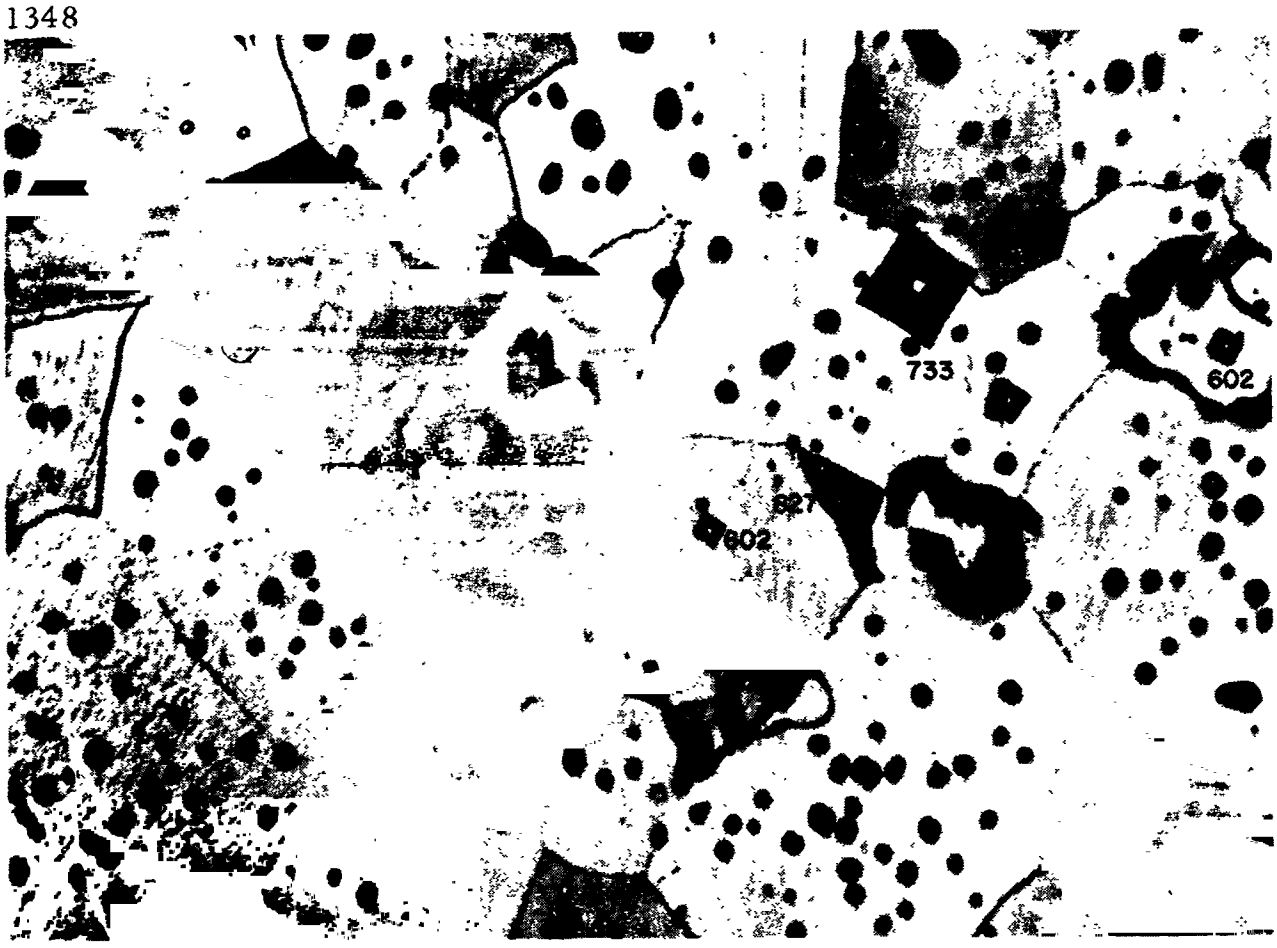


Fig. 32. Pellet No. 192; 91.3% dense, 501 to 748 VPH; 96W-4 Ir; 1000x.

1350

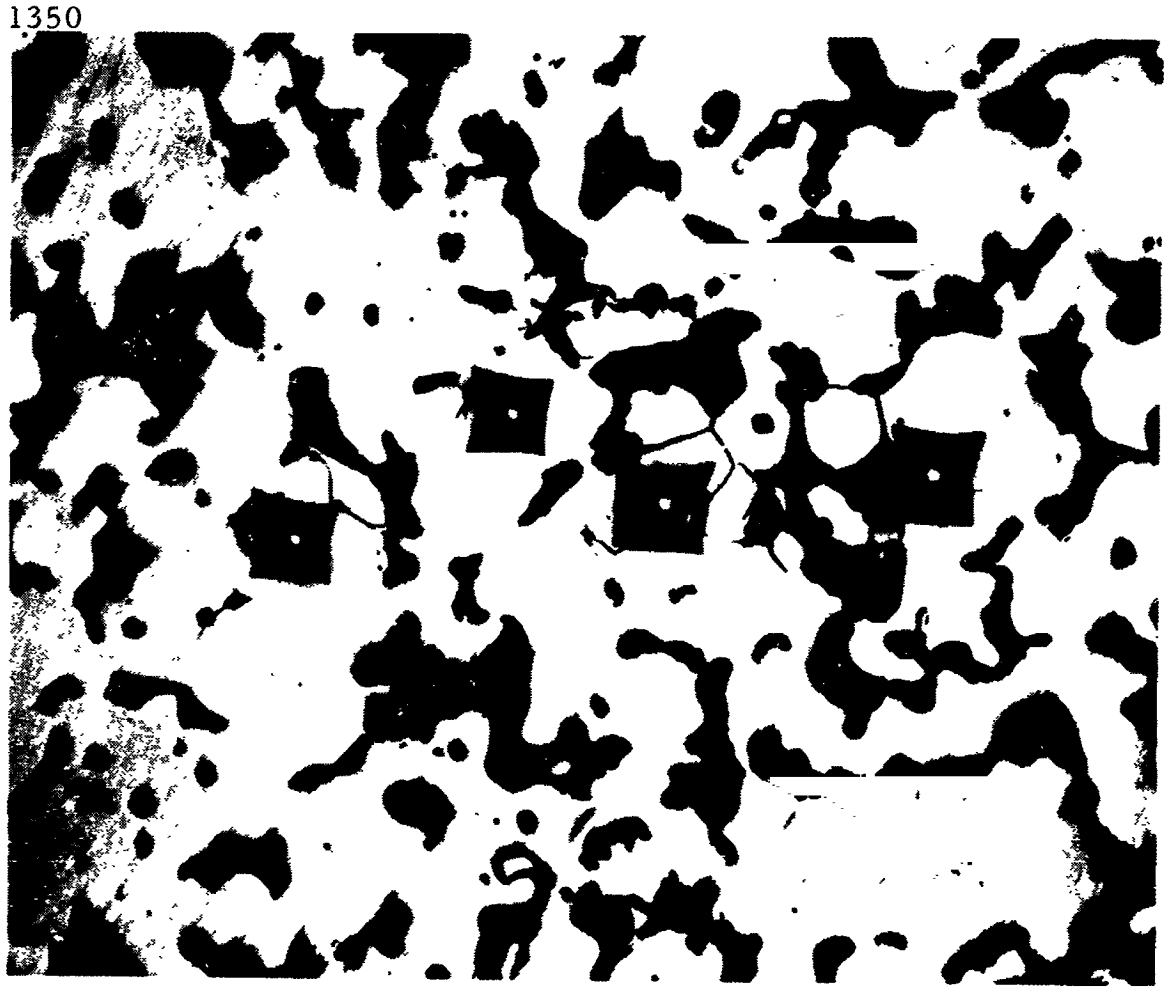

Fig. 33. Pellet No. 226; 70.9% dense, 753 to 802 VPH; 50 Ir-50 W; 1000x.

# TABLE XXIV

## Summary of Pellet Pressing and Sintering

| Pellet No. | Material | Powder Size, μ | PRESSING DATA | | | | | SINTERING DATA | | | REMARKS |
|---|---|---|---|---|---|---|---|---|---|---|---|
| | | | Pressure psi x $10^{-3}$ | Temp., °C | Ejection Temp., °C | Density, % of Theor. | Remarks | Temp., °C | Time, Minutes | Density, % of Theor. | |
| 161 | Iridium, spherical | 10-11 | 75 | 400 | Rm.Temp. | 78.4 | Good | 1500 | 60 | 77.4 | Weld test |
| 164 | " " | 6-9 | " | " | " | 75.6 | Good. Powder contaminated with phosphor | | | | |
| 166 | " " | 6-9 | " | " | " | 76.5 | Good. Powder contaminated with phosphor | | | | |
| 171 | " " | 6-9 | " | " | " | 74.6 | Good | 1630 | 90 | 78.6 | Silver filled. Weld test |
| 172 | " " | 3.7 | " | " | " | 75.3 | " | 1630 | 60 | 83.1 | Silver filled. Weld test |
| 173 | " " | 5.0 | " | " | " | 74.0 | " | 1700 | 60 | 84.6 | Silver filled. |
| 174 | " " | 3.7 | " | " | " | 74.3 | " | 1700 | 60 | 86.6 | |
| 175 | " " | 5.0 | " | " | " | 74.6 | " | 1600 | 60 | 81.9 | To ion test 12-3-64 |
| 177 | " " | 5.0 | " | " | " | 74.6 | " | 1600 | 60 | 81.4 | Machined pellet |
| 182 | " " | 6-9 | 100 | 500 | " | 81.5 | " | 1700 | 60 | 84.0 | Weld test |
| 183 | Tungsten, spherical | 3+6 | | | | 69.7 | 3/4" dia. x 7/8" long | 2200 | 180 | | |
| | | | | | | | | 2400 | 120 | 93.9 | |
| 184 | " " | 3+6 | | | | 69.8 | " " | 2200 | 180 | | |
| | | | | | | | | 2400 | 120 | 94.1 | To NASA 1-4-65 |
| 185 | " " | 3+6 | | | | 69.6 | " " | 2200 | 180 | | |
| | | | | | | | | 2400 | 120 | 93.9 | " " " |
| 191 | 4% Ir-96%W mixture | | 80 | 170 | " | 73.0 | Good | 2400 | 240 | 90.9 | " " 2-19-65 |
| 192 | " " " | | 90 | 160 | " | 74.2 | Laminations (no back pressure) | " | " | 91.3 | Metallographic examination |
| 194 | " " " | | " | " | " | 75.5 | Good | 2200 | 360 | 91.5 | To NASA 2-19-65 |
| 195 | " " " | | 100 | 400 | " | 79.2 | " | " | " | 91.4 | " " " |
| 196 | " " " | | " | " | " | — | Broken | | | | |
| 199 | " " " | | " | " | " | 79.5 | Good | " | " | 91.3 | " " " |
| 200 | " " " | | " | " | " | 79.6 | " | " | " | 91.4 | " " " |
| 201 | " " " | | " | " | " | 79.5 | " | " | " | 91.4 | " " " |
| 202 | " " " | | " | " | " | 79.4 | " | " | " | 91.6 | " " " |
| 203 | " " " | | " | " | " | 80.0 | " | " | " | 91.1 | " " " |

## TABLE XXIV (Cont'd)

| Pellet No. | Material | Powder Size, μ | PRESSING DATA | | | | | SINTERING DATA | | | REMARKS |
|---|---|---|---|---|---|---|---|---|---|---|---|
| | | | Pressure psi x $10^{-3}$ | Temp., °C | Ejection Temp., °C | Density, % of Theor. | Remarks | Temp., °C | Time, Minutes | Density, % of Theor. | |
| 207 | 2% Ir-98%W mixture | | 100 | 400 | Rm. Temp. | 77.4 | Good | 2200 | 360 | 91.2 | To NASA 2-19-65 |
| 208 | " " " | | " | " | " | 76.2 | " | " | " | 90.9 | " " " |
| 210 | " " " | | " | " | " | 76.0 | " | " | " | 90.7 | " " " |
| 211 | " " " | | " | " | " | 80.4 | " | " | " | 91.0 | " " " |
| 212 | " " " | | " | " | " | 79.5 | " | " | " | 91.8 | " " " |
| 213 | " " " | | " | " | " | 79.5 | " | " | " | 91.8 | " " " |
| 214 | " " " | | " | " | " | 79.4 | " | " | " | 91.8 | " " " |
| 215 | " " " | | " | " | " | 79.8 | " | " | " | 91.2 | " " " |
| 216 | " " " | | " | " | " | 79.4 | " | " | " | 91.8 | " " " |
| 219 | 50% Ir-50%W mixture | | " | " | " | 78.7 | " | " | " | 71.0 | Low density; resists sintering |
| 220 | " " " | | " | " | " | 78.6 | " | " | " | 71.2 | " " |
| 221 | " " " | | " | " | " | 77.8 | " | " | " | 70.9 | " " |
| 222 | " " " | | " | " | " | 78.0 | " | " | " | 70.9 | " " |
| 223 | " " " | | " | " | " | 78.6 | " | " | " | 71.0 | " " |
| 224 | " " " | | " | " | " | 77.8 | " | " | " | 70.9 | " " |
| 225 | " " " | | " | " | " | 78.6 | " | " | " | 70.9 | " " |
| 226 | " " " | | " | " | " | 78.1 | " | " | " | 70.9 | " " |
| 227 | " " " | | " | " | " | 77.9 | " | " | " | 70.7 | Density was 84.2% after 36 hrs at 2200°C |
| 238 | 23% Re-77% W mixture | | 75 | 400 | " | 67.9 | " | | | | |
| 239 | " " " | | " | " | " | 68.5 | " | | | | |
| 242 | " " " | | 85 | " | " | 70.9 | " | | | | |
| 243 | " " " | | " | " | " | 70.8 | " | | | | |
| 231 | 5% Re-95% W pre-alloyed* | | 75 | " | " | 70.8 | Looked Good | 1700 | 480 | 83.7 | Cracked |
| 232 | " " " | | " | " | " | 72.1 | " " | " | " | 84.3 | " |
| 233 | " " " | | " | " | " | 72.4 | " " | " | " | 85.4 | " |
| 234 | " " " | | " | " | " | 72.8 | " " | " | " | 85.1 | " |
| 235 | " " " | | " | " | " | 72.8 | " " | " | " | 84.5 | " |

# TABLE XXIV (Cont'd)

| Pellet No. | Material | Powder Size, μ | PRESSING DATA | | | | | SINTERING DATA | | | REMARKS |
|---|---|---|---|---|---|---|---|---|---|---|---|
| | | | Pressure psi x $10^{-3}$ | Temp., °c | Ejection Temp., °C | Density, % of Theor. | Remarks | Temp., °C | Time, Minutes | Density, % of Theor. | |
| 236 | 5% Re-95%W pre-alloyed* | | 75 | 400 | Rm. Temp. | 71.7 | Looked Good | 1700 | 480 | 84.3 | Cracked |
| 237 | " " " | | " | " | " | 72.0 | " " | " | " | 79.5 | " |
| 261 | " " " | | " | " | <100 | 73.0 | " " | 1600 | 240 | 77.6 | Possible Cracks |
| 262 | " " " | | " | " | " | 73.3 | " " | " | " | 78.1 | Cracked |
| 263 | " " " | | " | " | 25 | — | Laminated, crumbled | | | | |
| 264 | " " " | | 60 | 200 | " | — | " " | | | | |
| 265 | " " " | | 75 | 400 | 200 | 69.3 | Cracked | | | | |
| 266 | " " " | | " | " | | 71.3 | " | | | | |
| 267 | " " " | | " | " | | 72.9 | Looked Good | 1600 | 480 | 78.7 | Slight lamination crack |
| 269 | " | | " | 500 | 250 | 72.8 | " " | " | " | 78.5 | " " " |
| 257 | 50% Ir-50%W pre-alloyed* | | " | " | 200 | — | Crumbled, powdery | | | | |
| 258 | " " " | | 90 | 400 | " | — | Severe laminations | | | | |
| 259 | " " " | | 50 | 700 | Rm. Temp. | — | Powdery, laminated | | | | |
| 277 | 25% Rc-75%W pre-alloyed* | 2-3 | " | 400 | 250 | Low | Powdery sides | 1800 | 120 | | Poor ends, not measurable, cracked |
| 278 | " " " | " | 65 | 300 | 300 | 59.1 | " " | 2000 | 240 | 82.2 | |
| 282 | " " " | 4-5 | 75 | " | " | Low | Powdery | | | | |
| 285 | " " " | 2-3 | 85 | 400 | 200 | 61.0 | Powdery, broke | 1800 | 120 | | Broken (pressing) |
| 286 | " " " | " | 75 | 700 | " | 58.2 | Powdery. Stuck to plungers. No cracks | 2000 | 240 | 80.9 | |
| 287 | " " " | " | " | 400 | " | — | Washed powder. Not powdery. Laminated | | | | |
| 288 | " " " | " | " | " | " | — | Looked Good | 2000 | | ≈ 85 | Laminated |
| 289 | " " " | " | " | " | " | — | Looked Good Powdery | 1800 | 60 | 75.0 | 3.8 x $10^6$ pores/$cm^2$. Pellet to ion test. |
| 291 | " " " | 4-5 | " | " | " | — | Laminated. Mounted as pressed (W + Cu) | | | | |

*Supplied by NASA

Notes: Each pressing requires 1/2 day
Each sintering run requires one day

Sintering kinetics of four sizes of spherical tungsten powder was initiated, with samples prepared from 3.1, 3.9, 5.4, and 7.4 μ powder. Runs were made at 1200, 1400, 1600, 1800, and 2000°C, for various times from 2 hours to 180 hours. Densities and permeabilities were measured, but permeability measurements were found to be inaccurate. Nitrogen transmission test equipment was modified and calibrated, and a system for measuring comparative permeability constants was set up.

## VII. RECOMMENDATIONS FOR FUTURE WORK

The following recommendations are submitted for future work:

- Continue the kinetics of sintering of both tungsten and the highly stable 50 Ir-50W mixture.
- Examine the feasibility of coating a porous tungsten substrate with pre-alloyed powders rather than trying to press entire ionizers of these expensive materials.
- Try to obtain an isotropic surface of tungsten with a high work function plane (110) available for ionization by etching, deposition, or deformation techniques.
- Seek sources for pre-alloyed powders of rhenium-tungsten of good homoegneity and small particle size.

PRECEDING PAGE BLANK NOT FILMED.

# PART 2

# ENGINE MATERIALS STUDIES

PRECEDING PAGE BLANK NOT FILMED.

BLANK PAGE

# I. INTRODUCTION

The primary objective of this part of the alloy ionizer fabrication study has been the development of porous coatings of metals or alloys which have higher vacuum work functions than pure porous tungsten. These coatings for tungsten ionizers must be stable for thousands of hours in vacuum at 1200 to 1300°C in the presence of cesium vapor. The coating must also cause negligible impedance to flow of cesium vapor through the ionizer.

The advantage of having an ionizer surface with a work function higher than that of pure tungsten lies in the fact that the higher work function ionizer will emit fewer neutral cesium atoms compared with the cesium ions which it can produce, i.e., it has a lower neutral fraction than pure tungsten. The ultimate long term life of any well designed ionizer optical system depends to a large extent upon having a low neutral fraction. Neutral cesium atoms drifting through a focused beam of positive ions will be ionized by charge exchange with the high energy cesium ions. These secondary ions are essentially unfocused and so will be accelerated toward the negative accel electrodes. The resulting sputtering away of electrode material could eventually lead to engine failure.

Figure 34 shows the neutral efflux fraction from various metals as a function of vacuum work function.* From this it can be seen that rhenium and iridium surfaces will have neutral fractions which are less than 1% of that of pure tungsten. This reduction in neutral fraction can increase engine life, as limited by the accel electrode life, by a factor of 20 to 100 times.

There is an advantage in improving the contact ionization efficiency of porous tungsten by the coating approach. The techniques for making fine pore, uniform porosity tungsten are now well developed and dependable. In addition, large ionizers can be fabricated by special electron beam welding techniques which have been recently developed.

*O. K. Husmann, Bull. Am. Phys. Soc. 10, 740 (1965).



PRECEDING PAGE BLANK NOT FILMED.

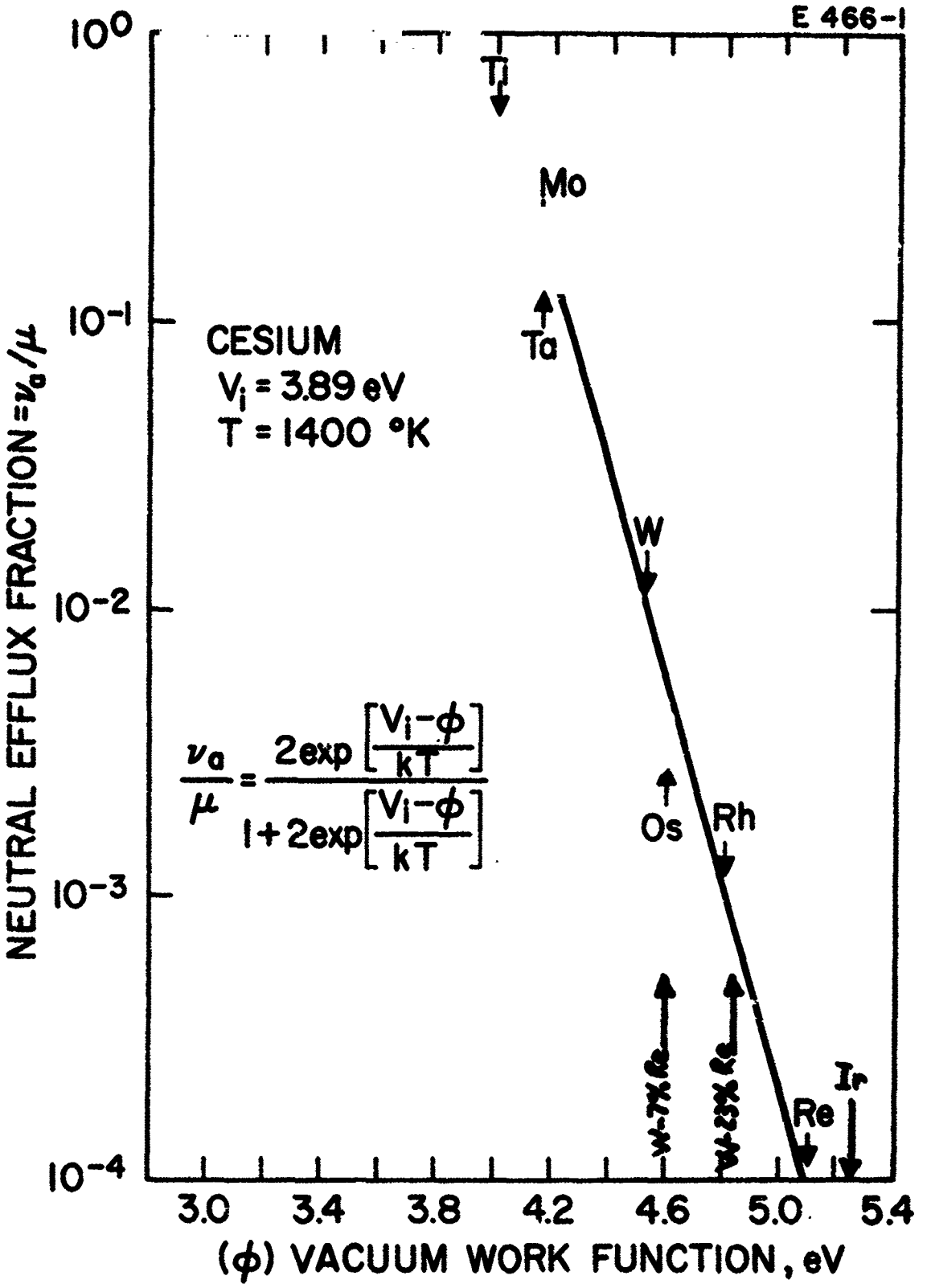


Fig. 34. Work function as a function of neutral efflux for iridium and tungsten-rhenium alloys (from O.K. Husmann, Bull. Am. Phys. Soc. 10, 740 (1965); and R. G. Wilson, data obtained under Contracts NAS 3-5249 and NAS 3-6278.

On the other hand, the production of porous ionizers made of other refractory metals and alloys is still in the early stages of development. Therefore, the quickest and most economical way to study the effect of other high work function metals is to coat them on the surface of available, well understood porous tungsten.

BLANK PAGE

## II. TESTING PROCEDURES

In this type of thin coating research, the testing and evaluating procedures are very important in directing the course of investigations. The electrical evaluations were performed under another program. The rate of diffusion of the coating away from the surface and measurements of changes in porosity were determined under this program. These latter properties had to be satisfactory before electrical tests were warranted. The rate of diffusion of the thin metallic surface films into the substrate had to be low enough to ensure permanence of the high work function layer.

The other requirement was that the surface coating must not diminish the surface porosity of the tungsten substrate to the point where the flow of cesium would be reduced by more than 10 to 20%. These conditions had to be satisfied before the more time consuming and elaborate electrical and surface physics measurements were warranted.

The coating thickness was most readily determined by metallurgical examination. However, special mounting techniques had to be used in order to see the thin coatings. Small pieces of the coated tungsten were either cracked from the test piece or sawed off with a wet silicon carbide wheel. The pieces were then placed in uranium glass tubing, Corning No. 3320, evacuated, and carefully heated until the glass collapsed around the tungsten. The encapsulated tungsten was cut with the wet silicon carbide wheel, mounted in Amber Bakelite, Bueller No. 1336AB, and polished. Wet silicon carbide papers down to 600 were used, followed by etch polishing with Linde A 0.3 μ alumina and dilute alkaline ferricyanide solution (Murakami etch) on a microcloth slow speed wheel. Using this mounting technique, it was possible to maintain coatings as thin as 0.2 μ on the edges of porous tungsten.

X-ray diffraction proved to be an invaluable method for nondestructively examining the surface after various coating and heating experiments. The tests were performed with a Norelco x-ray diffraction unit with wide angle goniometer, using either a zirconium filtered molybdenum target or

nickel filtered copper target. This method allowed a rough estimate of both the coating thickness and the degree to which it alloyed with the substrate. More precise measurements would have required a carefully prepared series of standard coatings which were not available under this program.

The other important characteristic to be determined after coating or heating was the porosity. Two types of measurements were employed. The most straightforward was the simple "nitrogen transmission" test in which the flow through the porous test piece was measured before and after testing. Machined ionizers which were welded into a manifold were connected directly to a flow meter and manometer. Unmounted ionizers were sealed into a manifold as shown in Fig. 35(a). Surface porosity of small flat pieces of porous tungsten over 1/2 in. in diameter was most conveniently measured by the "pressure decay" test using the apparatus in Fig. 35(b). This test measures the time required for the pressure of the 1550 $cm^3$ nitrogen supply tank to drop from 12 to 10 in. mercury pressure by flowing through area enclosed by a 1/4 in. by 1/16 in. wide O-ring. The O-ring is spring compressed against the test piece by pressing the pintle face against the surface and tightening the lock nut. It was found that this pressure was sometimes erratic so that O-ring compression varied, causing a variation in O-ring area. To improve this technique, a 3 mil shim was inserted between the pintle face and the porous surface, and the lock nut was then tightened. This was found to afford a more consistent degree of O-ring compression, and thus a more constant area was available for transmission. As the pressure decay test has been found to be very much more sensitive to extreme outer surface changes than the nitrogen transmission test, a more consistent O-ring compression would also give a more reproducible path length for gas escaping through the surface immediately underneath the O-ring.

The effects of high temperature on the coatings were first obtained using a Harper hydrogen atmosphere furnace with a 6 in. by 6 in. by 12 in. constant temperature zone. More satisfactory thermal tests were run in a vacuum furnace with liquid nitrogen cooled walls. The operating vacuum

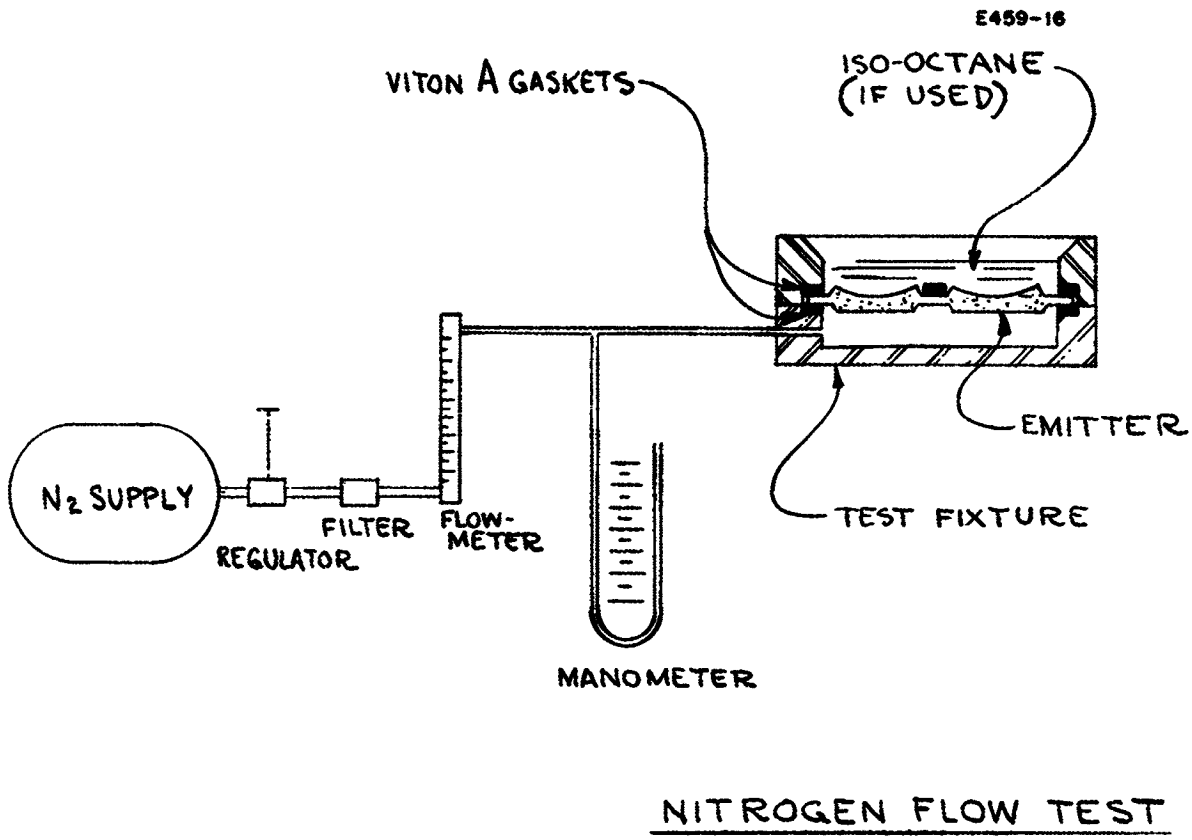


(a) Flow rate measurement.

Fig. 35. Schematics of test apparatus used at HRL.

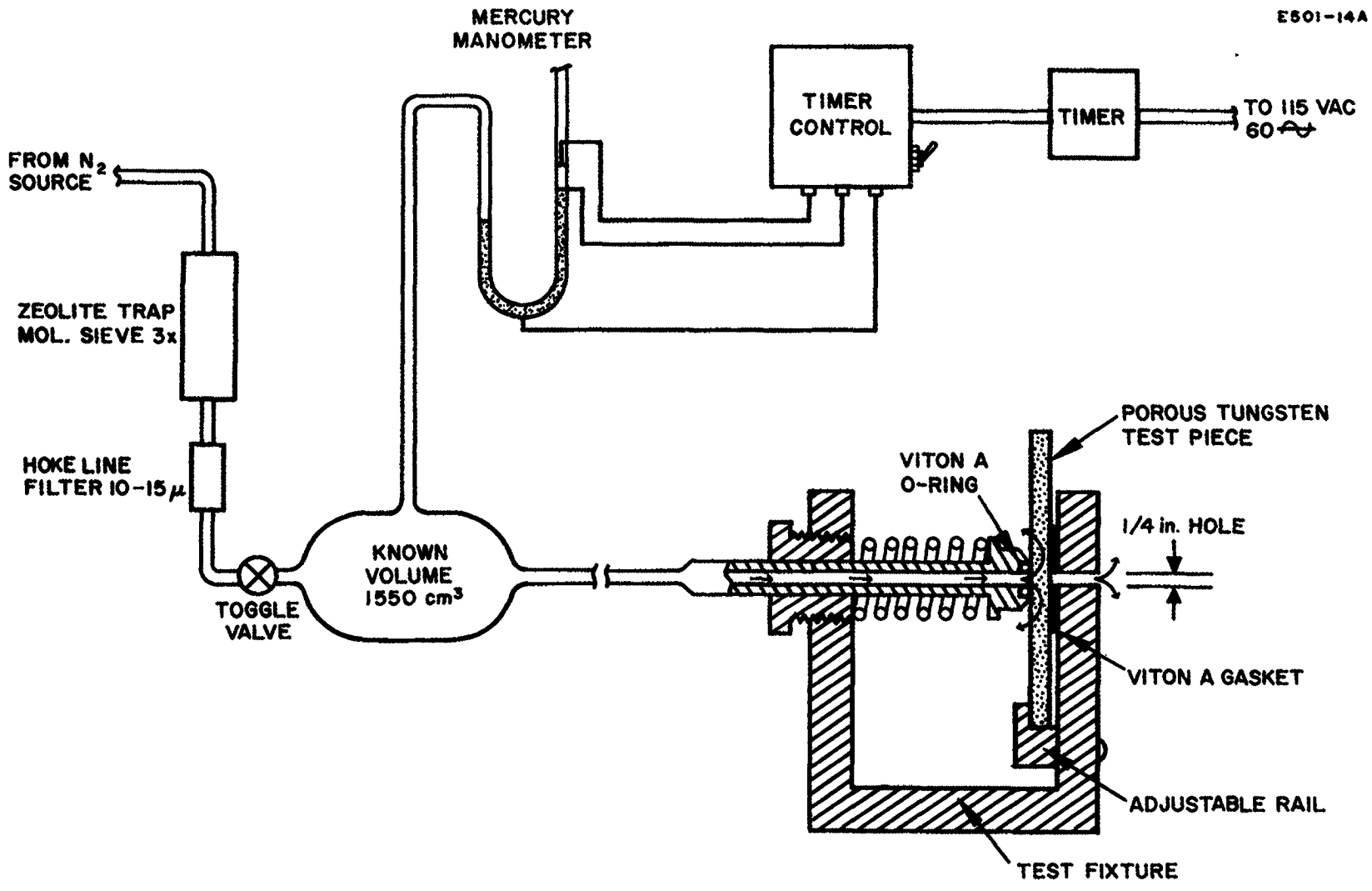


(b) Pressure decay test.

Fig. 35. Schematics of test apparatus used at HRL.

was approximately $1 \times 10^{-6}$ to $1 \times 10^{-7}$ Torr. Most of the thermal stability tests were run at 1500°C, as it was felt that this would give some acceleration to the diffusion effects. This temperature was 200° to 300°C higher than that usually used for ion engine operation. Moreover, at 1500°C, sintering effects in the porous tungsten itself, irrespective of the coating, should not be too significant.

The ultimate test of the coatings is of course the determination of vacuum electron work function, cesium ionization efficiency, and critical temperature. These measurements are very difficult, and require facilities not available in this program. The methods used are described in reports issued under Contracts NAS 3-6278 and NAS 3-6271. Preliminary results of these measurements are included in later sections of this report.

BLANK PAGE

## III. IRIDIUM COATING OF POROUS TUNGSTEN

Several methods have been explored for depositing thin adherent porous coatings of iridium on tungsten ionizers. A literature survey and personal contact with manufacturers of iridium indicated that there were no practical aqueous electrochemical methods. It was felt that iridium plating on porous tungsten from molten cyanides would cause serious contamination problems. * Unfortunately, there was insufficient time for its investigation under the present program.

The thermal or hydrogen reduction of platinum group metal chlorides to the metal was also a well known process and was studied in some detail. The simple chlorides of iridium and many other similar metals were available without the complicating presence of alkali or other metals. Thus it seemed that they might be dissolved in a suitable solvent, impregnated into porous tungsten, and then reduced to the pure metal. Two approaches have been used for impregnation. In one, the porous tungsten is impregnated by total immersion into the solution; in the other, the solution is sprayed on a heated surface in order to localize the deposition.

Another promising method was sputter coating with iridium. This process was also combined with the immersion process.

### A. COATING BY IMMERSION IN AN IRIDIUM SOLUTION

In this process, the porous tungsten was saturated with a solution of iridium chloride, the solvent was evaporated, and the iridium compound subsequently reduced to iridium metal by hydrogen firing at about 1000°C.

---

*R. N. Rhoda, Plating 49, 69 (1962).

Several solvents were tried as carriers for the iridium chloride. The requirements for a satisfactory solvent were that it dissolve appreciable iridium chloride, be volatile at reasonable temperatures, give a solution free of solids, and not react with tungsten. Tetrahydrofuran, pyridine, ethylene dichloride, isopropyl ether, anhydrous ethanol, and dilute and concentrated ammonia were tried. Of these, concentrated ammonia and alcohol showed the best characteristics. In later tests, distilled water was found to be an excellent solvent. It was not tried at first because the iridium chloride, as purchased, was supposed to be the trichloride, $IrCl_3$, which was essentially insoluble in water. It was later discovered that the compound was actually the tetrachloride, $IrCl_4$, which was more water soluble.

According to the manufacturer of the compound, iridium metal powder was chlorinated at red heat and it was not possible to stop the chlorination process at the precise moment when all the metal was converted only to the trichloride. The trichloride thus often reacts further to form the tetrachloride. Actually, the tetrachloride was a better compound to work with because of its higher solubility, and it reduced to the metal as easily as the trichloride.

1. Preparation of Iridium Solution

The iridium solution used for most of the impregnation work was prepared as follows (when larger amounts were needed, the amounts were scaled up accordingly): To 3 ml of concentrated ammonia in a 10 ml flask was added 0.1 gm $IrCl_4$. The flask was stoppered lightly and gently warmed on a hot plate with swirling. The solids dissolved in a few minutes, yielding a brownish green solution which was stable for 3 or 4 days when stoppered tightly. After that, a brownish precipitate began to form.

## 2. Preliminary Immersion Coating Tests

In order to define problem areas, a number of preliminary tests were performed. For example, it was found that the porous tungsten must be wet hydrogen fired at about 1000°C in order for it to wet completely with the impregnating solution. These tests were performed using type Mod E porous tungsten supplied by Philips Metalonics. This grade was made from unclassified angular tungsten powder which was sintered to about 75 to 80% dense and had 1 to 2 x $10^6$ pores/$cm^2$. In one exploratory test, Sample PW Ir No. 2 a piece of Mod E about 80% dense, weighing 4.4 g (0.5 in. by 0.5 in. by 0.087 in.), was allowed to saturate with the ammonia solution and was dried at 100°C. It was then dry hydrogen fired 30 min at 1000°C. After five saturations and firings, 7.7 mg of iridium, about 0.2% by weight, was deposited. From the porosity of the tungsten, it was calculated that approximately 9.5 mg could be absorbed assuming complete saturation each time.

Nitrogen pressure decay tests, as previously described, were used to follow changes in surface porosity. Before impregnation, the decay time of this sample was 40 sec. After impregnation, it was 48 to 49 sec. The color of the tungsten was changed from a dull grey to a brighter silver-grey. Surface examination at 500x showed that the pores were still visible, but that surface features had become less distinct. Metallurgical examination of mounted cross sections showed a brighter, more reflective metal coating on the outer layer or layers of pores. There was essentially none of this material visible in the interior pores. The rather irregular coating was about 0.2 to 0.5 $\mu$ thick.

X-ray diffraction patterns of the early samples were not very definitive because of the lack of standard curves for iridium-tungsten alloys. New and unidentified peaks were found which indicated that new phases were present. Peaks corresponding to pure iridium were often not present at all, and unfortunately, the principal iridium peak was obscured by the principal tungsten peak. The x-ray results of these alloys will be discussed in more detail later.

An emission spectrographic analysis of the above sample PW Ir No. 2 was made. Five milligrams of surface metal were scraped from an area approximately 0.25 in.$^2$ and 0.001 in. deep. This surface material proved to be 6.1% iridium, compared with an average composition of about 0.2% iridium by weight.

These preliminary findings supported further effort, because they indicated a surface concentration greater than had really been expected. Moreover, there appeared to be only a nominal loss of porosity. On the basis of these findings, more thorough tests were made to determine how much iridium could be deposited without impairing porosity and to determine the stability and permanence of the coating at ionizer operating temperatures.

a. Effect of Increasing Iridium Co[illegible] and Heating at 1500 to 1600°C

The effectiveness and permanence of an iridium coating might be a function of the amount of iridium deposited in the porous tungsten. Therefore, a series of tests were performed on various samples of Mod E porous tungsten so that the cumulative effect of iridium additions could be measured. Tungsten samples were from Billet N470, slab 477; and Billet N768, slab 466. Two types of samples were used. Small flat slabs 1/2 in. by 1 in. by 0.1 in. or 0.14 in. thick could be checked for porosity using the pressure decay method. Samples of a scrap ionizer from slab 477, about 0.04 in. thick, were impregnated to demonstrate the effect on thinner, curved samples. The effect of thermal aging on the diffusion of the coating away from the surface, or coating losses by evaporation, was determined by metallographic examination, weight change, and more qualitatively by x-ray diffraction. Slightly accelerated thermal stability tests at 1500 to 1600°C were used as a compromise (i.e., they were 250 to 350°C higher than ionizer operating temperatures, yet not high enough to introduce other changes which would not necessarily be a factor at the lower ionizer operating temperature). These tests could also be rather conveniently carried out for longer periods of time in hydrogen furnaces.

The impregnating solution and technique used were the same as discussed previously, with one exception. It was found that more iridium could be deposited in a shorter time if hydrogen firing was eliminated between each two saturations. In the revised procedure, the samples were saturated, dried at 100°C, resaturated, dried at 100°C, and dry hydrogen fired at 900° to 1000°C. Changes in weight due to iridium additions or loss, and changes in surface porosity as measured by pressure decay, are shown in Tables XXV and XXVI.

The tables indicate that similar materials of differing thickness will deposit about the same weight percent of iridium under the same number of saturations. Six impregnations will deposit about 0.3%, and 11 impregnations will deposit about 0.5%. The most significant result of these tests, however, was the manner in which the pressure decay returned to almost its original unimpregnated value when the samples were heated at 1500 to 1600°C in dry hydrogen for 2 hours or more. Microscopic examination of the unpolished flat surface after reduction of the iridium chloride showed a rough surface with very poorly defined pores. After firing at 1500°C, the pores were clearly defined. This indicates that the as-reduced iridium is probably fairly loose and tends to close the pores. After 1500°C firing, it diffuses into the surface and becomes an adherent dense coating which reduces the pore diameter only slightly.

Photomicrographs of a number of these samples are shown in Figs. 36 through 42. As a preliminary thermal stability test, some of the coated specimens of this group were heated for periods up to 25 hours at 1500°C in dry hydrogen.

These photomicrographs show that a 0.5% impregnation deposits a surface layer which is about 0.8 to 1.5 $\mu$ thick and quite irregular; this seems to cover most of the outer surfaces. The 0.3% samples are coated to about half thickness. There is a considerable amount of iridium within the pores, and occasional pores seemed to be filled with iridium. Since a pore may be cut through any part of its diameter, those which appear to be filled may merely be cut through one edge.

TABLE XXV

Deposition of Iridium in Porous Tungsten by Immersion
Flat Sample from Billet No. 466, Mod E[a]

| Number Impregnations | Total Iridium Added, g | % Increase Over Original Weight | Pressure Decay Time, Seconds | Treatment in Dry Hydrogen |
|---|---|---|---|---|
| None | (Sample Wt. 4.6161) | None | 41 | 1/2 hour at 1000° after each 2 impregnations |
| 2 | ---- | ---- | 42 | |
| 4 | 0.0090 | +0.2 | 48 | |
| 6 | 0.0128 | +0.3 | 53 | |
| 6 | (Sample Wt.[b] 4.0828) | | | |
| 6 | -0.0002 | | 43 | 2 hours at 1500° C |
| 6 | -0.0003 | | 42-43 | 4 hours at 1500° C |
| 6 | (Sample Wt. 4.0825) | | 42-43 | 4 hours at 1500° C |
| 10 | +0.0072 | +0.48[c] | 53 | 1/2 hour at 1000° C after 2 impregnations |
| 11 | +0.0094 | +0.53 | 54 | 1/2 hour at 1000° C after 1 impregnation |
| 11 | +0.0091 | +0.52 | 49 | 4 hours at 1500° C |

[a]Thickness 0.10 in., $1.9 \times 10^6$ pores/$cm^2$
[b]Piece removed for metallographic examination
[c]Percentage corrected to original weight basis

TABLE XXVI

Deposition of Iridium in Porous Tungsten by Immersion
Flat Sample No. 477, Mod E[a]

| Number Impregnations | Total Iridium Added | % Increase Over Original Weight | Pressure Decay Time, Seconds | Treatment in Dry Hydrogen |
|---|---|---|---|---|
| None | (Sample Wt. 7.8989) | ---- | 78 | 1/2 hour at 1000° after each 2 impregnations |
| 2 | ---- | ---- | 84 | |
| 4 | +0.0130 mg | +0.17 | 99 | |
| 6 | +0.0171 mg | +0.22 | 110-113 | |
| 6 | (Sample Wt.[b] 7.8355) | | | |
| 6 | -0.0005 mg | | 83 | 2 hours at 1600° C |
| 6 | -0.0003 mg | | 82-83 | 4 hours at 1600° C |

[a]Thickness 0.10 in., $1.9 \times 10^6$ pores/$cm^2$, Billet No. N470
[b]Piece removed for metallographic examination

M 3780

Fig. 36.
Uncoated No. 477 Mod E ionizer tungsten, 1500x.

M 3775

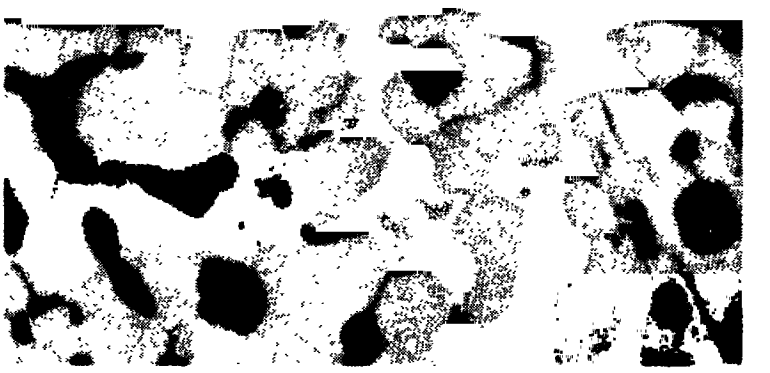

Fig. 37.
No. 477-2 Mod E ionizer tungsten after six impregnations with iridium (0.29% by weight) plus 4 hours heating at 1500°C in dry $H_2$, 1500x. After heating at 1500°C for 1 or more hours, all iridium coatings 1 to 2 μ thick contain about 50% tungsten by diffusion.

M 3779

Fig. 38.
No. 477-1 Mod E ionizer tungsten after six impregnations with iridium (0.29% by weight) plus 17 hours at 1500°C, 1500x.

M 3776

Fig. 39.
No. 477-2 Mod E ionizer tungsten after 11 impregnations with iridium (0.54% by weight) plus 8 hours at 1500°C, 1500 x.

M 3778

Fig. 40.
No. 466 flat Mod E tungsten after six impregnations with iridium (0.5% by weight) plus 4 hours at 1500°C, 1500x.

M 3777

Fig. 41.
No. 466 flat Mod E tungsten after 11 impregnations with iridium (0.53% by weight) plus 8 hours at 1500°C, 1500x.

M 3772

Fig. 42.
No. 466 flat Mod E tungsten after 11 impregnations with iridium (0.53% by weight) plus 25 hours at 1500°C, 1500x.

It is felt that coating the interior of the surface of the pores is important, because cesium ions may also be formed in and extracted from within the larger pores. These photomicrographs show that during the evaporation process the metal concentrates primarily in the outer two or three pores as well as the outer surface. This is an advantage because the gas flow will be restricted by iridium only in those pores where the iridium might have some beneficial effect in raising the work function.

This series of photomicrographs also indicates that the surface is converted almost to its final form during the first 2 to 4 hours of heating at 1500°C. It was then shown to be stable for at least the 25 hour test period at 1500°C. The coating thickness apparently increases only very slightly with time after the initial sintering into the tungsten. As described later, these diffused coatings contain about 50% tungsten and this composition would fall in the region of the $\epsilon$ phase of the iridium-tungsten binary phase diagram.

b. Effect of Using Larger Samples

Tests run on small porous samples about 0.5 in. by 0.5 in. by 1 in. did not reveal any problems caused by the possible uneven distribution of iridium. Therefore, it was necessary to perform similar tests on larger samples to determine what problems might arise if a full size ionizer were impregnated. The use of larger samples made it possible to perform actual nitrogen transmission tests which more closely reproduced the effect of the coating on cesium vapor transmission. Bubble patterns gave a visual indication of the uniformity of coating of all areas.

The porous tungsten samples used for these tests were two obsolete design 10-strip ionizers of Philips Mod E material approximately 2 in. by 4 in. by 0.04 in. They were in the finished machined condition and had been electron beam sealed in the area between the porous tungsten lenses. A fully machined one-strip ionizer with 1/10 the area of the 10-strip ionizer was treated in the identical manner as the two 10-strip ionizers. Sections of the one-strip ionizer were removed at appropriate intervals during impregnation and heating for metallographic examination.

The following procedure was used to impregnate and test the two 10-strip and one single-strip ionizers:

1. Nitrogen transmission measurements were made at 1 in. and 2 in. of mercury nitrogen pressure differential.
2. The ionizers were bubble checked to determine bubble emission at 5.6 in. mercury nitrogen pressure.
3. Ionizers were wet hydrogen fired at 1100°C for 30 min as a cleanup procedure, and weighed.
4. The iridium impregnating solution was prepared by dissolving 2 g anhydrous $IrCl_3$ in 60 mliter warm concentrated ammonia.
5. The ionizers were dipped slowly into the solution to permit displacement of air, and then allowed to drain for about 30 sec.
6. They were then dried in an air oven at 100°C for 30 min after which they were dipped and dried again.
7. The ionizers were fired at 1000°C in dry hydrogen for 15 to 30 min, cooled, and weighed.
8. Steps 5 through 7 were repeated twice, making a total of six impregnations.
9. The ionizers were fired for 90 min at 1500°C, weighed, and the nitrogen transmissions were determined. (One 10-strip ionizer was accidentally rendered useless at this point because of alumina pickup from a new ceramic boat.)
10. Steps 5 through 7 were repeated three more times on the remaining 10-strip ionizer and the single-strip sample, making a total of twelve impregnations.
11. The ionizers were fired for 4 hours at 1500°C in dry hydrogen, after which they were weighed, nitrogen transmission was determined, and bubble patterns were photographed. Total time at 1500°C was 5-1/2 hours.

The results of these impregnations are shown in Table XXVII. The ionizer which had been contaminated with alumina is not included in the table because the alumina coating on the bottom had seriously decreased the transmission. It will be noted that, as determined in previous small scale tests, about 0.5% by weight of iridium is added by 12 impregnations. The nitrogen transmission at 1 in. mercury pressure differential was reduced only about 9% and 7% at 2 in. mercury differential after 5-1/2 hours at 1500°C. This is somewhat less than the 16% loss indicated by pressure decay time tests on flat specimens previously measured, which had about the same iridium coating. After an additional 16 hours heating at 1500°C in dry hydrogen, the final loss in transmission was 7.5% at 1 in. mercury and 2% at 2 in. mercury pressure. There was no obvious reason for the difference between the 1 in. and 2 in. Q/P ratio. It may be due to increased leakage around the gaskets which seal ionizer into the flow checking manifold at the higher pressure.

These results show that the pressure decay measurement is influenced much more strongly by the surface coating than is the actual nitrogen transmission. In the pressure decay test, the nitrogen flows under the O-ring, so that a larger proportion of the flow is through surface pores whose diameter has been reduced by the iridium coating. Photomicrographs indicate that the pores are coated down about 0.001 in. from the surface. In contrast, the transmission test forces nitrogen to flow completely through the test piece. The flow limitations are therefore more dependent on the uncoated pores in the bulk of the tungsten. The reduction in nitrogen transmission is thus considerably less and is much more indicative of the probable effect on cesium vapor transmission. A thorough treatment of the flow measurements is to be found in reports issued under Contract NAS 3-6271.

The bubble pattern of the 10-strip ionizer was changed much more drastically than the change in nitrogen transmission would indicate. Photographs were taken of the ionizer immersed in distilled hexane and pressurized with 5.6 in. of mercury before and after the 12 impregnations, plus 5-1/2 hours of heating at 1500°C. At this pressure, only 10 to 15%

## TABLE XXVII

### Effect of Iridium Impregnation on Nitrogen Transmission of Porous Tungsten

| 10 Strip Ionizer No. 467. Total Area 47.5 $cm^2$ | | | | | | |
|---|---|---|---|---|---|---|
| Total Impregnations | Total Weight, g | Increase, g | ΔP, in. Mercury | Q, $cm^3$/min | Q/ΔP | Treatment |
| 0 | 82.685 | | 1 | 626 | 626 | None |
| | | | 2 | 1243 | 622 | |
| 2 | 82.753 | 0.067 | | | | 1000°C $H_2$ |
| 4 | 82.817 | 0.064 | | | | 1000°C $H_2$ |
| 6 | 82.899 | 0.082 | 1 | 611 | 611 | 1000°C $H_2$ + 1500°C for 90 min |
| | | | 2 | 1215 | 608 | |
| 8 | 82.956 | 0.057 | | | | 1000°C $H_2$ |
| 10 | | | | | | 1000°C $H_2$ |
| 12 | 83.107 | 0.151 | 1.1 | 611 | 556 | 1000°C + 4 hours at 1500°C |
| | | | 2 | 1148 | 574 | Total of 5-1/2 hours at 1500°C |
| 12 | 83.107 | 0.151 | 1 | 579 | 579 | 21-1/2 hours at 1500°C |
| | | | 2 | 1215 | 608 | |
| Total Iridium = 0.421 g<br>% Increase = 0.5 | | | | | | |
| One Strip Ionizer, Total Area 4.75 $cm^2$ | | | | | | |
| Total Impregnations | Total Weight, g | Increase, g | ΔP, in. Mercury | Q, $cm^3$/min | Q/ΔP | Treatment |
| 0 | 7.690 | | 1 | 38 | 38 | Treatment Same as Above |
| | | | 2 | 86 | 43 | |
| 2 | 7.696 | 0.006 | | | | |
| 4 | 7.702 | 0.006 | | | | |
| 6 | 7.710 | 0.008 | 1 | 38 | 38 | |
| | | | 2 | 86 | 43 | |
| 8 | 7.716 | 0.006 | | | | |
| 12 | 7.730 | 0.014 | 1 | 38 | 38 | |
| | | | 2 | 86 | 43 | Total of 5-1/2 hours at 1500°C |
| Total Iridium = 0.040 g<br>% Increase = 0.5 | | | | | | |

of the bubbles appeared ater the 12 impregnations, compared with the number seen before impregnating. If the pressure was increased to 8 to 10 in. of mercury, the bubble pattern was almost the same as at 5.6 in. prior to impregnation. One very noticeable change, however, was a distinct decrease in bubbles near the ends of the ionizer lenses. An area about 1/4 to 3/8 in. from the ends was affected. We have not included photographs because of the poor definition of bubbles, caused by the interference of the liquid layer.

Closer examination of the end areas showed that they were slightly darker and were probably more heavily coated. The pattern was quite similar on all the lenses. During saturation, it had been noted that a small amount of excess liquid tended to collect in these areas, probably because of surface tension effects. More iridium was thus deposited on the surface in these areas. This problem can be readily overcome by changing the impregnation technique slightly. Only one impregnation would be made before each 1000°C hydrogen firing, and any liquid observed near the ends of the lens would be carefully blotted away before drying at 100°C.

The 10-strip ionizer was given an additional 16 hours heating at 1500°C in an attempt to improve the bubble pattern. The pattern was unchanged, but the nitrogen transmission increased slightly, as shown in Table XXVII.

At best, interpretation of the bubble pattern is very qualitative. About the best one can expect to determine is a sort of pore size distribution. The larger pores will emit bubbles at a lower pressure than will the smaller pores. The smaller pores require a higher pressure to overcome the surface tension of the isooctane filling the surface pores. The bubble pattern obtained at 8 to 10 in. of mercury pressure after impregnation was the similar to that obtained at 5.6 in. before impregnation, indicating that the pores were not completely closed. Most of them were probably only reduced in size. Some pore closure had probably occurred near the ends of the lenses.

The single strip ionizer showed no significant change in transmission with the addition of 0.5% iridium, probably because the smaller flow rate of the one strip ionizer could not be measured as accurately as that of the larger 10-strip ionizer. The number of bubbles was reduced in about the same degree, but the excessive reduction near the ends was not as noticeable.

The single strip ionizer was used for metallographic examinations. It was cut into two sections, one 1/2 in. long and the other 1-1/2 in. long. The 1/2 in. length was given an additional 16 hours in hydrogen at 1500°C along with the 10-strip ionizer, making a total of 21-1/2 hours at 1500°C. The 1-1/2 in. length had accumulated 5-1/2 hours at 1500°C and was not heated further. Both samples were encapsulated in uranium glass Corning No. 3320, cut at six equally spaced intervals along the length of the 2 in. long lens to determine uniformity of distribution, and metallographically examined.

It was found that surface coating was not quite as thick or as uniform as that which was deposited on previous small samples. The coating, when examined using oil immersion at 2000x, actually appeared to cover the surface almost completely, but did not bridge many pores. However, photomicrographs did not show the coating as well as could be seen visually. The coating varied from 0.5 to 1 μ thick and seemed to have the same general appearance at several locations along the length of the lens. The 1/2 in. long section which had been heated for a total of 21 hours at 1500°C showed a slight thickening of the coating as a result of interdiffusion of the tungsten and iridium. The photomicrographs shown in Figs. 43 through 48 are representative of the variations seen along a 2 in. length of Mod E ionizer lens.

3. Coating Fine Pore Tungsten by Immersion

The Hughes Research Laboratories' type of porous tungsten made from uniform size spheroidized tungsten particles will be used for future improved high pore density ionizers. It was of interest to know how the fine pore tungsten was affected by iridium impregnation, compared with the larger pore Mod E.

M 3949

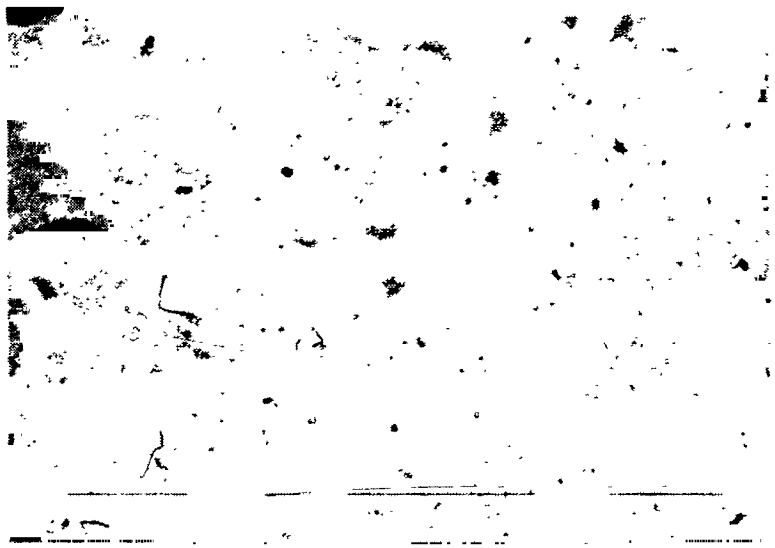

Fig. 43.
Photomicrograph (2000x) of a section of an iridium impregnated single strip ionizer hydrogen fired at 1500°C for 5-1/2 hours (Mod E tungsten, 12 impregnations, 0.5% iridium).

M 3948

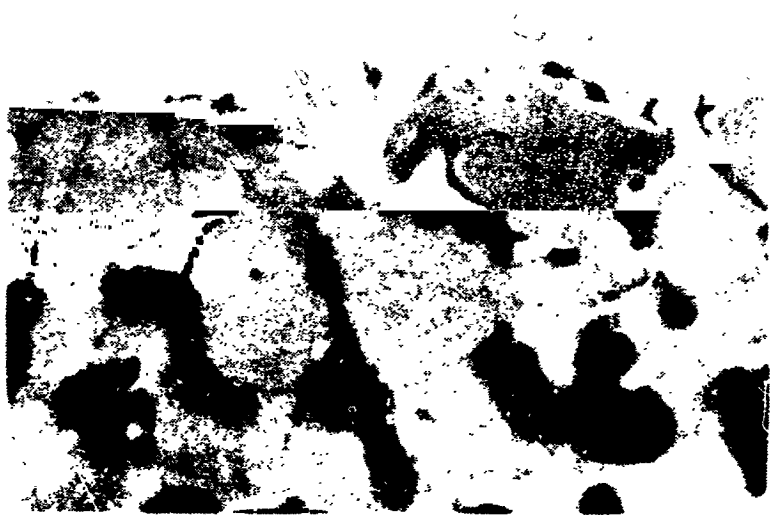

Fig. 44.
Photomicrograph (2000x) of another section of the same piece of iridium impregnated single strip ionizer shown in Fig. 43 (Mod E tungsten, 2 impregnations, 0.5% iridium, $H_2$ fired at 1500°C for 5-1/2 hours).

M 3954

Fig. 45.
Photomicrograph (2000x) of another section of the same piece of iridium impregnated single strip ionizer shown in Figs. 43 and 44 (Mod E tungsten, 12 impregnations, 0.5% iridium, $H_2$ fired at 1500°C for 5-1/2 hours).

M 3960

Fig. 46.
Photomicrograph (2000x) of another section of the same piece of iridium impregnated single strip ionizer shown in Figs. 43 through 45 (Mod E tungsten, 12 impregnations, 0.5% iridium, $H_2$ fired at 1500°C for 5-1/2hours).

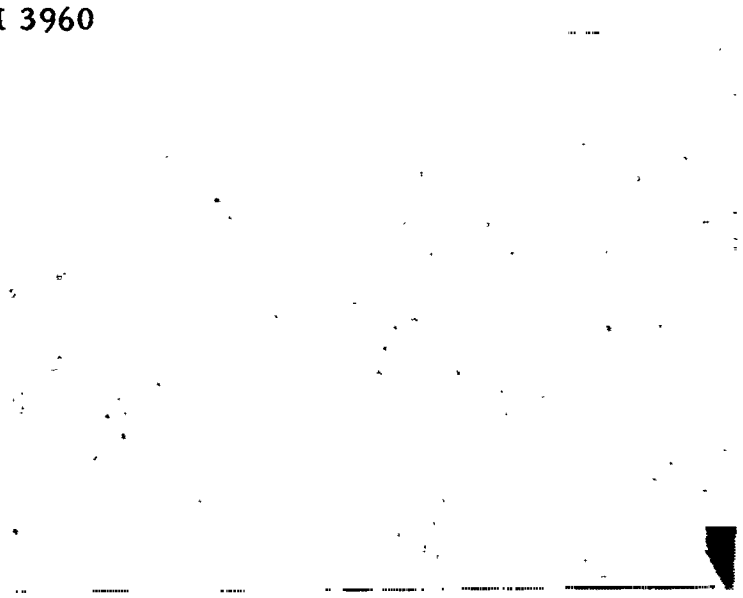

M 3959

Fig. 47.
Photomicrograph (2000x) of a section of an iridium impregnated single strip ionizer hydrogen fired at 1500°C for 21-1/2 hours (Mod E tungsten, 12 impregnations, 0.5% iridium). Same ionizer as shown in Fig. 43 through 48.

M 3958

Fig. 48.
Photomicrograph (2000x) of another section of the same piece of iridium impregnated single strip ionizer shown in Fig. 47 (Mod E tungsten, 12 impregnations, 0.5% iridium, $H_2$ fired at 1500°C for 21-1/2 hours).

The ion microscope can be used to determine work functions and critical temperatures for ionizer materials. To use this technique, two pellets were fabricated from HRL 3.9 μ sintered spherical tungsten (Plate No. 188-S). The pellets were 0.20 in. in diameter by 0.020 in. thick. They were given six impregnations with iridium chloride solution, as previously described, with a 1000°C hydrogen firing after each impregnation. They were then fired for 4 hours at 1500°C in dry hydrogen. The nitrogen transmission was reduced about 50%, which is rather substantial. Weight increases were not determined because of the small size of the pellet. However, from past experience, the pellets should contain about 0.2% iridium. The results of the ion microscope tests will be reported under Contract 3-6270.

The substantial flow reduction measured on this small pellet of the very fine pore material indicated the need for more detailed and reliable data which might be obtained from larger samples. A 1/2 in. by 1/8 in. pressed and sintered disk of the same type 3.9 μ spherical tungsten (Pellet No. 104) was selected for more quantitative treatment. This pellet was 78% dense and had been sintered 8 hours at 1500°C. It was impregnated as described above for the ion microscope pellet.

Table XXVIII shows that this particular 3.9 μ material had an increase of pressure decay time of about 12% after impregnation with 0.24% iridium, and 32% after 0.29% had been added. Both measurements were taken after 1500°C diffusion. Figure 49 shows a promising coating about 1 μ thick after the addition of about 0.3% iridium.

4. Comparison of Immersion Coating of Mod E and Fine Pore Tungsten

Data collected from Tables XXV through XXVIII and shown in Table XXIX indicate that the Mod E, because of its larger pores and grain size, is apparently less susceptible to flow reduction when coated with iridium by the impregnation process and heated to 1500-1600°C than is the fine pore HRL 3.9 μ material. Indications are that about 0.5% iridium could be added to Mod E without detriment to flow, but only about 0.2% could be added to the 3.9 μ material.

M 4013

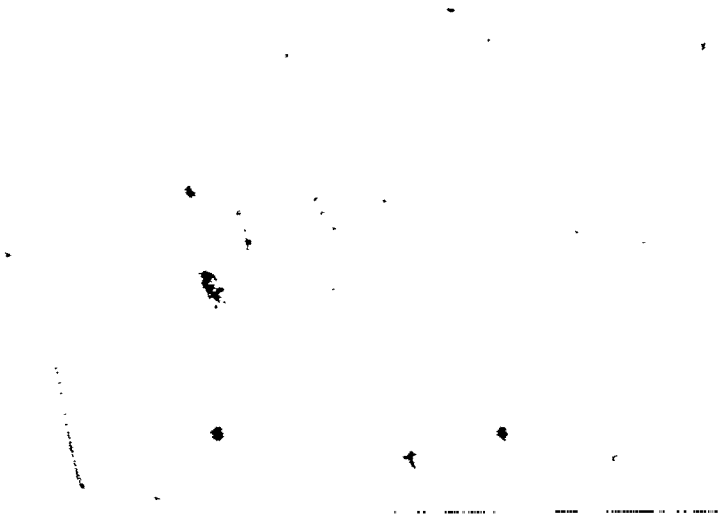

Fig. 49. Pellet No. 104, 3.9 μ spherical tungsten impregnated with 0.3% by weight iridium, 2000x, Murakami etch.

## TABLE XXVIII

### Impregnation by Immersion of Pellet No. 104[a] with Iridium

| Number of Impregnations | Side Measured | Decay Time, Sec | Total Weight, g | Weight Gain (Iridium), mg | Treatment |
|---|---|---|---|---|---|
| 0 | 1<br>2 | 385<br>375 | 5.300 | - | |
| 1 | 1<br>2 | 391<br>378 | 5.3020 | 2.0 | 1000°C $H_2$ fire.<br>20 min. |
| 2 | 1<br>2 | 418<br>411 | 5.3036 | 1.6 | 1000°C $H_2$ fire |
| 3 | 1<br>2 | 437<br>423 | 5.3059 | 2.3 | 1000°C $H_2$ fire |
| 4 | 1<br>2 | 500<br>494 | 5.3084 | 2.5 | 1000°C $H_2$ fire |
| 5 | 1<br>2 | 514<br>506 | 5.3104 | 2.0 | 1000°C $H_2$ fire |
| 6 | 1<br>2 | 426<br>427 | 5.3132 | 2.8 | 2 hours at 1500°C |
| 7 | 1<br>2 | 503<br>507 | 5.3155 | 1.7<br>14.9 | 1000°C $H_2$ fire |
| - | 1<br>2 | 496<br>503 | | | 75 min at 1500°C |
| Total Increase After 7 Impregnations | | 32% | | 14.9<br>(0.3%) | |

[a]Dimensions: 1/2 inch diameter by 1/8 inch thick; 3.9 μ spherical tungsten, pressed and sintered to 78% density.

TABLE XXIX

Comparison of Mod E and HRL 3.9 μ Porous Tungsten

| Type | Iridium Added, % | Test | % Reduction | Source |
|---|---|---|---|---|
| Mod E | 0.5 | Transmission | 4.8 | Table III |
| Mod E | 0.3 | Pressure Decay | 5.0 | Table I |
| Mod E | 0.52 | Pressure Decay | 19.5 | Table I |
| Mod E | 0.22 | Pressure Decay | 6.4 | Table II |
| HRL 3.9 μ | 0.24 | Pressure Decay | 12.0 | Table IV |
| HRL 3.9 μ | 0.29 | Pressure Decay | 32.0 | Table IV |

The HRL 3.9 μ tungsten has an average pore size of about 1.9 μ, while the Mod E is about 2.8 μ. Equivalent amounts of iridium will obviously cause a greater percentage decrease in pore cross section in the 1.9 μ pore than in the 2.8 μ pore. The amount of impregnation which can be tolerated by the fine pore tungsten will have to be determined from a consideration of the allowable reduction in nitrogen transmission and the minimum amount of iridium which will yield a stable high work function surface. The former will have to be determined by a button or ionizer engine test. The photomicrographs of Mod E and HRL 3.9 μ tungsten show that about the same coating thickness is obtained with a 0.3% addition of iridium to HRL 3.9 μ as by a 0.5% addition to Mod E.

## B. COATING WITH IRIDIUM BY SPUTTERING

Several sputtered iridium coated samples were prepared by Philips Metalonics using equipment which was not available at the Hughes Research Laboratories. Thicknesses of 0.5 μ and 1.5 μ were deposited on Mod E porous tungsten. The coatings were of very uniform

thickness on the 1/2 in. diameter samples and did not bridge or cover the pores. On the other hand, they did not appreciably coat the interior of the pores. Recent findings indicate that the pores may actually be an important source of ions, so it would be advantageous to have an iridium lining on the outer pores. Figures 50 and 51 show a 1.5 $\mu$ sputtered coat. The sputtered coating in Fig. 50 was deposited on tungsten at a relatively low temperature, so that the interaction or alloying with the substrate was negligible. Figure 51 shows approximately the same original thickness of coating which has been heated for 4 hours at 1800°C. It is apparent from these pictures that the coating has increased in thickness about 100%, making an approximately 50:50 alloy. As the temperature of diffusion is about 550 to 600°C higher than the usual operating temperature of ion engines, thermal stability at operating temperatures could be orders of magnitude greater. This of course depends upon whether the ionizing characteristics of the iridium-tungsten alloy are satisfactory.

One possible disadvantage of sputtered coatings of any type compared with chemically deposited coatings stems from the fact that sputtered material tends to entrap gases and other impurities which are present in the vacuum deposition chamber. On the other hand, chemical coatings will contain only the elements in the solutions used in the depositions. In one case described later, a problem arose from the non-adherence of the sputtered layer on a smooth weld area.

## C. COATING WITH IRIDIUM BY COMBINING SPUTTERING AND IMMERSION

In order to utilize the uniform coatings produced by sputtering, it would be possible to combine this process with impregnation. Impregnation would serve the purpose of coating the interior surfaces of the outer layer of pores. One of the Mod E samples with a 0.5 $\mu$ thick sputtered coating was immersed six times in the iridium solution using the usual process. The sample was then diffused for 2 hours at 1500°C. No

M 3773

Fig. 50. Sputtered iridium on Mod E tungsten, unheated, 1500x.

M 3774

Fig. 51. Sputtered iridium on Mod E tungsten after 4 hours at 1800°C in vacuum, approximately same original thickness as in Fig. 17, 1500x. An approximately 50:50 tungsten-iridium alloy is formed.

pressure decay data were taken on the sample because the Mod E substrate material had very low transmission even before coating. Figure 52 shows the resulting coating. Although it does not show up well in the photomicrograph, the iridium can be detected visually in the pores in areas where the sputtering could not reach.

## D. COATING BY SPRAYING WITH IRIDIUM SOLUTIONS

The immersion method has the advantage of coating the interior surfaces of the outer two or three pores as well as the extreme outer surface. It has the disadvantage of coating both sides of an ionizer, in addition to putting some iridium too deep to be of any benefit to the surface work function. This causes a greater reduction in transmission than may really be necessary. The sputter coating method coats only one side, but it deposits very little within the surface pores.

Spraying the iridium solution on the surface in such a manner that there would be only a minimal penetration into the pores might be expected to have the advantages of both the sputtering and immersion methods. It was found possible to use a water solution of the iridium chloride and to spray it on a heated tungsten surface in order to obtain a very satisfactory surface coating.

### 1. Spray Coating Procedures

The spray apparatus used was simply an all glass nasal spray powered by a rubber squeeze bulb. The spray solution was composed of 0.5 g $IrCl_4$ in 6 $cm^3$ water plus 0.2 $cm^3$ concentrated HCl. About 1 to 2 $cm^3$ at a time was placed in the aspirator for coating small specimens. Best coating results were obtained when the porous tungsten was heated to about 120°C. If the sample was much hotter, the solution dried in flakes on the surface. If the sample temperature was less than 100°C, the solution was absorbed too deeply. The surface was sprayed

lightly and evenly until the dark color of the iridium chloride was just visible. After further drying at 100°C, the sample was wet or dry hydrogen fired at 1000°C for about 30 min.

2. Thermal Stability of Sprayed on Coatings

The first sample for quantitative coating was a 1/2 in. by 1 in. by 0.1 in. flat cut from slab 313-S. The slab was made from Ampro C 3.8 μ spheroidized material which had been sintered to 80% density. This material has less thermal stability than Mod E because it is made up of much smaller particles. The sample, Ir No. 3, was given seven spray coats with a 30 min hydrogen fire between each coating. After the seventh coat, the sample was fired at 1500°C for 2-1/3 hours. The sample surface was slightly rough even before coating, so that the nitrogen pressure decay values were rather inconsistent and difficult to reproduce. However, they are presented in Table XXX and show only a slight increase after the initial 2-1/3 hour 1500°C diffusion. X-ray diffraction showed a very heavy coating of alloyed iridium. Figures 53 and 54 show the coating as it appeared after 2-1/3 hours at 1500°C. Visual inspection showed that a considerably greater amount of iridium was present in the pores than in the sputter coated samples. The very small pores in the 3.9 μ tungsten make it very difficult to see the thinner deposit within the pores. The iridium 1-1/2 to 2 μ coating appears to be almost a solid layer; because there is still high porosity, however, this appearance probably results because iridium smears during polishing and is not etched away as is the smeared tungsten.

The x-ray diffraction and metallographic studies indicate that for the spray coated samples the iridium is essentially on the surface or near it; therefore, we are justified in calculating a surface concentration in milligrams per square centimeter, based on the calculated area covered and the weight of iridium added. These figures are also shown in Tables XXX and XXXI etc.

M 4012

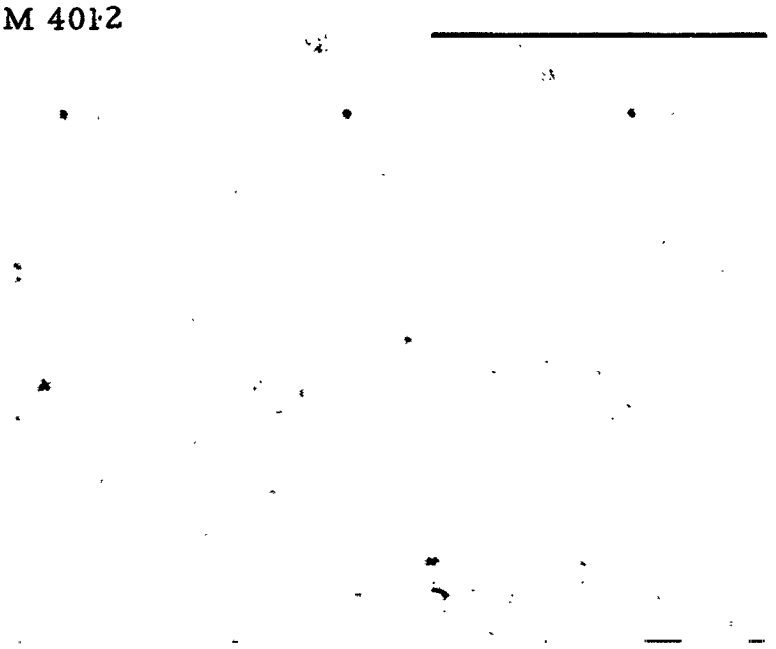

Fig. 52.
Sample I-12 Mod E;
0.5 μ sputter coating
plus six impregnations
with iridium; 2000x,
Murakami etch.

M 4094

Fig. 53.
Sample No. 3, iridium
spray coat, 3.1 mg/cm$^2$
on 3.8 μ porous tungsten.
Heated 2-1/3 hours at
1500°C, 2000x, Murakami
etch.

TABLE XXX

Effect of 1500°C Hydrogen on Surface Porosity of Iridium Coated Porous Tungsten[a] as Measured by Pressure Decay Test

Sample Ir No. 3

| Time at 1500°C | 0 Hours | 2-1/3 Hours | 58-1/2 Hours |
|---|---|---|---|
| Before Coating - Side 1 | 350 Sec | | |
| After Seven Coats - Side 1 | | 384 Sec | 8700 Sec |
| Uncoated Side 2 | | 369 Sec | 911 Sec |

[a]An 80% dense, high pore count material made by Hughes Research Laboratories of Ampro C 3.8 μ spheroidized powder. Seven coats of iridium were applied by the spray method to give 3.1 mg of iridium/cm$^2$ over 4.5 cm$^2$ area. Total iridium added was 13.9 mg, or 0.07% by weight.

In a preliminary thermal stability test, the sample was heated for 58-1/2 hours at 1500°C in dry hydrogen. Referring to Table XXX, the pressure decay time showed the surface to be essentially nonporous. However, the back of the piece, which had been resting on a flat tungsten sheet, also showed considerable loss of porosity. Figure 55, which was taken after this heating, shows that the coating is still there, although it may be slightly thinner. Not shown in this photograph, however, are the underlying pores which appeared to have sintered excessively, to a depth of several mils. The loss of porosity probably resulted not from the presence of the coating but from other causes. During the weekend when the sample was run, a haze was noted in the furnace hydrogen atmosphere, which may have resulted from a high water content. This could have caused a "water cycle" in the surface pores which resulted in considerable pore sintering. Two other samples which were rhenium coated were heated at the same time and they also experienced a loss of porosity, which will be discussed later. It was not as great a loss as that suffered by the tungsten sample, but it was considerable.

M 4095

Fig. 54.
Sample No. 3, iridium spray coat, 3.1 mg/cm$^2$ on 3.8 μ porous tungsten. Heated 2-1/3 hours at 1500°C, 2000x, Murakami etch. These iridium coatings and others reach a stable composition containing about 50% tungsten after a few hours at 1500°C. This corresponds to a composition in the $\epsilon$ phase.

M 4173

Fig. 55.
Sample No. 3, iridium spray coat, 3.1 mg/cm$^2$ on 3.8 μ porous tungsten, heated 58-1/2 hours at 1500°C in Hydrogen; 2000x Murakami etch.

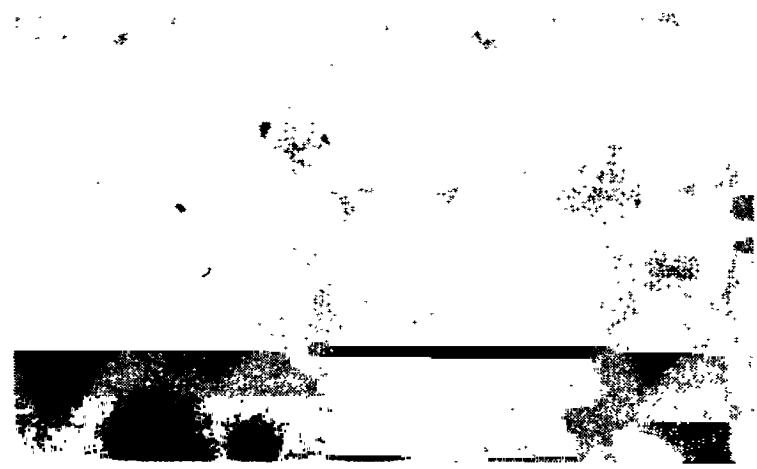

X-ray diffraction patterns taken before and after the extended heating at 1500°C were essentially identical. This indicated that the average coating thickness and composition remained essentially unchanged. Emission spectrographic analysis of the surface did not show any traces of molybdenum, alumina, or other materials which might have altered the surface.

The previous test indicated a need to eliminate the unknowns of the furnace atmosphere and to study the coating on porous tungsten with better stability. The effect of the coating could then be isolated better.

Two types of Mod E tungsten were coated for these tests. A small slab of Mod E 1/2 in. by 3/4 in. by 0.1 in. and an obsolete design three-strip ionizer approximately 1-1/2 in. by 2-1/2 in. by 0.040 in. were iridium spray coated as before. The iridium chloride solution was diluted 1:1 with water (0.042 g/mliter compared with previously used 0.084 g/mliter. The pieces were sprayed more lightly each time, in the hope that the slower process with a more dilute solution would be less likely to clog pores.

After spraying with the iridium solution, the parts were placed in molybdenum boats and fired for 30 min at 1000°C in wet hydrogen. Weights, permeability (nitrogen transmission of the ionizer), and pressure decay (small slab) were then determined. After six coatings, the samples were fired for 2 hours at 1500°C in dry hydrogen. Permeability, pressure decay, and x-ray diffraction measurements were made.

The vacuum furnace used for this test could operate for extended periods without direct supervision. As it was lined with a liquid nitrogen cooled cryowall, there was little chance of diffusion pump oil contaminating the samples. The vacuum was steady at about $1 \times 10^{-6}$ to $1 \times 10^{-7}$ Torr for the heating period. As indicated in Table XXXI, the furnace was shut down at 15, 31, 100, and 200 hours and the samples removed for testing. A small piece of sample 4V iridium was removed after 31 hours for metallographic examination. A sample could not be removed after 100 hours because that would have left insufficient area for pressure decay tests.

# TABLE XXXI

## Changes in $N_2$ Permeability and Weight After Spray Coating Porous Tungsten with Iridium and Heat Treating in Vacuum

| Sample | Number of Coatings | Iridium Added, $mg/cm^2$ | Accumulated Weight Loss, mg | $Q/\Delta P$, $cm^3/min/in$ Mercury | | Heat Treatment |
|---|---|---|---|---|---|---|
| 3 Strip Ionizer, Mod E, 16.5 $cm^2$ area, 27.8915 g | 0 | 0 | | 378 | | 1 hour, 1000°C, wet $H_2$ |
| | 1 | 0.22 | | 378 | | 30 min, 1000°C, wet $H_2$ |
| | 2 | 0.36 | | 378 | | 30 min, 1000°C, wet $H_2$ |
| | 3 | 0.60 | | 374 | | 30 min, 1000°C, wet $H_2$ |
| | 4 | 1.0 | | 354 | | 30 min, 1000°C, wet $H_2$ |
| | 5 | 1.2 | | 354 | | 30 min, 1000°C, wet $H_2$ |
| | 6 | 1.6 | | 354 | | 30 min, 1000°C, wet $H_2$ |
| | 6 | 1.6 | 0.0 | 368 | | 2 hours, 1500°C, dry $H_2$ |
| | 6 | 1.6 | 32.6 | 378 | | 15 hours, 1500°C, vacuum[a] |
| | 6 | 1.6 | 34.7 | 378 | | 31 hours, 1500°C, vacuum |
| | 6 | 1.6 | 38.7 | 354 | | 100 hours, 1500°C, vacuum |
| | 6 | 1.6 | 43.4 | 388 | | 200 hours, 1500°C, vacuum[b] |
| | | | | Pressure Decay Time, Sec | | |
| | | | | Coated Side | Uncoated Side | |
| No. 4 V iridium, Flat Test Slab, Mod E, 8.5352 g Area, 2.25 $cm^2$ | 0 | 0 | | 46.1[d] | 44.5 | 1 hour, 1000°C, wet $H_2$ |
| | 1 | 0.31 | | 49.1 | | 30 min, 1000°C, wet $H_2$ |
| | 2 | 0.49 | | 46.0 | | 30 min, 1000°C, wet $H_2$ |
| | 3 | 0.71 | | 49.6 | | 30 min, 1000°C, wet $H_2$ |
| | 4 | 0.93 | | 48.8 | | 30 min, 1000°C, wet $H_2$ |
| | 5 | 1.24 | | 48.0 | | 30 min, 1000°C, wet $H_2$ |
| | 6 | 1.51 | | 50.3 | 44.9 | 30 min, 1000°C, wet $H_2$ |
| | 6 | 1.51 | 0.0 | 44.9 | 43.7 | 2 hours, 1500°C, dry $H_2$ |
| | 6 | 1.51 | 3.0 | 48.4 | 45.5 | 15 hours, 1500°C, vacuum |
| | 6 | 1.51 | 3.9 | 44.1 | 44.6 | 31 hours, 1500°C, vacuum |
| | | | -- | 50.0[d] | 46.7 | 100 hours, 1500°C, vacuum |
| | | | -- | 54.8[e] | 56.1 | 100 hours, 1500°C, vacuum |
| | | | 4.5[c] | 58.7[e] | 56.6 | 200 hours, 1500°C, vacuum[b] |

[a] Average pressure $1 \times 10^{-6}$ to $1 \times 10^{-7}$ Torr
[b] Total accumulated time at 1500°C
[c] Weight loss occurring between 100 and 200 hour measurements only
[d] Old method of pressure decay
[e] New method - see text

The photograph in Figs. 56 and 57 were taken after 31 hours and 200 hours of heating at 1500°C in vacuum. The coating has an average thickness of 0.5 to 1.0 μ. From these it can be seen that there was very little change in the coating during the 169 hour interval. Previous experience had shown that the most noticeable change in coating structure occurs in the first few hours at 1500°C when the initial alloy formation takes place. Microscopic examination of the actual metallurgical mounts showed the coating to be more continuous and to have better coverage in the pores than is visible in Figs. 56 and 57.

The flow tests on these samples were very encouraging and demonstrated that the presence of iridium on the surface will not in itself cause catastrophic pore closure. The amount of pore closure indicated by the pressure decay test was essentially the same on the side which was coated with 1.5 mg iridium/$cm^2$ as it was on the side which was not coated. Therefore, the reduction resulted mainly from surface pore shrinkage which was not caused by the coating.

The nitrogen transmission tests confirmed the findings of the surface sensitive pressure decay test. In fact, the transmission may have increased slightly as a result of causes which are not clear at this time. Table XXXI shows that there has been a slight weight loss in both specimens, amounting to about 2 to 3 mg/$cm^2$ of exposed area during the 200 hour heating period. It is possible that some material had vaporized from the pores, slightly enlarging them. Tungsten could also have been lost by vaporization of tungsten oxides due to traces of oxygen in the vacuum chamber.

In any event, the changes in transmission which are insignificant after 200 hours at 1500° would be less at temperatures of 1250°C for more extended periods.

X-ray diffraction patterns were taken after 2, 15, 31, 100, and 200 hours at 1500°C. There was essentially no change in the x-ray pattern. This indicates that the layer 3 to 4 μ deep was essentially unchanged, thus confirming the photomicrographs.

M 4172

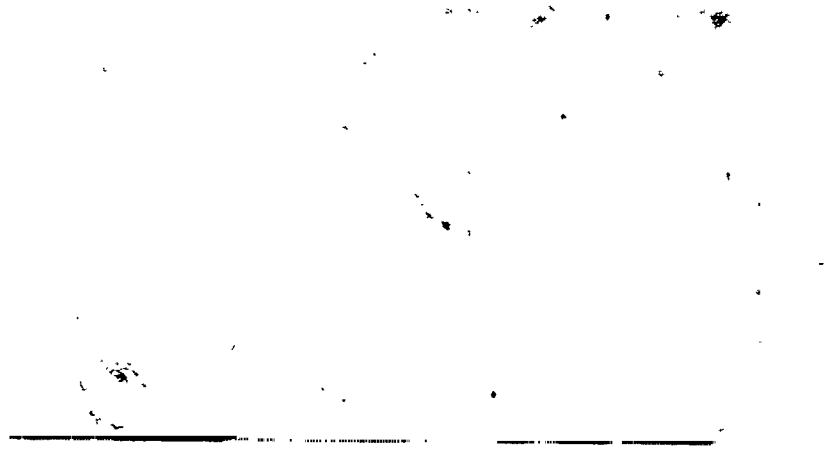

Fig. 56.
Sample 4V Ir, iridium coating on Mod E. 1.4 mg Ir/cm$^2$ after 31 hours at 1500°C in 1 x $10^{-6}$ Torr vacuum; 2000x, Murakami etch.

M 4238

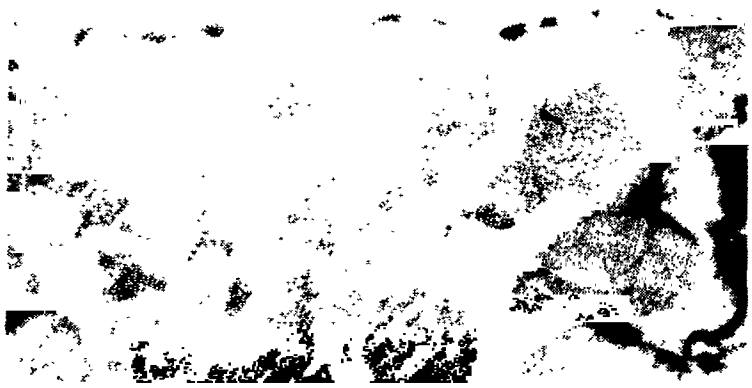

Fig. 57.
Sample 4V Ir, iridium coated, 1.5 mg/cm$^2$, 200 hours at 1500°C in vacuum, 2000x.

## E. TESTING OF IRIDIUM COATED TUNGSTEN

### 1. X-ray Diffraction Studies

X-ray diffraction has been a valuable tool for obtaining a qualitative idea of the iridium coating thickness and the changes which the coating undergoes during high temperature exposure. Although a minor effort was made to determine the nature of the iridium alloy formed by the coating, a complete determination was beyond the scope of this program. The standard alloys necessary for comparison were not available, except for a 50:50 weight basis alloy which was obtained by the high temperature sintering of the tungsten and iridium powders. Fortunately, this sample was in the general composition range of the coatings formed by the impregnation process. Sintered pellets containing 2 and 4% iridium showed essentially nothing but tungsten x-ray diffraction patterns. At this level, iridium forms a solid solution which probably has the same x-ray diffraction pattern as pure tungsten.

X-ray diffraction showed that 0.5 to 1.5 μ iridium coatings deposited by sputtering onto a relatively cool tungsten substrate had essentially no interaction. However, as soon as these were heated even briefly to 1200°C, new phases or alloys with different d-spacings began to appear. Coatings deposited by immersion or spraying, followed by reduction at 1000°C, showed an immediate alloying with the tungsten. The principal peaks which could be attributed to the alloy showed interplanar spacings of d = 2.40 Å and 2.10 Å. These peaks became stronger when the samples were heated to 1500°C, and the overlapping principal iridium and tungsten peaks at d = 2.22 to 2.24 Å diminished in intensity. As more iridium was added and heated at 1500°C, the intensity of the x-ray reflections from 2.40 Å and 2.10 Å spacings continued to increase, while the 2.22 to 2.24 peak began to disappear. In the case of thin iridium coatings of less than about 0.5 μ, the underlying tungsten substrate also showed its typical diffraction pattern, with the intensity of its reflections somewhat reduced by the absorption of the alloy coating.

Table XXXII shows the d-spacing values for a limited number of pure metals, coated samples, and alloys. Two particular coated samples are tabulated because they were heated for extended periods of time at 1500°C, and, being very thin, they should have been in some sort of stable condition. They were also coated by the spray process, so that an approximate value for the surface coverage (in milligram per square centimeter) could be assigned. Sample 4V iridium was coated with 1.5 mg/cm$^2$, and heated for 200 hours at 1500°C in vacuum. Sample iridium No. 3 was coated with 3.1 mg/cm$^2$ and was heated 58-1/2 hours at 1500°C in hydrogen. The thickness of the alloy coating on 4V iridium after heating was 0.5 to 1.0 $\mu$. The coating on iridium No. 3 was 1 to 2 $\mu$ thick. (These were seen previously in Figs. 56 and 57.) Sample No. 227 was made from a 50:50 by weight mixture of Ir:W powder which was sintered for 36 hours at 2200°C. It is assumed to be completely alloyed. Sample No. 276 was prepared from a three times arc melted 50:50 mixture which was then crushed, spheroidized, and sintered two hours at 1600°C. The prominence of the tungsten peaks in this sample compared with No. 227 indicates that there may still be free tungsten and that arc melting was not complete. Number 276 is included merely for comparison.

Comparison of the x-ray data obtained from the coated samples with data from alloy No. 227 shows rather clearly that the coating must be roughly a 50:50 alloy of tungsten and iridium which would lie in the $\epsilon$ phase region. (See Fig. 58) This estimate is upheld by the fact that the unalloyed coatings deposited by sputtering increase in thickness by about 100% after being heated to about 1500° C. The thickness then remains essentially constant for at least 200 hours at 1500°C.

Most of the d-spacings of the alloy coatings correspond to the close-packed hexagonal structure of the $\epsilon$ phase. However, the most prominent d-spacing at 2.10 to 2.11 Å does not fit this structure. Thus the true structure is still in doubt at this time. In this type of diffusion coating, structural determinations are complicated by the fact that a

## TABLE XXXII

### X-ray Diffraction Patterns of Iridium, Tungsten, and Coatings of Iridium on Tungsten

| d spacing, Å | Iridium Pure Powder | Tungsten Pure Powder or Solid | No. 227[a] 50:50 Sintered Alloy | No. 276[b] 50:50 Arc Melted | 4V Ir[c] 1.5 mg/cm Coating | Ir No. 3 3.1 mg/cm$^2$ Coating | Probable Identity |
|---|---|---|---|---|---|---|---|
| Relative Reflection Intensity (Peak Height) | | | | | | | |
| 2.40 | | | 10 | 26 | 25 | 28 | Alloy 2[d] |
| 2.22[e] | 100 | | 5 | 42 | 100 | 19 | Ir 1 |
| 2.24[e] | | 100 | | | | | W 1 |
| 2.11 | | | | 100 | 81 | 100 | Alloy 1 |
| 2.10 | | | 100 | | | | Alloy 1 |
| 1.92 | 50 | | | | | | Ir 2 |
| 1.63 | | | 2 | 21 | 13 | 16 | Alloy |
| 1.58 | | 15 | | 1 | 50 | 6 | W 3 |
| 1.38 | 41 | | 30 | 17 | 13 | 30 | Ir 4 |
| 1.30 | | | | | | 15 | W 2 |
| 1.29 | | 23 | 1 | 2 | 50 | | W 2 |
| 1.27 | | | 2 | | | | Alloy |
| 1.26 | | | | 2 | 19 | 20 | Alloy |
| 1.20 | | | 8 | | | | Alloy |
| 1.19 | | | | 5 | 5 | 10 | Alloy |
| 1.18 | | | 12 | | | | Alloy |
| 1.17 | | | | 15 | 15 | 25 | Alloy |
| 1.16 | 47 | | 21 | 5 | | | Ir 3 |
| 1.15 | | | | | | 19 | Ir 3 |
| 1.12 | | 8 | 9 | 3 | | 9 | W 4 |
| 1.11 | 15 | | | | | | Ir 5 |

[a] 50:50 mixture of W and Ir powder, pressed and sintered 36 hours at 2200°C
[b] 50:50 mixture of W and Ir arc melted three times, crushed spheroidized and sintered 2 hrs at 1600°C — possible incomplete alloy.
[c] spray coated Mod E - heated 200 hrs. at 1500°C in vacuum
[d] number indicates relative magnitude of peak usually found within the W, Ir, or alloy diffraction pattern
[e] these two peaks usually overlap and are indistinguishable

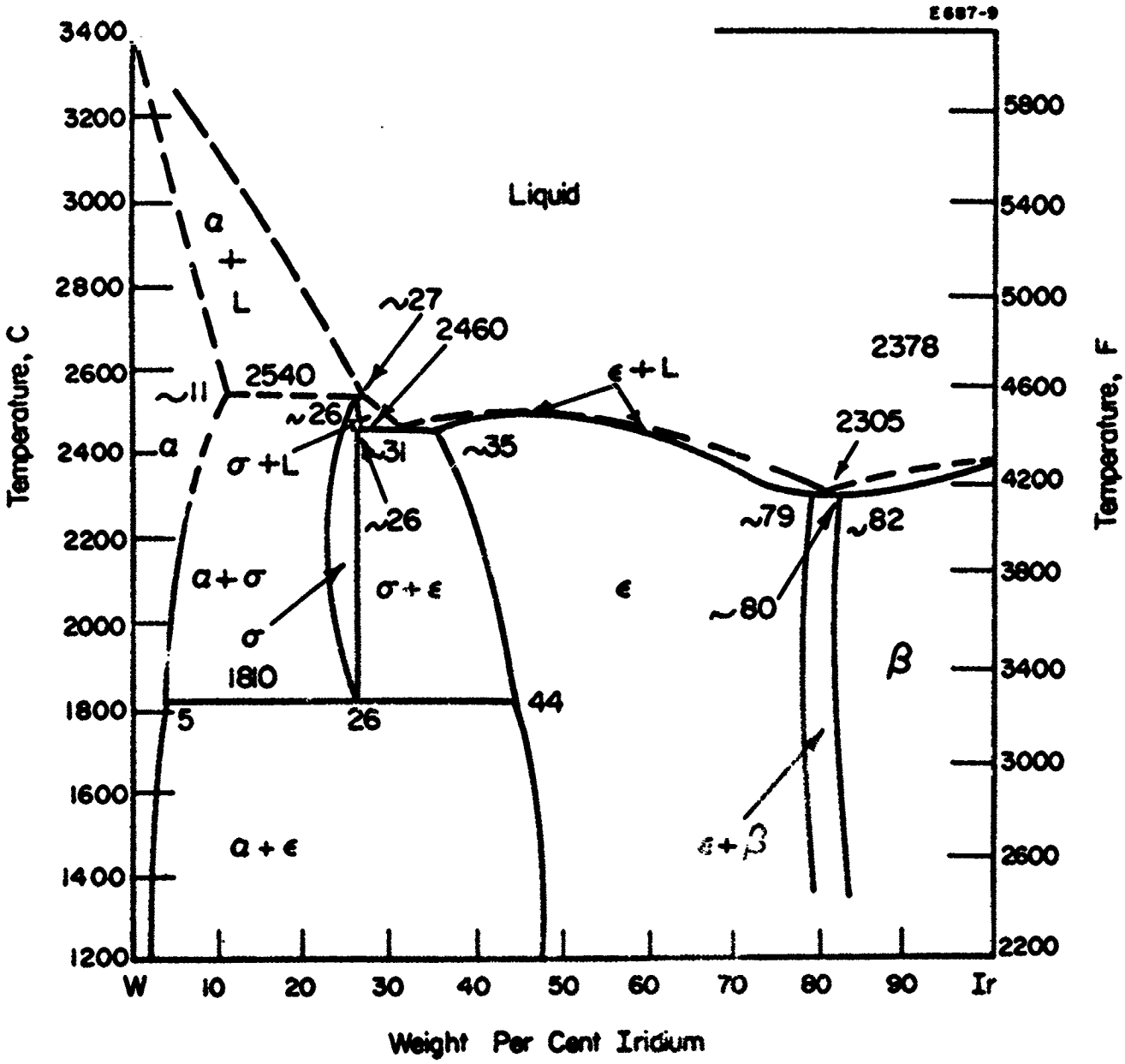


Fig. 58. Phase diagram for tungsten-iridium system. (From DMIC Report No. 183, February 7, 1963, (84-1)-63.)

gradation of composition can exist because of the inexhaustible supply of tungsten and the limited supply of iridium.

The photomicrographs of sample 4V iridium after 31 and 200 hours at 1500°C show that there is a high degree of resistance to further diffusion after the alloy is once formed. X-ray diffraction patterns taken after 2, 15, 31, 100, and 200 hours at 1500°C also showed that there was essentially no change. The diffraction peak height ratios over this period changed very little, as shown in Table XXXIII. Throughout all the x-ray studies, the power settings were held constant so that the true diffraction amplitudes from the coatings themselves could be recorded faithfully. The graphs showed little change in absolute peak heights, indicating a constant coating thickness for the samples after heat treatment.

TABLE XXXIII

Changes in Ratios of Principal X-ray Reflections From Iridium Coated Mod E Porous Tungsten During Heating at 1500°C

| Interplanar Spacing Ratio | Reflection Peak Height Ratio After Various Times at 1500°C | | | | |
|---|---|---|---|---|---|
| | 2 hours | 15 hours | 31 hours | 100 hours | 200 hours |
| $\frac{2.23\ \text{Å}}{2.10\ \text{Å}}$ | 1.43 | 1.35 | 1.39 | 1.39 | 1.24 |
| $\frac{2.23\ \text{Å}}{2.39\ \text{Å}}$ | 4.3 | 3.67 | 4.4 | 4.2 | 4.1 |

2. Electrical Tests

Several work function and cesium ionization tests have been performed on iridium coated tungsten. The data are still too incomplete to say more than that the results are promising and that more thorough testing seems warranted. In preliminary tests, the work function has been raised and the neutral fraction has been lowered without undue elevation of the critical temperature.

Dr. R. G. Wilson of HRL under Contracts NAS 3-5249 and NAS 3-6278 used a vacuum tube type test in which the iridium coated tungsten was held in vacuum and in various cesium vapor pressures for tests as a front fed ionizer. The alloyed surface was found to have an effective thermionic work function of 5.28 ±0.03 eV compared with 5.27 ±0.03 eV for pure outgassed iridium and 4.51 ±0.03 eV for solid tungsten. The critical temperature was found to be not more than 50°K higher than tungsten. This sample had been coated by the immersion technique with 0.3% iridium, then heated 4 hours at 1500°C in hydrogen.

Two 0.18 in. diameter button ionizers were spray coated with iridium for testing by D. F. Hall and H. Shelton under Contract NAS 3-7109 at TRW Systems. The base material was HRL 3.9 μ porous tungsten. Sample B, which was coated with 0.5 to 1.0 μ gave a 4.88 eV work function at 5 mA/cm$^2$ and a neutral efflux of 0.35% at 20 mA/cm$^2$. According to Hall and Shelton, the results obtained on this sample were better than for any previous good clean or carbided tungsten which they had tested up to that time. The ionizer was subsequently treated with $5 \times 10^{-6}$ Torr oxygen according to their standard procedures and was adversely affected. Recovery to its original level was not complete.

Sample A was unintentionally given a heavier coating than anticipated, so that its nitrogen transmission was reduced to about 50% of its original value. The coating was estimated to be 1 to 2 μ thick, but it was probable that many of the small pores were sealed. The work function of this ionizer was estimated to be 4.8 eV at 1 to 5 mA/cm$^2$, but it dropped to about 4.6 eV at 20 mA/cm$^2$. The neutral fraction was no better than that of pure tungsten. As they also had considerable trouble with this ionizer in bringing it to a clean condition, it should probably not be considered a representative test.

---

Tests conducted after the close of this contract indicated that Hall and Shelton were probably losing the coating by negative copper ion sputtering while their tests were being performed.

A single strip ionizer coated with 3.6 mg/cm$^2$ by the spray process was tested at HRL. In one short series of measurements, it gave a work function of 5.1 to 5.2 eV and a neutral fraction of about 0.02% at 7.5 mA/cm$^2$. System problems prevented further testing. A second single strip ionizer was coated with 0.6 mg iridium/cm$^2$, a much thinner coating. This was not tested in time to be reported herein.

A single strip ionizer which was sputter coated with 1.5 $\mu$ of iridium had a neutral fraction of 0.035% at 10 mA/cm$^2$. Over the testing range, the neutral fraction was 5 to 10% of the tungsten value.

## F. CONCLUSIONS AND RECOMMENDATIONS CONCERNING COATING WITH IRIDIUM

These electrical tests, even though incomplete, indicate that the iridium coatings will afford a very significant improvement over a pure tungsten surface. However, the true value of this type of coated ionizer can be accurately determined only by extended operation as a practical ion engine. Such a test is required to determine the actual effect on ionization efficiency as a result of the loss of surface alloy by inward diffusion, the long term effect of cesium vapor and the ionization process, and iridium loss by oxidation or vaporization. Another important unknown is the effect of materials from the test environment which strike the ionizer surface as a result of sputtering by the cesium ion beam.

In addition to actual engine tests, more information should be obtained on the relationship between pore size, pore concentration, coating thickness, and thermal stability. These data could be obtained from a series of iridium coatings of differing thicknesses on porous tungsten of various pore counts. After thermal aging at 1500°C for periods of several hundred hours, the optimum combination could be determined by nitrogen transmission tests, metallographic examination, and x-ray diffraction.

BLANK PAGE

## IV. RHENIUM COATING OF POROUS TUNGSTEN

From the theoretical standpoint, rhenium should be practically as efficient an ionizer as iridium. It has the proper physical properties and has a work function which is almost as high as that of iridium. As its chemical properties are somewhat similar to those of iridium, the same general techniques for coating were tried. Many of the techniques evolved for iridium were almost directly applicable to rhenium. However, more emphasis was placed on iridium than on rhenium during the program, primarily because the early work on iridium was very promising. It seemed advisable to bring iridium to the stage where electrical and stability tests could be made in more detail before switching to a more concentrated study of rhenium.

Four methods of coating were briefly investigated. A commercial rhenium electroplating solution was tried with some success. Porous samples were coated by immersion and spraying in a manner similar to iridium. Sputtering was also found to be a satisfactory method for deposition. One minor test was performed on the thermal reduction of $ReCl_5$ vapors on heated tungsten.

### A. COATING WITH RHENIUM BY ELECTROPLATING

Using a proprietary "Rhenium A" salt (Technic, Inc.), some exploratory plating tests were performed first on solid tungsten. Various cleaning procedures were used (such as hot NaOH followed by HF and $H_2O$ rinses, and an etch made from equal volumes of formic acid; $H_2O_2$ (30%):, and $H_2O$ at 50°C). It was found that at 0.15 A/cm$^2$ at 65°C about 1 $\mu$ of rhenium was deposited in 20 min, but adhesion was poor.

Porous samples had their surfaces prepared by first saturating with water and then chemical etching in the above formic acid, $H_2O_2$, $H_2O$ solution. Other samples were wet hydrogen fired. The latter process was preferred because it did not enlarge the pores.

A sample of Mod E was etched by the above solution and plated at 0.22 A/cm$^2$ for 16 min at 65°C. A second sample of Mod E, PW Re No. 3, was wet hydrogen fired at 1000°C and plated at 0.15 A/cm$^2$ for 12 min at 65°C. Both plating conditions produced a grey to black deposit which was converted to a silvery grey by heating for 30 min at 1050°C in hydrogen.

The samples were potted in uranium glass and metallurgically examined at 2000x. Both samples were plated in the center with ~0.6 to 0.8 μ of rhenium. The coating was considerably thicker at the edges. The chemically etched sample showed gross pore enlargement and so was not studied further. Sample PW Re 3 is shown in Fig. 59. The coating follows the contours of the pores even down into the pores. However, it appears to have shrunk away from the substrate and to have developed shrinkage cracks.

These results suggested that the technique should be changed to give a more uniform coating and to minimize the shrinkage problem. The shrinkage is believed to result from decomposition of rhenium hydride, which is formed during plating. The hydride is also probably responsible for the dark grey or black color before firing.

In order to minimize shrinkage, two shorter plating cycles were used in the next test. The plating test was performed on Sample PW Re 4, pellet No. 66, a 0.5 in. by 0.125 in. disk of sintered spherical 5.3 μ powder. It was wet and dry hydrogen fired as a preliminary cleanup procedure. The disk was mounted on a glass holder and sealed against the flat glass surface with a rubber gasket. In this manner, only the front surface of the disk was exposed for plating. A small positive pressure of distilled water was applied behind the disk. The slight flow of water through the disk thus prevented the plating solution from penetrating into the porous tungsten.

Using "Rhenium A" solution, the sample was plated twice at 0.08 A/cm$^2$ and 65 to 75°C with a 30 min dry hydrogen fire at 1000°C after each plating. The dark grey as-plated deposit was converted to a silver grey by the firing process.

Examination of the surface at 1000x showed no gross closing of pores. The deposit appeared adherent, but the flat surface of the polished grains had a wrinkled appearance. Examination of the cross section at 2000x showed a single layered coating about 0.6 to 0.8 $\mu$ thick. Compared with the previous single plating cycle, the coating was much more adherent and had fewer noticeable discontinuities due to shrinkage. Figure 60 shows the coating in an area near the center of the sample after the last 1000°C firing. The plate was slightly thicker at the edges. After heating for 3-3/4 hours at 1500°C, the coating was just barely visible, but it seemed to be in better contact with the substrate. Efforts to obtain satisfactory photomicrographs of the coating after the 1500°C treatment were unsuccessful.

X-ray diffraction showed very well the presence of the as-plated coating after the 1000°C heating. After the 1500° treatment, the peaks were reduced about 20%. The placement of the peaks was not changed by the second heating; this indicated that, as in the case of the iridium, alloying takes place at 1000°C.

In order to improve the plating uniformity, another sample was plated with two coats under the same conditions as above, except that the bath was stirred. A 0.27 in. diameter button ionizer was used so that the effect of the curved surface could be observed. The color of the as-deposited coating was about the same as previously, but the coating thickness was more uniform. There was no significant effect caused by slight concavity of the ionizer surface. The plating process might thus be suitable for machined ionizers. The coating is shown in Fig. 61 as it appeared after 30 min of 1000°C heating.

## B. COATING BY IMMERSION IN A RHENIUM SOLUTION

The impregnation with rhenium was performed essentially in the same manner as with iridium. The solubility of the rhenium pentachloride, $ReCl_5$, in the solvents used for $IrCl_4$ was determined.

M 4708

Fig. 59.
Sample PW Re No. 3.
Electroplated rhenium on
Mod E tungsten, 2000x.

M 4710

Fig. 60.
Pellet No. 66, Sample
PW Re No. 4. Rhenium
electroplated twice in
still bath, 2000x.

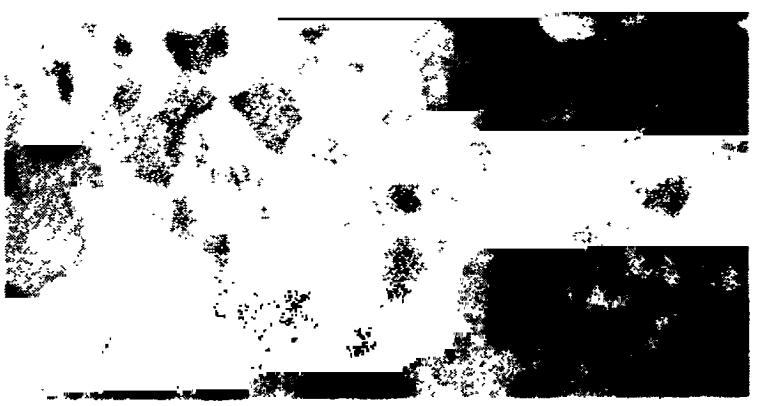

Anhydrous ethyl alcohol and tetrahydrofuran were found to be excellent solvents. The dark greenish-brown solutions formed were clear and stable.

Tests were performed on two types of HRL spheroidized porous tungsten. After wet hydrogen firing, the pressure decay method was used to determine surface porosity, so that the effect of the added rhenium could be measured. A solution of 0.5 of $ReCl_5$ in 5 $cm^3$ of alcohol was the impregnating solution used for Pellet 102, and 0.5 g of $ReCl_5$ was dissolved in 5 $cm^3$ of tetrahydrofuran (THF) for impregnating Pellet 137. The pellets were immersed in their respective solutions, dried at 100°C, and wet hydrogen fired at 1000°C for 30 min. The wet hydrogen was used to act as an oxidizer to remove traces of organic matter which might be deposited from the solvents. It would also help hydrolyze $ReCl_5$ in order to reduce its tendency to vaporize. $ReCl_5$ can vaporize in dry hydrogen at 200 to 300°C. The results of these tests are shown in Table XXXIV. Nitrogen pressure decay tests were performed on each side of the pellet after each 1000°C firing and after the final firing for 2.5 hours at 1500°C in dry hydrogen. As in the case of iridium, the nitrogen pressure decay showed that the 1500°C heating improved the surface porosity.

Although these more concentrated solutions of $ReCl_5$ added rhenium metal at a faster rate than the previous ammonia-$IrCl_4$ solution, the rhenium was apparently deposited throughout the pores rather than on the surface. An x-ray diffraction pattern taken from a 0.5 μ sputtered rhenium coating which had been heated for 1 hour at 1200°C showed about five times as much rhenium as the impregnated samples after the addition of 0.3% rhenium. Iridium at this concentration would have showed up strongly in x-ray diffraction.

The lack of concentration on the surface could also have been caused by a partial vaporization of $ReCl_5$ during the hydrogen reduction. Immediately after this experiment, the spray method was used very successfully with iridium to give a high surface concentration. The method was therefore tried for rhenium, as described below.

## TABLE XXXIV

### Rhenium Impregnation by Immersion

| Number of Impregnations | Addition of Rhenium in Alcohol Pellet No. 102 | Pressure Decay,[a] Sec | Addition of Rhenium in THF, Pellet No. 137 | Pressure Decay, Sec | Treatment (Same for both Pellets) |
|---|---|---|---|---|---|
| . | Total Weight | | Total Weight | | |
| 0 | 5.4072 | 402/404 | 4.9528 | 133/136 | -- |
| 1 | 5.4106 | 412/418 | 4.9565 | 157/172 | 30 min 1000°C, $H_2$ |
| 2 | 5.41476 | 418/423 | 4.9612 | 170/173 | 30 min 1000°C $H_2$ |
| 3 | 5.4178 | 460/483 | 4.9647 | 173/193 | 30 min 1000°C, $H_2$ |
| 4 | 5.4212 | 500/509 | 4.9688 | 183/208 | 30 min 1000°C, $H_2$ |
| -- | 5.4211 | 468/469 | 4.9686 | 155/173 | 2 hours 1500°C, $H_2$ |
| 5 | 5.4242 | 472/502 | 4.9713 | 164/183 | 30 min 1000°C, $H_2$ |
| 6 | 5.4272 | 496/500 | 4.9745 | 177/199 | 30 min 1000°C, $H_2$ |
| -- | -- | 467/485 | -- | 147/165 | 2.5 hours 1500°C, $H_2$ |
| % Rhenium Added | 0.37% | | 0.44% | | |

[a]Side 1/Side 2
Pellet No. 102 3.9 μ spherical tungsten - 79% dense
Pellet No. 137 6.9 μ spherical tungsten - 76.7% dense
Both pellets were 1/2 inch in diameter by 1/8 inch thick

## C. COATING BY SPRAYING WITH A RHENIUM SOLUTION

In general, the spray method was found to be a vast improvement over the immersion method because it concentrated the rhenium almost exclusively on one surface. X-ray diffraction of the sprayed coating gave essentially the same patterns as the sputtered iridium coatings. Metallographic examination confirmed this, although the thinner coatings were hard to see after heating to 1500°C. Thus, it was possible to assign a millimeter per square centimeter value to the coating so that it could be conveniently described.

The spray impregnation tests were performed on sections 1/2 in. by 1 in. by 1/8 in. cut from slab 313-S which was made of Ampro C 3.8 μ spheroidized tungsten powder which had been sintered to 80% density. The surface was in the as-pressed condition, which was smooth but not metallurgically polished.

The spray apparatus used was an all glass nasal spray powered by a rubber squeeze bulb. Two solutions were used. For sample 1R, 0.25 g of $ReCl_5$ were dissolved in 5 $cm^3$ of anhydrous alcohol. For sample 2R 0.25 g of $ReCl_5$ were dissolved in 5 $cm^3$ of tetrahydrofuran (THF). The flat porous tungsten sample was placed on a hot plate and brought to the desired temperature (finally determined to be about 80°C). The surface was sprayed slowly and evenly to allow the solvent to evaporate. As soon as the surface darkened, as a result of a surface buildup of the $ReCl_5$, coating was discontinued and the sample was dried further at 100°C. It was then wet hydrogen fired at 950 to 1000°C for 30 min. Weights and nitrogen pressure decay were measured after each impregnation and firing.

The first series of rhenium coatings were applied at a sample temperature considerably above the boiling point of the solvent. This caused a loose, curling deposit. An adherent deposit was obtained if the tungsten was only slightly above the boiling point, so that the deposit had more chance to penetrate into the porous surface.

The results of the coating experiments are shown in Table XXXV. The nitrogen pressure decay tests were somewhat erratic, but they generally showed a rather modest loss in porosity, considering the heavy surface coating. A similar degree of loss was noted in the iridium coated sample No. 3 Ir, which was prepared at the same time.

As shown in Fig. 62, sample 1R had an excellent surface layer of rhenium alloy about 1-1/2 $\mu$ thick. This was formed by a deposit of 2.7 mg/cm$^2$ from an alcoholic solution. Sample 2R, which had a 1.2 mg/cm$^2$ coating, did not show up nearly as well in the photomicrograph, although it could be seen visually.

TABLE XXXV

Impregnation of Porous Tungsten with Rhenium by the Spray Method

| Sample | 1R Alcohol Solution Rhenium | 2R THF Solution Rhenium | No. 3 $H_2O$ Solution Iridium |
|---|---|---|---|
| No. Spray costs | 5 | 5 | 7 |
| Initial Sample Weight[a] | 14.9894 g | 15.4804 g | 18.1860 |
| Weight Added | 8.5 mg | 4.0 mg | 13.9 mg |
| mg/cm$^2$ | 2.7 | 1.2 | 3.1 |
| Pressure Decay Before Coating | 402 sec | 334 | 350 |
| Final Pressure Decay | 428 sec | 388 | 384 |

[a]There was no weight gain or loss after firing the samples for 4 hours in 1500°C dry $H_2$.

M 4709

Fig. 61.
Sample PW Re No. 5.
Rhenium electroplated twice in stirred bath, 3000x.

M 4090

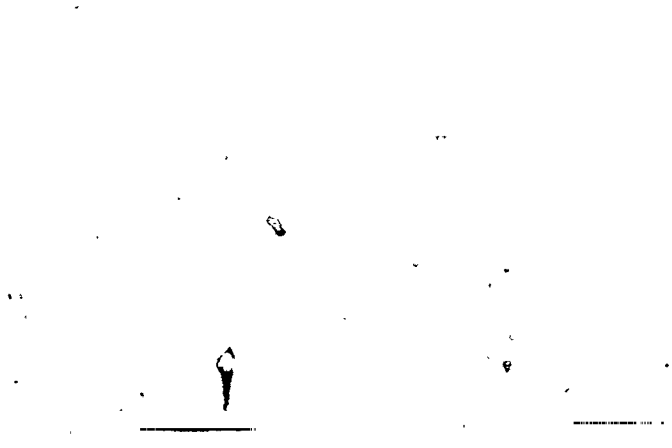

Fig. 62.
Sample 1 R, rhenium spray coat of 2.7 mg/cm$^2$ on 3.9 μ porous tungsten heated 4 hours at 1500°C, 2000x, Murakami etch.

One preliminary series of spray coatings with ammonium perrhenate was carried out. It was thoughtpossible that this compound would be more desirable for use in spray coating because it is water soluble. Rhenium pentachloride, as described previously, had to be dissolved in oxygenated organic solvents such as alcohol or tetrahydrofuran. X-ray diffraction patterns of rhenium coatings obtained from these organic solvents had occasionally shown very faint peaks which might be attributable to WC. This indicated a possible interaction of the $ReCl_5$ solvent complex and the tungsten. If a WC impurity were concentrated on the surface, it could mask or alter the work function obtained from the rhenium coating.

To utilize a nonorganic system, ammonium perrhenate (0.25 g), was dissolved in 6.0 mliter $H_2O$. A Brinkman Instruments all-glass atomizer was used to spray the solution lightly onto the porous tungsten, which was heated to about 120°C. Since the deposit was colorless to white, it was difficult to judge how much had been sprayed on. The area coated was approximately 2.5 $cm^2$. As the ammonium perrhenate was quite volatile, the tungsten sample was first reduced at temperatures between 400° and 300°C where the volatility was low. It was then heated to 1000°C.

The first 400°C reduction indicated that there was enough volatility of the perrhenate to cause it to be transferred to and reduced on the alumina boat. The reduction temperatures were then lowered to 300 to 350°C. Table XXXVI shows the results of six spray coatings which deposited up to 3.1 $mg/cm^2$.

It can be seen that there was a slight increase in pressure decay time after only 1.75 mg $Re/cm^2$ was added. However, there was no x-ray diffraction pattern from rhenium at this level. The previous $ReCl_5$-THF solution deposit gave a distinct pattern at only 1.2 $mg/cm^2$. As the perrhenate sample had not been x-rayed before the 1500°C firing, it was given two additional coatings using only the 1000°C firing to minimize diffusion. After the addition of another 1.35 mg $Re/cm^2$ without

## TABLE XXXVI

### Results of Spray Coating with Ammonium Perrhenate Solution

| Number of Coats | Sample Weight, g | Total Rhenium Added, mg | Amount Deposited Per Unit Area, $mg/cm^2$ | Pressure Decay Time, Sec | | Comment |
|---|---|---|---|---|---|---|
| | | | | Coated Side | Uncoated Side | |
| 0 | 17.5109 | 0 | 0 | 344.8 | 351.6 | Initial |
| 1 | 17.5115 | +0.6 | 0.24 | 351.7 | --- | Reduce at 400°C, 15 min, wet $H_2$ then 1000°C, 15 min, wet $H_2$ |
| 2 | 17.5127 | +1.8 | 0.73 | 367.8 | --- | 350°C, 15 min, wet $H_2$; 1000°C, 15 min, wet $H_2$ |
| 3 | 17.5142 | +3.3 | 1.34 | 381.5 | --- | 300°C, 15 min, wet $H_2$; 1000°C, 15 min, wet $H_2$ |
| 4 | 17.5152 | +4.3 | 1.75 | 377.9 | --- | 1000°C, 15 min, wet $H_2$ |
| 4 | 17.5148 | --- | --- | 385.2 | --- | 1 hour 10 min, 1500°C, dry $H_2$ - X-ray pattern absent |
| 4 | 17.5150 | --- | --- | --- | --- | 1 hour, wet $H_2$ fire |
| 5 | 17.5155 | +4.8 | 1.96 | --- | --- | 300°C, 15 min, wet $H_2$; 1000°C, 15 min, wet $H_2$ |
| 6 | 17.5183 | +7.6 | 3.10 | 368.7 | 371.8 | 1000°C, 15 min, wet $H_2$ very slight X-ray pattern[a] |

[a]Sample - 3.9 μ HRL porous tungsten, 2.45 $cm^2$ area
Spray coating solution - 0.25 g of ammonium perrhenate in 6.0 mliter of $H_2O$

the 1500°C firing, a very faint rhenium diffraction pattern was seen. However, it was still only about 5% as intense as a pattern obtained from 1.2 mg Re/cm$^2$ spray deposited from the THF, even after the latter was heated for 70 min at 1500°C.

A metallographic examination performed on this sample showed an irregular diffuse coating less than 0.5 μ thick. It was very difficult to see.

The x-ray diffraction tests indicate that before it is reduced to the metal, most of the ammonium perrhenate tends to vaporize from the outer surface, where it must be located for surface work function modifications. However, the pressure decay tests showed that the pores below the depth of x-ray penetration (3 to 4 μ) were constricted by a rhenium deposit. The weight gain also confirmed the presence of rhenium.

The perrhenate method will undoubtedly give a cleaner rhenium deposit than will the organic solutions of $ReCl_5$. However, the exact conditions of time and temperature will have to be determined, in order that it can be reduced on the outermost surface without being lost by evaporation.

## D. COATINGS WITH RHENIUM BY VAPOR PLATING

The vapor pressure of $ReCl_5$ is sufficiently high that it can be used as a source of rhenium in vapor plating. One simple experiment was tried which showed that an identifiable rhenium layer could be deposited by this process using the thermal decomposition of $ReCl_5$.

About 1 g of $ReCl_5$ was placed in a small effusion cup with a 0.15 in. outlet. The tungsten piece about 3/8 in. by 3/8 in. which was to be plated, was placed 1 in. in front of the effusion cup. This target could be heated to 700 to 800°C by a heater coil mounted behind it. The heater elements were shielded from the effusing $ReCl_5$ vapor. The apparatus was placed in a larger glas tube and evacuated. When the tungsten target was heated to 700 to 800°C, the effusion cup was

heated to 120°C. After a 20 min plating period, the sample was removed and analyzed by x-ray diffraction. A weak but definite rhenium pattern was detected and was estimated to be 0.1 to 0.2 μ thick. No further tests were performed on this process, but it obviously could be used under the proper conditions.

## E. COATING WITH RHENIUM BY SPUTTERING

Porous rhenium coatings which were 0.5 and 1.5 μ thick were successfully sputtered onto tungsten by Philips Metalonics. Several of these 0.5 μ coatings are shown in Figs. 63 through 65. A one-strip ionizer was also sputter coated and tested briefly under Contract NAS 3-6270. However, the coating was suspected of developing a loose flake which caused a disabling arc. The porosity of these coatings is apparently as good as that of the iridium coatings.

## F. TESTING OF RHENIUM COATED TUNGSTEN

### 1. Thermal Stability Tests

The thermal stability of the rhenium coatings was studied only briefly. The little information obtained indicated that the thin coatings might be less stable than similar iridium coatings. As in the case of iridium, heating at 1500° converts a thin, pure rhenium coating into an alloy. Previously described samples 1R and 2R coated with 2.7 mg/cm$^2$ and 1.2 mg/cm$^2$ were heated for 58-1/2 hours in 1500°C dry $H_2$. After this, the formerly distinct x-ray diffraction pattern caused by the surface alloy had essentially disappeared. Sample 1R was shown (Fig. 62) to have a very distinct coating after 4 hours at 1500°C; however, after 58-1/2 hours at 1500°C in hydrogen, it was no longer visible. It is possible that the coating may have diffused inward and been diluted to the point where the alloy solid solution looked the same as tungsten both

M 3947

Fig. 63.
Photomicrograph (2000x) of a sample of Mod E tungsten sputter coated with a 0.5 μ thick coating of rhenium.

M 3952

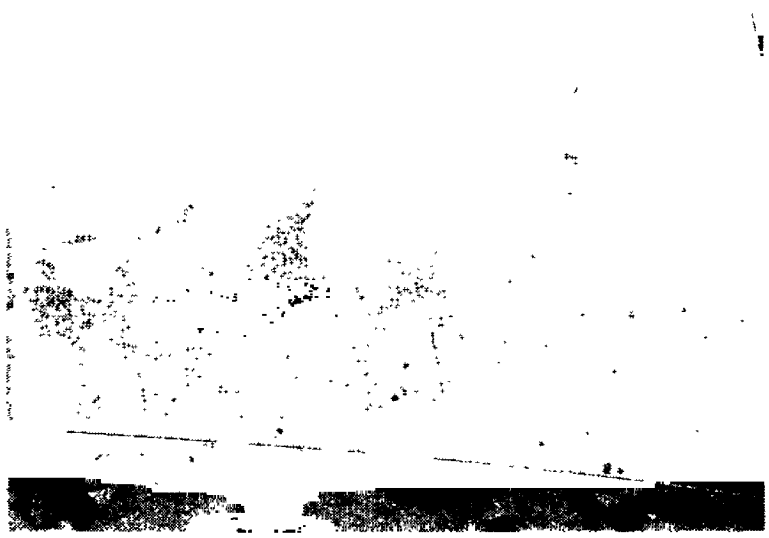

Fig. 64.
Photomicrograph (2000x) of Mod E tungsten sputter coated with rhenium and vacuum fired at 1200°C for 4 hours (0.5 μ thick original coating).

M 3946

Fig. 65.
Photomicrograph (2000x) of Mod E tungsten sputter coated with rhenium and vacuum fired at 1800°C for 4 hours (0.5 μ thick original coating).

on the photomicrograph and x-ray diffraction. Another possibility is that is may have been vaporized by water or oxygen in the hydrogen atmosphere. Some rhenium was present in the outer 0.001 in., however, because an emission spectrographic analysis of surface scrapings showed about 4% rhenium.

Rhenium may have better stability in vacuum than in hydrogen, as illustrated by Figs. 63 through 65. These photomicrographs show that the 0.5 $\mu$ coating remains even after 4 hours at 1800°C, although it is not as prominent or easy to see as similar iridium coatings. X-ray fluorescence data by Philips Metalonics indicated that the coating which was originally 0.5 $\mu$ thick still contained rhenium in the surface layer to a depth of 3 to 5 $\mu$ or less even after 4 hours at 1800°C in vacuum. It was diluted to somewhat less than a 50% concentration by the underlying tungsten. X-ray diffraction did not show an alloy pattern after the 1800°C treatment.

In another test, a 1.5 $\mu$ sputtered coating was heated for 100 hours at 1500°C in vacuum. X-ray diffraction showed that a substantial surface alloy still existed. The patterns of 1.5 $\mu$ coatings after 4 hours at 1800°C and 100 hours at 1500°C were quite similar.

These limited tests probably signify that there may be a lower limit in coating thickness which must be exceeded before the rhenium alloy remains on the surface during extended heating in a form which is identifiable by x-ray diffraction.

## 2. X-Ray Diffraction Studies

The x-ray patterns obtained from various coatings of rhenium indicate that alloying definitely takes place when the samples are heated to 1500°C. Several representative patterns are shown in Table XXXVII. These reflection intensities at various interplanar spacings were normalized to show the highest peak on the pattern as 100. The patterns are considerably more complicated than those from iridium, and no attempt has yet been made to identify the composition of the coating from the various d-spacings. Some qualitative observations are possible, however.

# TABLE XXXVII

## Interplanar Spacings of Rhenium, Tungsten, and Coatings of Rhenium on Tungsten

| Sample<br>d-spacings, Å | Pure Porous Tungsten | Pure Rhenium Powder | R-23[a, b]<br>3.1 mg/cm$^2$<br>100 hours at 1500°C<br>In Vacuum | R-28<br>3.1 mg/cm$^2$<br>4 hours at 1800°C<br>In Vacuum | 1R<br>2.7 mg/cm$^2$<br>2 hours at 1000°C<br>In $H_2$ | 1R<br>2-1/2 hours<br>1500°C<br>In $H_2$ | 1R<br>58-1/2 hours<br>1500°C<br>In $H_2$ | Probable Identity |
|---|---|---|---|---|---|---|---|---|
| | | | | Relative Peak Heights | | | | |
| 2.58 | | | 6 | 9 | | 11 | | Alloy |
| 2.50 | | | 9 | 24 | | 47 | | Alloy |
| 2.32 | | 30 | | 2 | 23 | 52 | | $Re_3$[c] |
| 2.82 | | | 81 | 100 | | 26 | 5 | Alloy |
| 2.26 | | | 35 | 49 | | 1 | | Alloy |
| 2.24[d] | 100 | | | | 100 | 100 | 100 | $W_1$ |
| 2.23[d] | | 37 | 100 | 79 | 20 | | | $Re_2$ |
| 2.16 | | | 32 | 59 | | 29 | | Alloy |
| 2.11 | | 100 | 73 | 100 | 98 | 16 | | $Re_1$ |
| 2.06 | | | 38 | 55 | | 13 | 4 | Alloy |
| 2.01 | | | 8 | 12 | | | | Alloy |
| 1.92 | | | 8 | 12 | | | 3 | Alloy |
| 1.88 | | | 1 | 3 | | | 4 | Alloy |
| 1.82 | | | 2 | 5 | | | | Alloy |
| 1.79 | | | 3 | 5 | | | | Alloy |
| 1.76 | | | 3 | 4 | | | | Alloy |
| 1.68 | | | 3 | 4 | | 10 | | Alloy |
| 1.63 | | 27 | | | 12 | 18 | | $Re_5$ |
| 1.58 | 15 | | | | 29 | 10 | 30 | $W_3$ |
| 1.57 | | | 26 | 13 | | | | Alloy |
| 1.52 | | | 3 | 4 | | 13 | | Alloy |
| 1.50 | | | 3 | 4 | | | | Alloy |
| 1.45 | | | 4 | 5 | | | | Alloy |
| 1.38 | | 38 | 12 | 13 | 18 | 24 | | $Re_4$ |
| 1.35 | | | 11 | 22 | | 26 | | Alloy |
| 1.34 | | 36 | 2 | 6 | | 55 | | $Re_4$ |
| 1.33 | | | 3 | 5 | | | | Alloy |
| 1.32 | | | 9 | 11 | | | | Alloy |
| 1.31 | | | 4 | 6 | | 10 | | Alloy |
| 1.29 | 23 | | | | 71 | 10 | 60 | $W_2$ |
| 1.28 | | | 42 | 23 | | | | Alloy |
| 1.26 | | 35 | 3 | 8 | 15 | | | $Re_4$ |
| 1.20 | | 10 | | | 5 | 16 | | $Re_5$ |
| 1.17 | | 32 | | | 15 | | | $Re_4$ |
| 1.15 | | 32 | 11 | 6 | 15 | | | $Re_4$ |
| 1.12 | 8 | | | | 30 | | | $W_4$ |
| 1.11 | | 7 | | 6 | 12 | | | $Re_5$ |

[a] Mg Re/cm$^2$

[b] See text for more complete description

[c] Subscript indicates relative magnitude within tungsten, alloy, or rhenium group of peaks

[d] These peaks are usually overlapping

It has been observed that a 0.5 μ coating was optically visible after both 1 hour at 1200°C and 4 hours at 1800°C. A distinct alloy pattern was visible after the 1200°C heating. After 4 hours at 1800°C, the x-ray pattern showed essentially nothing but pure tungsten. This probably indicates that composition of the terminal solid solution has been reached by interdiffusion during the 4 hour, 1800°C heating, and that this β phase at compositions containing less than 26% Re has essentially the same crystal structure as pure tungsten.

Samples R-23 and R-28, which were sputtered coated 1.5 μ thick on Mod E (3.1 mg/cm$^2$), showed essentially the same distinct alloy pattern after 4 hours at 1800°C as after 100 hours at 1500°C. These coatings, being thicker, still retained the complicated alloy pattern.

Sample 1R in Table XXXVII was a spray coating on HRL 3.9 μ porous tungsten. This coating at 2.7 mg Re/cm$^2$ was thinner than R-23 and R-28. Comparing the curves from 2 hours at 1000°, 2-1/2 hours at 1500°C, and 58-1/2 hours at 1500°C, it is noted that separate rhenium peaks were still visible after the 1000°C heating. After 2-1/2 hours at 1500°C, alloy peaks were visible; after 58-1/2 hours at 1500°C, the rhenium peaks and alloy peaks had essentially disappeared. A few indications of the strongest alloy peaks were left, but these were almost indistinguishable from background noise.

Emission spectrographic analysis of surface scrapings about 0.001 in. deep from sample 1R still showed about 4% rhenium, even though metallographic examination did not reveal a discrete surface layer. This rhenium concentration is about what would be expected when the 2.7 mg/cm$^2$ later was mixed with a 1 mil layer of tungsten.

Samples R-23 and R-28 were heated in vacuum and 1R was heated in hydrogen. It is not known whether this had an effect on the difference in retention of alloy in the outer 2 to 3 μ surface. Another possible difference may stem from the fact that Mod E has a larger pore and grain size than the HRL 3.9 μ porous tungsten.

Summarizing these qualitative results, it appears that a thin coating of 0.5 μ or less dilutes with tungsten fairly rapidly until it cannot be detected by x-ray diffraction. A 1.5 μ sputtered coat is still quite easily seen after at least 100 hours at 1500°C in vacuum. A slightly thinner sprayed coat showed essentially no alloy pattern after 58-1/2 hours at 1500°C. The x-ray pattern of the alloy would be expected to disappear and leave only the pattern of tungsten when the surface composition reaches 26% rhenium or less. This is the approximate level at which the β-phase solid solution of rhenium in tungsten exists.

### 3. Electrical Tests

At this time, work function and neutral fraction tests have been performed and reported under Contract NAS 3-6271 on only one single-strip ionizer coated by sputtering with 1.5 μ of rhenium. Information obtained before the coating flaked and caused a disabling arc indicated that the rhenium may be superior to iridium. The work function at 2.2 $mA/cm^2$ was about 5.2 eV, with a neutral fraction of 0.005%.

After the ionizer was disassembled, it was found that the sputtered rhenium coating was not completely adherent in the smooth weld areas between the porous tungsten and the manifold. When the ionizer was heated to operating temperatures, and operating potentials were applied, loose pieces of the coating apparently were pulled toward the accel structure until electrical contact was made. This problem could be easily eliminated in future ionizers by masking off the weld areas during sputtering or by diffusing the coating at 1500°C before use. The diffusion step was not used for this particular coating which was deposited by Philips Metalonics.

## G. CONCLUSIONS AND RECOMMENDATIONS CONCERNING COATING WITH RHENIUM

The limited work on rhenium coatings shows sufficient promise to warrant further testing and development under essentially the same

approaches as indicated previously for iridium coatings. The operation of a practical ion engine with a rhenium coating will undoubtedly be affected by the same environmental and other factors as iridium coated ionizers. Because of the higher solubility of rhenium in tungsten compared with iridium in tungsten, it is expected that thin rhenium coatings will be generally less stable from the diffusion standpoint than equivalent iridium coatings. The work functions of two of the resulting solid solutions that would be formed after loss of the discrete second phase layer by diffusion were shown in Fig. 34.

## APPENDIX I

## SPECTROGRAPHIC ANALYSES OF PRE-ALLOYED SPHERICAL POWDERS

| Element | Parts Per Million | | |
|---|---|---|---|
| | 5 Re-95W | 25 Re-75W | 50 Ir-50W |
| Silver | 5 | ND < 1 | ND |
| Aluminum | 5 | 230 | 200 |
| Arsenic | ND < 20[a] | ND | ND |
| Boron | ND < 1 | ND | ND |
| Barium | ND < 1 | ND | ND |
| Beryllium | ND < 1 | ND | ND |
| Bismuth | ND < 1 | ND | ND |
| Calcium | ND < 1 | 160 | 5 |
| Cobalt | ND < 1 | 10 | 10 |
| Chromium | | 170 | 30 |
| Copper | 10 | 100 | 100 |
| Iron | 100 | 280 | 150 |
| Hafnium | ND < 20 | ND | ND |
| Indium | ND < 1 | ND | ND |
| Iridium | ND < 5 | ND < 5 | |
| Lithium | ND < 1 | ND | ND |
| Magnesium | 5 | 50 | 10 |
| Manganese | ND < 1 | 20 | 5 |
| Molybdenum | 10 | 120 | 120 |
| Sodium | 30 | 50 | 15 |
| Columbium | ND < 5 | ND | ND |
| Nickel | 10 | 170 | 150 |
| Osmium | ND < 200 | ND | ND |
| Lead | ND < 1 | ND | ND |
| Palladium | ND < 1 | ND | ND |
| Platinum | ND < 5 | ND | ND |
| Rhodium | ND < 5 | ND | 100 |
| Ruthenium | ND < 200 | ND | ND |
| Antimony | ND < 20 | 20 | ND |
| Silicon | 10 | 250 | 150 |
| Tin | ND < 1 | 100 | ND |
| Strontium | ND < 1 | ND | ND |
| Tantalum | ND < 30 | ND | ND |
| Titanium | 1 | 15 | 15 |
| Vanadium | ND < 1 | ND | ND |
| Zirconium | ND < 1 | 15 | 80 |
| Thorium | ND < 50 | 200 | ND |
| Rhenium | Medium | ND < 500 | ND < 500 |
| Potassium | 5 | 50 | 15 |
| Rubidium | ND < 1 | ND | ND |

[a]ND < not detected less than